YRKESHÖGSKOLAN NOVIA

Topological Optimisation of Bicycle Frame Connections Using 3D Printing Design

Font i Codinachs, Roc

Zurita Sánchez, Raúl

Degree Thesis

Thesis for NOVIA (UAS)

Degree Programme in Energy Technology

Vaasa, Finland, 2023

DEGREE THESIS

Author: Roc Font i Codinachs and Raúl Zurita Sánchez
Degree Programme and place of study: Mechanical Engineering
Specialisation: Energy Technology
Supervisor(s): Philip Hollins and Miguel Zamora

Title: Topological optimisation of bicycle frame connections using 3D printing design

---

Date: 19.05.2023 Number of pages: 110 Appendices: 5

Abstract

This thesis discusses the Additive Manufacturing design, optimisation and 3D metal printing of the union nodes of a bicycle frame. A first prototype was already developed, hence this second model had to improve the previous in terms of visual aspects and weight reduction.

The components were printed using the Prima Additive - Print Sharp 250 printer installed in the laboratory, using Stainless Steel 316L as the material. The joint tubes between the union nodes were made of Aluminium 6060 and assembled through an engineered mechanical joint.

The average reduction of 50% of the components' mass was achieved using Design for Additive Manufacturing techniques in Altair and nTopology software. The head tube experienced an 81% mass reduction while the seat tube weight increased by 28%, the maximum and minimum accomplished. The complexity of the parts, with an estimated cost of 15,800€, made it impossible to print them in metal because of the more than 200 hours of printing time, the limitations of the machine, and the high demand for the equipment used, which led to limited printing sessions.

Potential improvements that could be applied to this project are a change of printing material or the use of a more advanced machine model that allows more complex structures to be printed.

Language: English
Key Words: Additive Manufacturing, 3D Design, Topology Optimisation, Lattices, Mass Reduction

Table of Contents

1 Introduction 1
1.1 Aim and objectives 1
1.2 Project purpose 2
1.3 Document structure 2
2 Theoretical background 3
2.1 3D printed bikes background 3
2.1.1 Evolution of 3D printed bikes: An historical overview 4
2.1.2 Challenges and limitations of 3D printed bikes 5
2.1.3 First prototype of the University of Vaasa Additive Manufacturing Laboratory 5
2.2 Additive Manufacturing 6
2.2.1 Types of Additive Manufacturing 7
2.2.2 Advantages of Additive Manufacturing 13
2.2.3 Usable materials 14
2.2.4 Defects in additive manufactured parts 15
2.3 Laser Powder Bed Fusion 16
2.3.1 Operation principle 16
2.3.2 Post-processing 17
2.3.3 Prima additive – Prima Sharp 250 19
2.4 Design for Additive Manufacturing 19
2.4.1 Topology Optimisation 20
2.4.2 Lattice structures 21
3 Materials and methodology 22
3.1 Original frame and bicycle components 22
3.2 Materials to be used 23
3.3 3D CAD design workflow 24
3.4 Topology Optimisation workflow 25
3.5 Lattice structure workflow 27
3.6 Printing preparation workflow 28
4 Stress analysis 29
4.1 Loads and reactions 30
4.2 Analysis of deflections and internal forces 32
5 Assembly type analysis 35
5.1 Design option one 35
5.2 Design option two 35

5.3 Design option three 36
5.4 Design option four 36
5.5 Design option five 37
5.6 Design option six 37
5.7 Design option seven 38
6 3D design and optimisation of the parts 39
6.1 Right dropout 39
6.2 Left dropout 48
6.3 Head tube 54
6.4 Bottom bracket 61
6.5 Seat tube 66
7 3D plastic printing 71
7.1 Joints 72
7.2 Right dropout 74
7.3 Left dropout 76
7.4 Head tube 78
7.5 Bottom bracket 80
7.6 Seat tube 81
8 3D metal printing 83
8.1 Preparation process 83
8.2 Printing supervision 86
8.3 After-printing process 87
8.4 Component post-processing 88
9 Results 90
9.1 Joints 90
9.2 Plastic parts 92
9.3 Metal parts 93
9.4 Cost analysis 94
10 Discussion 95
10.1 Aim and objectives 95
10.2 Limitations 96
10.3 Inconsistencies within the assessment's results 97
10.4 Suggestions for assessment improvements 97
11 Conclusion 98
12 References 101
Appendix 1. Stainless Steel 316L Technical Datasheet I

Appendix 2. Aluminium 6060 Technical Datasheet II
Appendix 3. Metal printing times III
Appendix 4. Estimated cost of the parts VI
Appendix 5. Project scheduler IX

List of Figures

Figure 1. Bicycle frame parts.. 3
Figure 2. Components of the first bicycle prototype 6
Figure 3. Diagram of Material Extrusion operation 7
Figure 4. Diagram of Material Jetting operation. 8
Figure 5. Diagram of Binder Jetting operation 9
Figure 6. Diagram of Sheet Lamination operation 10
Figure 7. Diagram of Vat Photopolymerization operation. 11
Figure 8. Diagram of Powder Bed Fusion operation 11
Figure 9. Diagram of Direct Energy Deposition operation 12
Figure 10. Laser Powder Bed Fusion machine scheme 16
Figure 11. Post-processing workflow 17
Figure 12. Rapid Prototyping workflow 20
Figure 13. Lattice unit cell examples 21
Figure 14. Project reference bicycle 22
Figure 15. CAD design workflow 24
Figure 16. Optimisation process workflow 25
Figure 17. Lattice structure process workflow 27
Figure 18. Printing preparation workflow with Materialize Magics 28
Figure 19. Printing preparation workflow with EP Hatch 29
Figure 20. Graphic representation of the frame with applied loads and bearing points ... 31
Figure 21. Axial forces diagram of the frame scaling 5 times the actual value 33
Figure 22. Shear forces and bending moment, respectively, scaling 5 the actual value 34
Figure 23. Deflection of the frame scaled 300 times larger 34
Figure 24. Sketch of the first option 35
Figure 25. Sketch of the second option 36
Figure 26. Sketch of the third option 36
Figure 27. Sketch of the fourth option 37
Figure 28. Sketch of the fifth option 37
Figure 29. Sketch of the sixth option 38
Figure 30. Sketch of the seventh option 38
Figure 31. Original right dropout 39
Figure 32. Right dropout first design 40
Figure 33. Right dropout second design and modification 40
Figure 34. Derailleur support 41
Figure 35. Rapid Prototyping of the notch for the derailleur 41
Figure 36. Right dropout third design 42
Figure 37. Right dropout partitions 42
Figure 38. Optimised right dropout with and without unions 43

Figure 39. Component in Materialize Magics baseplate. 43
Figure 40. Materialize Magics fix wizard 44
Figure 41. Mesh errors in the right dropout 44
Figure 42. Mesh errors fixing process 45
Figure 43. Support perforation parameters 45
Figure 44. Generated support for right dropout 46
Figure 45. Right dropout final modification and close-up 47
Figure 46. Right dropout final design and optimisation 47
Figure 47. Original left dropout 48
Figure 48. Left dropout first design 48
Figure 49. Left dropout second design and modification 49
Figure 50. Left dropout partitions 49
Figure 51. Left dropout first optimisation 50
Figure 52. Left dropout final design 50
Figure 53. Left dropout final optimisation 51
Figure 54. Left dropout Materialize Magics baseplate 51
Figure 55. Mesh errors of the left dropout 52
Figure 56. Support generation for the left dropout 52
Figure 57. New support generation for the left dropout 53
Figure 58. Internal support to fix left dropout 53
Figure 59. Original head tube 54
Figure 60. Head tube first design 54
Figure 61. Head tube back modifications (Left: first design. Right: Second design) 55
Figure 62. Head Tube partitions 55
Figure 63. Topology optimisation of the head tube (From left to right; first design - first modification - second modification) 56
Figure 64. Head tube with back nerves 57
Figure 65. Head tube with lattices structure 57
Figure 66. Back reinforcements with embedded lattices 58
Figure 67. Embedded lattice parameters 58
Figure 68. Final head tube with unions 59
Figure 69. Mesh errors of the head tube. 60
Figure 70. Support generation for the head tube 60
Figure 71. Original bottom bracket. 61
Figure 72. CAD design of the bottom bracket 61
Figure 73. Geometry sketch of the rear part of the frame 62
Figure 74. Bottom bracket partitions 63
Figure 75. Different views of the bottom bracket optimised 63
Figure 76. Bottom bracket optimised with unions 64
Figure 77. Lattices added to the bottom bracket perimeter 64
Figure 78. Surface lattices parameters 65
Figure 79. Mesh errors of the bottom bracket 65
Figure 80. Support generation for the bottom bracket 66
Figure 81. Original seat tube 66
Figure 82. First CAD design of the seat tube 67
Figure 83. Second CAD design of the seat tube 67
Figure 84. Third CAD design of the seat tube 68
Figure 85. Seat tube partitions 68

Figure 86. Different views of the first optimised seat tube 69
Figure 87. Fourth CAD design of the seat tube 69
Figure 88. Final seat tube with unions 70
Figure 89. Mesh errors of the seat tube..... 70
Figure 90. Support generation for the seat tube 71
Figure 91. Plastic tests of the fifth type joint 72
Figure 92. Plastic test of the sixth type joint 73
Figure 93. Plastic test of the seventh type joint..... 74
Figure 94. First plastic printing of the right dropout..... 74
Figure 95. Second plastic printing right dropout..... 75
Figure 96. Final plastic printing of the right dropout 75
Figure 97. First plastic printing of the left dropout 76
Figure 98. Second plastic printing of the left dropout 77
Figure 99. Third plastic printing of the left dropout..... 77
Figure 100. Final plastic printing of the left dropout 78
Figure 101. Generated support in the CURA software for both dropouts..... 78
Figure 102. Plastic printed head tube 79
Figure 103. Generated support in the CURA software for the head tube 79
Figure 104. Generated support in the CURA software for the bottom bracket 80
Figure 105. Plastic printed bottom bracket..... 80
Figure 106. First plastic version of the seat tube 81
Figure 107. Generated support in the CURA software for the seat tube 82
Figure 108. Definitive plastic parts of the seat tube 82
Figure 109. Oven to bake the powder..... 83
Figure 110. Baseplate calibration and control rule 84
Figure 111. Silicon blade placement and fixing..... 84
Figure 112. Silicon blade calibration 85
Figure 113. Laser lens cleaning..... 85
Figure 114. Environment Settings 86
Figure 115. First layer drawing of the dropouts..... 87
Figure 116. Baseplate covered in metal powder..... 88
Figure 117. Sifting machine 88
Figure 118. Example of a component with supports 89
Figure 119. Baseplate being milled (left) and the baseplate result (right) 89
Figure 120. Section view of the two different diameters of the final joint 90
Figure 121. Definitive plastic joints 91
Figure 122. Printed metal joints 91
Figure 123. Metal printing error on the left and aborted printing result on the right 93

List of Tables

Table 1. First prototype bicycle component weights 6
Table 2. Bike frame measurements..... 30
Table 3. Bar properties inserted to Barras, Young module (N/mm^2), inertia (mm^4), area (mm^2) 33
Table 4. Numeric results for Barras' calculation of forces (N) and moments (Nmm)..... 33

Table 5. Numeric results for the displacements (mm) and rotation (rad) of the joints. ... 34
Table 6. Table of measures for the rear part angles 62
Table 7. Summary of the printed parts compared with the first bicycle prototype 92
Table 8. Component's mass analysis 93
Table 9. Parts metal printing time 94
Table 10. Estimated price of the metal 3D printed parts 95

Glossary

Acronyms

3D	Three-Dimensional
AM	Additive Manufacturing
BJ	Binder Jetting
CAD	Computer Aided Design
CNC	Computer Numerical Control
DED	Direct Energy Deposition
DfAM	Design of Additive Manufacturing
EPI	Encapsulated Postscript Interchange
LPBF	Laser Powder Bed Fusion
ME	Material Extrusion
MJ	Material Jetting
PBF	Powder Bed Fusion
RP	Rapid Prototyping
SL	Sheet Lamination
SLC	Stereolithography Contour
STEP	Standard for Exchange of Product Data
STL	Stereolithography
TM	Traditional Manufacturing
TO	Topology Optimisation
UV	Ultraviolet
VP	Vat Photopolymerization

Units

mm	Millimetre
N	Newton
°	Degree
MPa	Megapascal
mm^2	Square millimetre
mm^4	Millimetre to the power of four
Nmm	Newton per millimetre
rad	Radian
N/mm^2	Newton per square millimetre

1 Introduction

The bicycle has been one of the most popular modes of transportation for over a century, thanks to its efficiency, versatility, and environmental friendliness (Hiles, 2015). However, Traditional Manufacturing (TM) methods for bicycle components have been a bottleneck in terms of design complexity and production costs. With the advent of 3-Dimensional (3D) printing technology, the bicycle industry has an opportunity to revolutionize the way bicycles are designed and manufactured (Mythos, 2014).

This thesis focuses on the application of Additive Manufacturing (AM) and Topology Optimisation (TO) techniques to produce the nodes of a bicycle. The purpose of this thesis is to explore the potential benefits and limitations of 3D printing technology for producing complex bicycle components. Additionally, the redesign of the bicycle frame is necessary to ensure that the printed parts can be assembled correctly, without compromising the structural integrity and performance of the bike.

The methodology used in this study involves a combination of Computer-Aided Design (CAD), finite element analysis, and AM techniques. The TO process will be used to generate optimal designs for the bicycle nodes, taking into consideration the weight, stiffness, strength requirements and applied loads. The aim is to produce 3D-printed components that are structurally sound and perform to the required standards. The 3D printing process will be used to produce the final parts, and their mechanical properties and dimension accuracy will be checked to ensure they meet the design specifications.

The main contributions of this study are expected to be the validation of 3D printing technology for producing bicycle components and the development of a new methodology for designing and optimising bicycle nodes.

1.1 Aim and objectives

This thesis aims to design and 3D metal print the union nodes of a bicycle frame. Consequently, the whole bicycle has to be redesigned, including its structure, to make it possible to assemble with the new nodes. Also, to validate the feasibility of using AM and TO techniques to produce the nodes of a bike.

To achieve the aim and purpose of this thesis, the following objectives have to be fulfilled:

- Design an easy-to-assemble mechanical fitting method.
- Produce the 3D printed joints with the lowest mass but the highest resistance.
- Improve the design and weight compared to the first 3D printed bicycle prototype.
- Manufacture 3D printed components.
- Undertake performance testing benchmark.

The purpose of this study is to determine the advantages and disadvantages of 3D printing technology for bicycle component production, as well as to explore a new technique for designing and optimising bicycle frames.

1.2 Project purpose

This thesis has been commissioned by Dr. Rayko Toshev, manager of the Additive Manufacturing Laboratory from the University of Vaasa, and supervised by Miguel Zamora, Laboratory Engineer of the University of Vaasa and the technical responsible of the lab. After the first prototype was printed and assembled years ago, in 2021, the lab keeps an interest in creating a feasible bike frame by using Additive Manufacturing methods. Success in this field would represent the laboratory's first major project, creating a precedent and a way of presenting the laboratory's achievements. It would also represent the earliest AM project in the Finnish bicycle industry.

1.3 Document structure

This thesis begins with a brief introduction to the additive manufactured bicycles topic and an overview of the thesis aims, objectives and purpose (Section 1). Section 2 is an introduction to the manufacturing principles and techniques which will be used for this project and a look back at what has already been done in the bicycle industry.

The methodology followed for each step of the process, as well as the materials used, will be explained in Section 3. Sections 4 to 8 will discuss all aspects of applied loads, joint type selection, design and optimisation, printing, and post-processing of the bicycle nodes.

Finally, Section 9 presents the results obtained for this work, Section 10 a discussion of these results and lastly the conclusion in Section 11.

2 Theoretical background

The chapter provides a theoretical background on the fundamental principles, techniques, and applications of AM. It explores important topics to find out the main features, such as Design for Additive Manufacturing (DfAM), types of AM, usable materials, defects in additive manufactured parts and a short review of main advantages when applying this new industrial technology.

A short review of 3D printed bicycle background and the first prototype made by the University of Vaasa are presented, followed by an overview of the AM technology implemented.

TO is one of the strong points of the chapter. As Bendsøe & Sigmund (2013) describe, it is a design method used in AM that mathematically analyses and optimises the material distribution within a given design space to achieve desired performance while minimizing material usage. Lattice structures design is also another main topic related to AM techniques (Tao & Leu, 2016). Altogether are included in the DfAM section.

2.1 3D printed bikes background

To know which parts of the bicycle will be referred to in this section, the following figure (Figure 1) shows in a comprehensive way all the parts of a bike.

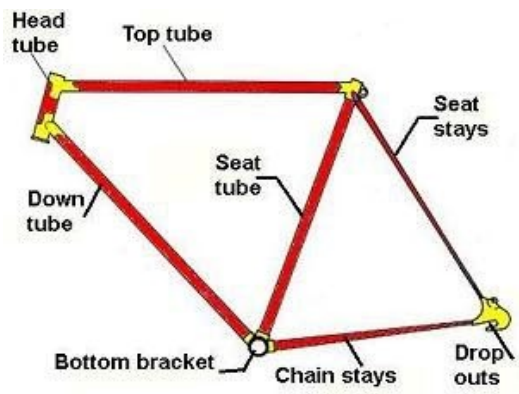

Figure 1. Bicycle frame parts. (Century Cycles, 2023).

The parts of the bicycle to be optimised are the junction areas between tubes. From now on they will be referred to as head tube, seat tube, bottom bracket, and left and right dropouts.

3D printing has revolutionized the way of producing and manufacturing goods. Some of the benefits of this type of manufacturing are the ability to create complex and intricate designs with precision and relative speed. In the cycling sector, using this manufacturing method allows to have a lightweight construction, unique design and the ability to customize the bike to the rider's needs.

In this section will be discussed the history and challenges of 3D printing bicycles.

2.1.1 Evolution of 3D printed bikes: An historical overview

3D printing was born in the 1980s, with its developer Chuck Hull. Since then, the industry has evolved and improved to where we are today (Structuralia, 2022).

Due to the great development of 3D printing, it branched out into other sectors such as the cycling industry. The first printed bicycle was designed by James Novak in 2014. It was printed in mammoth resin and exhibited in Australia (Ginsberg, 2017).

In the June of 2015 the company MX3D printed a functional metal bicycle using a robotic arm, that allowed them to print the frame's complex structures without the need of supports (Miller, 2016). This same year, the company Arevo Labs launched a 3D printed carbon fiber bike frame, which used the same manufacturing process as the MX3D, and resulted in being lightweight and strong (Carlota V., 2019).

The latest major milestone in the cycling industry has been the manufacturing of a 3D printed bicycle that allowed Filippo Ganna to beat the global Hour Record. The bike was tailor-made for the cyclist and used materials from the aerospace industry (Fotheringham, 2022). This has created a precedent for 3D printing techniques to be introduced more noticeably in the creation of bicycles, in view of their versatility and good performance and to further develop bicycles using AM techniques.

2.1.2 Challenges and limitations of 3D printed bikes

The 3D printing industry has evolved exponentially these last years, this means that technologies that were once cutting-edge are now available to the majority of the public.

The metal printer has a high cost that most people could not afford to pay for. Although it is expected to have further development in this type of machines and their price is expected to go down, they still have a high cost (Kauppila, 2023).

Other materials, such as plastic or carbon fibre, can be used to print bicycles (Bourell et al., 2017). The machinery needed for these processes is much cheaper than that used for AM, which means more widespread use of these methods.

Another major challenge is getting these bikes to market. The price is still high enough to still opt for a conventionally manufactured bicycle, but as printing technology develops, the price will start to come down and become more competitive. This is when the potential of a 3D printed bicycle will become visible and comparable to that of conventional bicycles.

2.1.3 First prototype of the University of Vaasa Additive Manufacturing Laboratory

In section *1.2 Project purpose*, it is presented that a bicycle had already been designed in this laboratory. This first prototype also used AM techniques such as TO and the usage of lattices, which will be further explained in this thesis.

The components designed were the same that the ones to be done for this project. Below can be seen how the first design of the components of this bicycle looked like (Figure 2).

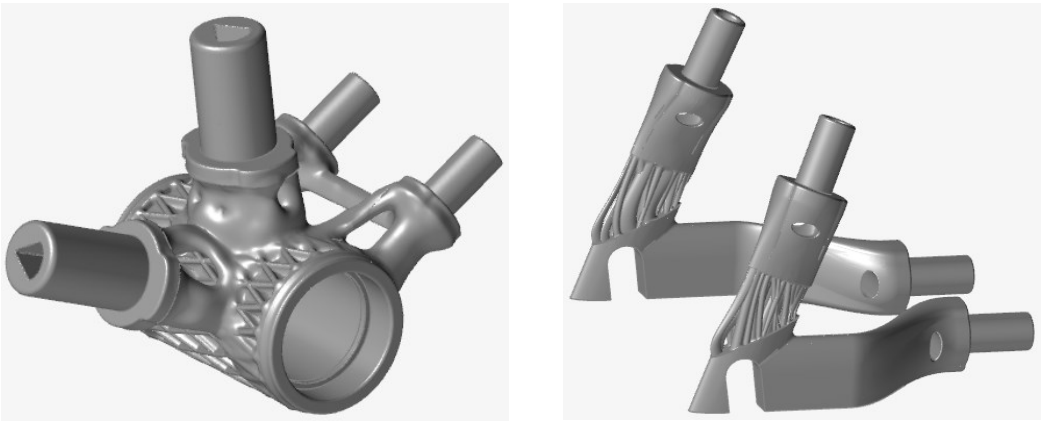

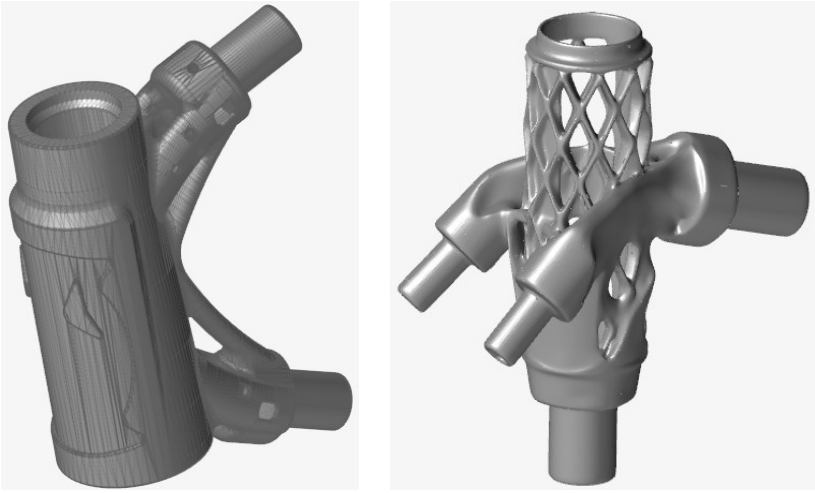

Figure 2. Components of the first bicycle prototype. (Author's own).

Although the design may appear to be complex and intricate, not all the components were optimised to reduce their mass and the lattices used are merely aesthetic. The mass of each component was analysed in the 3D optimisation software and is shown in Table 1.

Table 1. First prototype bicycle component weights

	Head tube	Seat tube	Bottom Bracket	Left Dropout	Right Dropout
Original mass (kg)	1.963	2.600	2.190	0.320	0.320
Optimised mass (kg)	1.963	1.185	1.260	0.320	0.320

(Author’s own).

There are three of the components whose original and the optimised weight is the same, this is because these parts were not optimised or had any modification applied. For this first prototype, the connecting rods between the designed parts were made of carbon fibre and the union between component and tube was by pushing and gluing them together.

2.2 Additive Manufacturing

Additive Manufacturing, also known as 3D printing, is a process of creating physical objects from digital models (Kim et al., 2015). It involves laying down successive layers of material, such as plastic or metal among others, until the final object is complete. This contrasts with TM methods, such as machining or moulding, which typically involve removing material from a solid block to achieve the final shape.

AM offers advantages over TM processes, including greater geometric flexibility, reduced waste production, portability, and ease of use (Singh & Davim, 2019). Researchers from government, universities, and industry anticipate that AM will become a major player in the next industrial revolution, and ongoing research efforts are aimed at realizing the practical applications of AM in various domains such as manufacturing, biomedical, and energy applications (Dilberoglu et al., 2017).

2.2.1 Types of Additive Manufacturing

Several different types of AM technologies vary in terms of materials used, precision, speed, and complexity of the parts that can be produced. Its classification is split into fusion and non-fusion-based processes (Alfattni, 2022). Each of these technologies has its strengths and limitations and can be used to produce a wide range of objects from simple prototypes to highly complex parts.

2.2.1.1 Material Extrusion

Material Extrusion (ME), also known as Fused Deposition Modelling or Fused Filament Fabrication, is a common process used in AM to create three-dimensional objects.

In ME, a thermoplastic filament is fed into a heated nozzle, where it is melted and then deposited layer by layer to form the desired shape (TWI Global, 2023) (Figure 3). The molten material is extruded through a nozzle that moves in the x, y, and z directions, guided by a CAD file. As each layer is deposited, it solidifies and fuses with the previous layer, creating a strong bond between the layers.

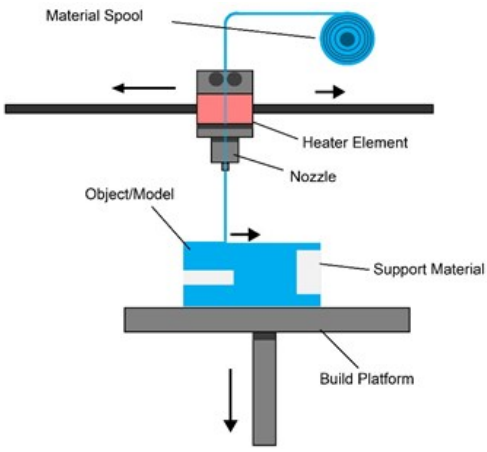

Figure 3. Diagram of Material Extrusion operation. (Loughborough University Website, 2023).

The ME process is widely used because it is relatively simple, fast, and can produce parts with high accuracy and repeatability (Braconnier et al., 2020). It is commonly used to create prototypes, small production runs, and customized parts for a variety of applications in industries such as aerospace, automotive, and medical devices.

2.2.1.2 Material Jetting

Elkaseer et al. (2022) define that Material Jetting (MJ) is a type of AM technology that involves the deposition of droplets of photopolymer materials using inkjet printing technology (Figure 4). In this process, a print head dispenses tiny droplets of a liquid material onto a build platform, where they are rapidly cured using ultraviolet (UV) light. The droplets are deposited layer by layer to create a 3D object.

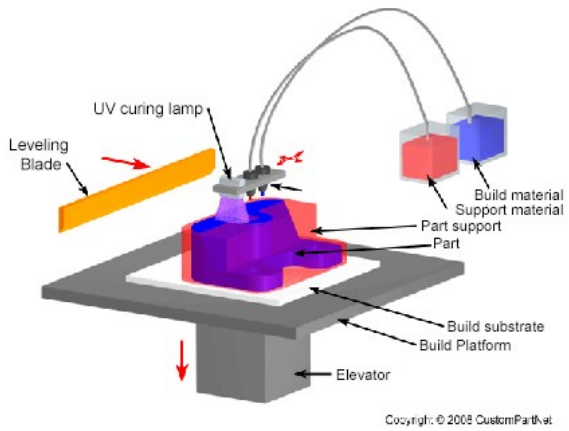

Figure 4. Diagram of Material Jetting operation. (Loughborough University Website, 2023).

MJ is a highly precise AM method, capable of producing parts with very fine details and smooth surfaces. It is commonly used in applications such as dental and medical models, jewellery, and other highly detailed objects (Gülcan et al., 2021). The process allows for the use of multiple materials in a single print, as the print head can dispense different types of materials at different times during the printing process. This enables the creation of objects with a range of properties, such as varying levels of stiffness or flexibility.

2.2.1.3 Binder Jetting

Binder Jetting (BJ) is a type of AM technology that uses a binder solution to selectively bind together powder particles to create a 3D object (Arnold, 2022) (Figure 5). In this process, a thin layer of powder material is spread evenly across a build platform, and a print head

selectively deposits a liquid binder onto the powder layer in a pattern that corresponds to the cross-section of the object being printed. The binder causes the powder particles to adhere to each other, forming a solid part (Du et al., 2020). This process is repeated layer by layer until the final object is formed.

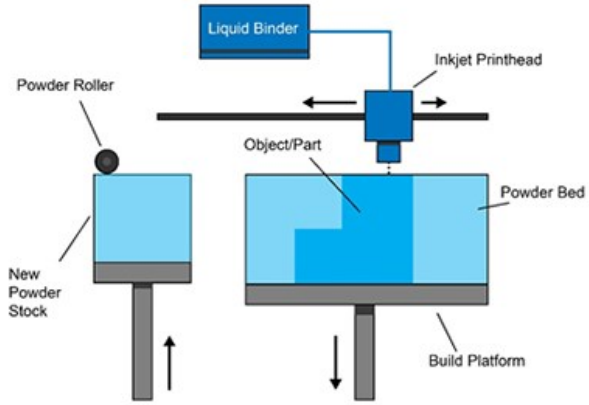

Figure 5. Diagram of Binder Jetting operation. (Loughborough University Website, 2023).

BJ is a fast and cost-effective method of AM that is commonly used for producing metal and ceramic parts. It can also be used with other materials such as sand and polymers. The process allows for the creation of complex shapes and internal structures, and the use of multiple materials in a single print. However, the resulting parts may have lower strength and precision compared to other AM methods (Mirzababaei & Pasebani, 2019). The finished parts are often sintered or otherwise post-processed to increase their strength and durability.

2.2.1.4 Sheet Lamination

As Gibson et al. (2020) say, Sheet Lamination (SL) is a type of AM technology that involves the layer-by-layer bonding of sheets of material to create a 3D object (Figure 6). In this process, thin sheets of material such as paper, plastic, or metal are bonded together using an adhesive or heat to form a solid object. The sheets can be cut or shaped prior to lamination to achieve the desired geometry.

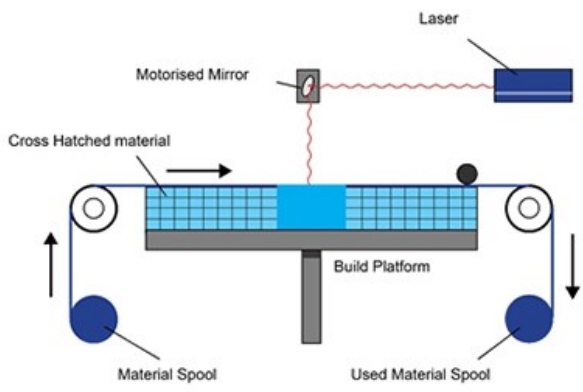

Figure 6. Diagram of Sheet Lamination operation. (Loughborough University Website, 2023).

SL is a low-cost AM method that is commonly used for producing large, low-resolution objects such as architectural models, packaging materials, and temporary structures (Zhang et al., 2017). It can also be used for producing small parts with complex shapes, although the resolution may be limited. The process is relatively fast and can be used with a variety of materials, including recycled materials, making it an environmentally friendly option. However, the resulting parts may have lower strength and durability compared to other AM methods.

2.2.1.5 Vat Photopolymerization

Vat Photopolymerization (VP) is a type of AM technology that uses a liquid photopolymer resin that is solidified layer by layer using UV light (Pagac et al., 2021) (Figure 7). In this process, a build platform is submerged in a vat of liquid resin, and a UV light source is used to selectively cure the resin in a pattern that corresponds to the cross-section of the object being printed. The cured resin forms a solid layer, and the build platform is lowered to create a new layer of uncured resin on top of the previous layer. The process is repeated layer by layer until the final object is formed.

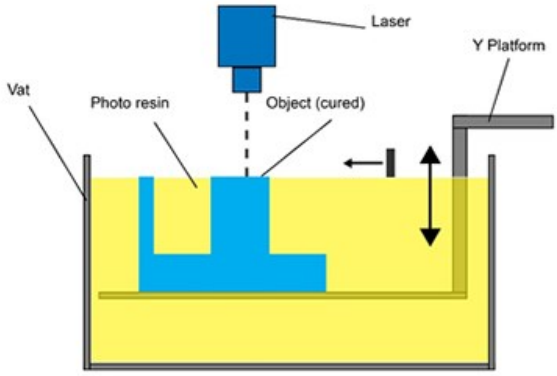

Figure 7. Diagram of Vat Photopolymerization operation. (Loughborough University Website, 2023).

Al Rashid et al. (2021) say that VP is a high-precision AM method that is commonly used for producing small, intricate parts with high accuracy and resolution. It can be used with a range of materials, including plastics, ceramics, and composites. The resulting parts have a smooth surface finish and can have very fine details and features. However, the process can be relatively slow compared to other AM methods, and the finished parts may be brittle and have lower strength and durability compared to other manufacturing methods.

2.2.1.6 Powder Bed Fusion

Powder Bed Fusion (PBF) is a type of AM technology that uses a laser or electron beam to selectively melt and fuse together layers of metal, plastic, or ceramic powder to create a 3D object (Dev Singh et al., 2021) (Figure 8). In this process, a thin layer of powder is spread evenly across a build platform, and a laser or electron beam is used to selectively melt the powder in a pattern that corresponds to the cross-section of the object being printed (Snow et al., 2020). The melted powder solidifies and fuses with the previous layer, forming a solid part. This process is repeated layer by layer until the final object is formed.

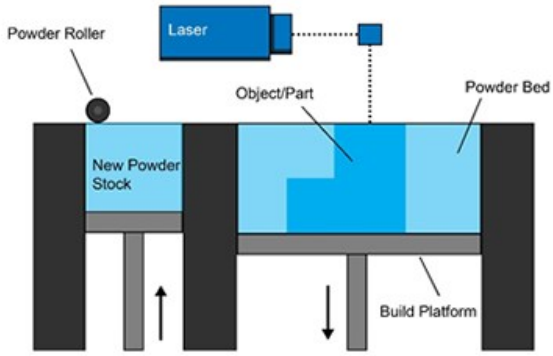

Figure 8. Diagram of Powder Bed Fusion operation. (Loughborough University Website, 2023).

PBF is a high-precision AM method that is commonly used for producing metal parts with complex geometries and internal structures. It can produce parts with high accuracy and surface finish, and can be used with a range of materials, including titanium, aluminium, and steel (Hossain et al., 2016). The process allows for the creation of parts with high strength and durability and can produce parts with properties similar to those of conventionally manufactured parts. However, the process can be relatively slow, and the finished parts may have residual stresses that can affect their mechanical properties.

2.2.1.7 Direct Energy Deposition

Direct Energy Deposition (DED) is a type of AM technology that uses a focused energy source, such as a laser or electron beam, to melt and fuse together layers of metal, plastic, or ceramic material to create a 3D object (Piscopo & Iuliano, 2022) (Figure 9). In this process, the energy source is directed onto the surface of the material, causing it to melt and form a small pool of molten material. A feedstock material, in the form of wire or powder, is then fed into the pool of molten material, where it solidifies and fuses with the previous layer. This process is repeated layer by layer until the final object is formed.

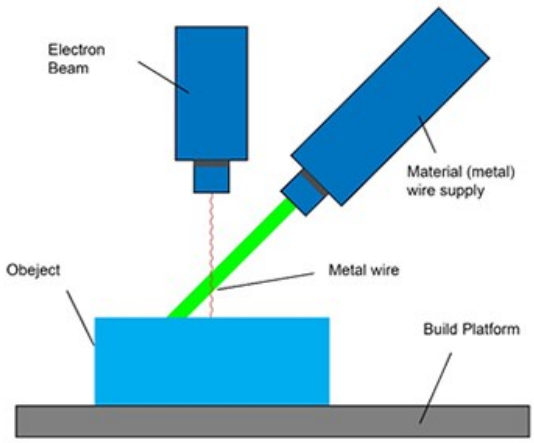

Figure 9. Diagram of Direct Energy Deposition operation. (Loughborough University Website, 2023).

DED is a high-precision AM method that is commonly used for repairing or modifying existing parts, as well as for producing new parts with complex geometries and internal structures (Ahn, 2021). It can be used with a range of materials, including titanium, aluminium, and steel, and allows for the creation of parts with high strength and durability. The process can also be used to create parts with graded material properties, as different materials can be fed into the pool of molten material to create a desired property profile.

As other methods, the process can be relatively slow, and the finished parts may have residual stresses that can affect their mechanical properties.

2.2.2 Advantages of Additive Manufacturing

Additive Manufacturing, or 3D printing, offers several advantages over Traditional Manufacturing methods.

As Attaran (2017) explains on its review, AM allows for the creation of complex and intricate shapes that may be difficult or impossible to achieve with TM methods. That design flexibility enables designers to create highly customized, optimised, and innovative products that may have superior performance characteristics. It also enables Rapid Prototyping (RP), allowing for faster iterations of design and product development. This can result in shorter product development cycles, reduced time to market, and increased innovation.

TM methods often result in significant material waste, as parts are machined or moulded from larger blocks of material. In contrast, AM typically builds parts layer by layer, only using the material needed for the final object (Ford & Despeisse, 2016). The reduced material waste can result in lower material waste and reduced costs associated with material usage.

It can be cost-effective for producing small runs of specialized or low-volume parts (Pérez et al., 2020). TM methods often require expensive tooling or moulds, which may not be feasible for small production runs. AM, on the other hand, can produce parts with minimal setup costs, making it suitable for small-scale production.

AM allows for on-demand production, where parts can be produced as needed, eliminating the need for large inventory stockpiles. This can result in reduced inventory costs and more efficient supply chain management. In addition, it can enable decentralized production, as digital design files can be sent electronically and produced locally. This geographical flexibility can potentially reduce transportation costs, lead times, and environmental impacts associated with long-distance shipping (Bandyopadhyay et al., 2022).

AM allows for easy customization and personalization of products, as digital design files can be easily modified to meet individual needs or preferences (Klahn et al., 2015). This

opens possibilities for unique, tailor-made products and mass customization. It also can enable the creation of complex assemblies as a single printed object, reducing the need for assembly of multiple individual parts. The reduced assembly complexity can simplify manufacturing processes, reduce assembly time, and labour costs, and improve product performance.

2.2.3 Usable materials

AM has revolutionized the way objects are designed and produced. One of the critical factors is the availability of a wide range of usable materials (Bandyopadhyay & Bose, 2016). From metals and polymers to ceramics and composites, the choice of materials in AM plays a crucial role in determining the properties, performance, and applications of the printed objects (Bourell et al., 2017).

Bhatia & Sehgal (2021) define all groups of materials that are currently in use in AM processes. Polymers are one of the most common. They are lightweight, flexible, and can be easily moulded into different shapes. In front of those, metals and alloys are used to create strong and durable objects. Materials such as titanium, stainless steel, aluminium, and copper are commonly used in 3D printing.

Biomaterials are also used in AM to create objects that are biocompatible and can be used in medical applications such as hydrogels, biodegradable plastics, and synthetic bone. These items tend to be composite materials, which is a group that encompasses a wider range of materials. In turn, composites are used to create objects with unique properties (Kumar & Sathiya, 2021). They are made by combining two or more materials to create a new material with different properties.

Ceramics are another material group used in AM to create objects that are strong and heat resistant (Travitzky et al., 2014). Some examples are porcelain, clay, and zirconia. In addition, building materials such as concrete, cement, and sand are used also to create objects that are large and strong. 3D printing of building materials is being used to create structures such as houses, bridges, and other large objects.

In addition to the materials mentioned above, Yadav et al. (2021) say that there are also other specialized materials used in AM. For example, food printing materials such as

chocolate, sugar, and dough are used to create edible objects such as desserts and pastries. And smart materials, such as shape-memory alloys and conductive polymers, can also be used in AM to create objects with unique properties, such as objects that can change shape in response to temperature or objects that can conduct electricity (Mondal & Tripathy, 2021). These specialized materials are expanding the potential uses of AM and enabling the creation of even more complex and innovative objects.

2.2.4 Defects in additive manufactured parts

AM, like any manufacturing process, can have various types of defects that may affect the quality, structural integrity, or appearance of the printed objects.

Implementing AM technology is still difficult since quality, repeatability and mechanical properties of the part issues have not yet been fully resolved to meet industrial standards (Yao et al., 2018). The quality of final constructs will be affected by processing variables including laser power, scan velocity, and hatch spacing. Due to the discontinuity of the printing process and other unrelated causes, defects frequently appear in the build component.

Chen et al. (2021) define the main categories of defects as cracking, residual stresses, porosity and balling. The first one is a common defect in AM parts, and it is mainly caused by thermal stresses, which are caused by temperature changes of the printed part. Pores are caused by trapped gas and a lack of fusion, which immediately impact on the density and mechanical characteristics of final components and their performance. And the last one, called balling, is the phenomena of molten material solidified into spheres instead of solid layers, which is a severe impediment to interlayer connection (Demir & Previtali, 2017).

Other researchers as Cerniglia & Montinaro (2018), Brennan et al. (2021) and Wu et al. (2018) mention other minor defect categories as surface roughness, layer misalignment, geometric defects, incomplete fusion, delamination, oxidation, inaccurate material deposition, contamination, support structure defects and post-processing defects.

2.3 Laser Powder Bed Fusion

One of the most widely used 3D printing techniques is Laser Powder Bed Fusion (LPBF). A laser beam with a specific spot size fuses several layers of powder, one by one, following a determined strategy to build a component of desired geometry (Sabzi & Rivera-Díaz-del-Castillo, 2022). It can print complex designs, optimised geometries and lightweight parts.

2.3.1 Operation principle

As mentioned before, this method is based on melting metal powder by its exposure to laser radiation. The main parts of this machine are shown in the figure below (Figure 10).

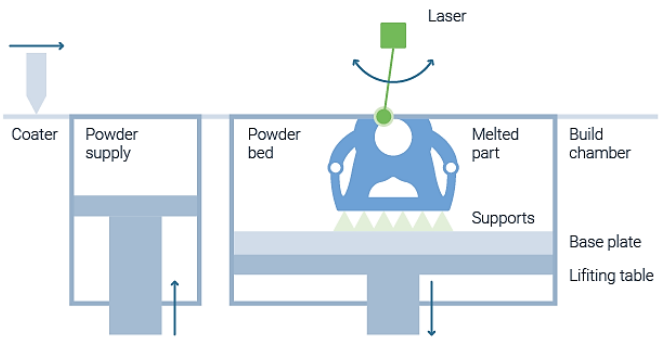

Figure 10. Laser Powder Bed Fusion machine scheme. (AM power, 2019).

To create a part, a predetermined amount of metallic powder is applied to a base plate using a blade, brush or roller (Hendrixson, 2021). At that point, the laser selectively melts the powder to shape the desired shape for that layer of the part (Duda & Raghavan, 2016). Since the base plate is also made of metal, when the metal powder is melted, it welds the plate and needs further machining (Protolabs, 2020).

When the exposure process is completed, the base plate is lowered by the same distance as the workpiece is raised, which is the thickness of the melted layer. On the other side, the powder supply raises the same distance to keep providing metal powder (AM Power, 2019). The powder which hasn't been reached by the laser remains loose and thus can be recycled and reused for other printings.

As metallic powders have a strong reaction potential, this process is conducted in a controlled atmosphere. Prior to the procedure, the chamber is purged with nitrogen or argon until the level of oxygen is lower than 0.1% (Sabzi & Rivera-Díaz-del-Castillo, 2022).

2.3.2 Post-processing

The post-processing of 3D-printed metal components usually involves several steps to improve the overall's piece quality, mechanical properties and surface finish (Gadagi & Lekurwale, 2021). The figure below illustrates the usual post-processing workflow (Figure 11).

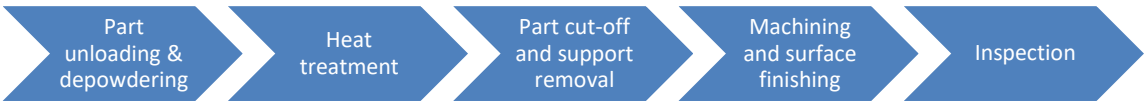

Figure 11. Post-processing workflow. (Author's own).

All the steps will have further theoretical and practical explanation below.

2.3.2.1 Part unloading and depowdering

Once the impression is done, the components are covered in non-melted metal powder. This powder is removed from the printed part with a brush and taken out from the workspace through a vacuum cleaner.

Depowdering means to remove the trapped metal powder from the inside of the printed component (Kotturkar, 2021). For emptying the trapped powder, holes have to be designed in the workpiece to allow the dust to drain out.

2.3.2.2 Heat treatment

Heat treatment may be necessary after some metal 3D printing procedures to reduce residual tension and improve the part's mechanical characteristics (Gadagi & Lekurwale, 2021). This entails heating the component to a specified temperature and then, cool it gradually.

It should be noted that heat treatment is carried out before the components are removed from the build plate in order to prevent part surface roughness.

2.3.2.3 Part cut-off and support removal

Once the heat treatment is done the piece has to be removed from the baseplate. To do so usually is used a Computer Numerical Control (CNC) machine, and it is obtained the component with the supports attached to it (Protolabs, 2023).

After the baseplate is no longer attached to the baseplate, removing supports becomes easier. The most common way of removing supports is manually, with the drawback of needing further machining (Naramore, 2019). For more complex configurations that require a better surface finish, it is used CNC. And at last, if the supports are inaccessible to remove by hand or using CNC it is applied a thermal deburring method to make them weaker (Kotturkar, 2021).

2.3.2.4 Machining surface and finishing

Usually, 3D printed metal components have a rough surface finish, and it has to be improved and sharp edges removed. Some of the most common techniques are polishing, sandblasting or electrochemical polishing (Bigrep, 2018).

Other pieces may need threads, holes, or flat surfaces. All these features are carried out in this part of the process (Markforged, 2023).

Surface finishing techniques are chosen based on the type of surface finish and the desired aesthetic appeal. Some of the most commonly used techniques are vibro-tumbling, sandblasting, electropolishing or applying a protective coating (Kotturkar, 2021).

2.3.2.5 Inspection

Inspection is the final stage of post-processing. Usually, three types of inspection are carried out, all of them being non-destructive (Iacopo et al., 2022).

The first one is a dimensional inspection to ensure that the component's dimensions are consistent with the drawing dimensions. Depending on the type of measurement and its magnitude, the measuring tool is chosen.

Secondly, a mechanical inspection is carried out to ensure all the properties fulfil the needs of the project and compare them to the material's datasheet (Graf et al., 2023). Some of the tests are tensile, microstructure, density, hardness, and shear.

Finally, it is conducted a structural inspection to check if the piece has internal cracks or porosity (Wang et al., 2022). Some of the tests are Dye Penetrant Inspection, Ultrasound, X-Ray or Computer Tomography scanning.

2.3.3 Prima additive – Prima Sharp 250

Prima Additive is one of the few manufacturers and distributors of metal AM machinery (Prima Additive, 2023a). They are specialized in laser technologies, which are PBF and DED.

For this project, the machine used will be Prima Additive – Print Sharp 250. This machine has recognition for its high-quality and precise printing capabilities, with an installed laser that ensures accuracy in printing complex geometries and high-resolution parts. It can work with different materials such as titanium, aluminium, stainless steel, and cobalt-chrome (Prima Additive, 2023b).

The Print Sharp 250 features a $500\ W$ single-mode Infra-Red Fibre Laser, which ensures high-speed and accurate printing. The laser needs to be refrigerated, so an advanced cooling system maintains a proper and constant temperature during the whole printing. The machine's building volume is $258 \times 258 \times 330\ mm$, and a build rate of $12000 - 30000\ mm^3/h$. The deposition layer height goes around 0.02 and $0.1\ mm$ and its width is $0.1\ mm$ in a single track (Prima Additive, 2021).

2.4 Design for Additive Manufacturing

Torosian (2023) defines the Design for Additive Manufacturing as the art, science and skill used to manufacture ordinary object in a non-traditional way: using 3D printers. Engineers can produce things with more complex shapes and with less material use and weight thanks to the additive design process. It involves taking advantage of the unique capabilities and limitations of AM technologies to create functional, efficient, and optimised parts.

The piece-by-piece, line-by-line, surface-by-surface, or layer-by-layer construction method, material qualities, resolution, and limits of the AM technology being utilised are only a few

of the distinctive attributes of AM that DfAM takes into account (Thompson et al., 2016). It attempts to maximise the advantages of AM, including design flexibility, decreased material usage, increased performance, and quicker production, by designing with these factors in mind.

Rapid Prototyping basic operation is described on the schematic below (Figure 12) and it is one of the most important techniques in AM. This process involves quickly creating functional or visual prototypes of a product or system using advanced technologies such as 3D printing (Wong & Hernandez, 2012).

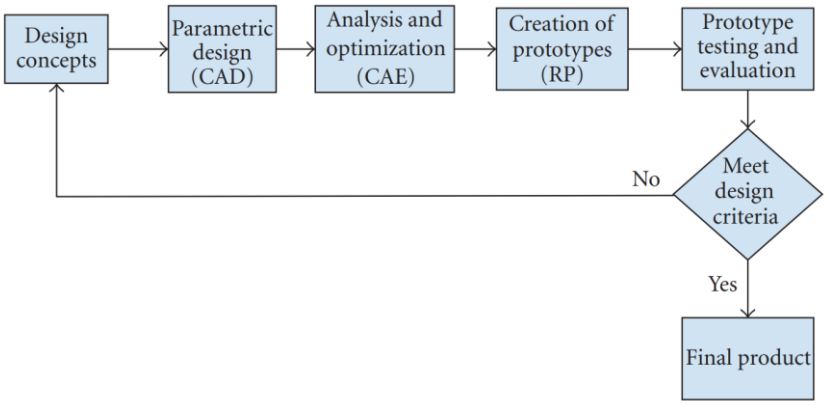

Figure 12. Rapid Prototyping workflow. (Wong & Hernandez, 2012).

It allows for fast iteration and testing of design ideas, accelerating the development cycle and enabling efficient validation of concepts before committing to full-scale production.

As Jiang et al. (2018) explain in their review, support generation is a crucial step in AM design. It involves creating temporary structures to support overhanging or complex features of a 3D-printed object during the printing process. These supports are usually generated automatically by the slicing software based on the geometry of the part, and they are printed simultaneously with the object using the same or a different support material (Jin et al., 2015). The designer has to create the shape of the part according to minimize the support generation, reduce the wasted material, and facilitate the post-processing.

2.4.1 Topology Optimisation

Topology Optimisation is a mathematical method that optimises the material distribution in a defined domain and maximizes the performance and efficiency of the design (Formlabs,

2023), based on the loads, structure restrictions and supports of the component (Rosinha et al., 2015). An analysis is carried out through all the design space, and shows which regions work efficiently. The elements that are not picking up stress, have little strain energy or are redundant, are removed from the mesh (Abbey, 2018).

The process of removing pieces from the mesh is complex and computationally demanding. Instead, the stiffness and density of the elements to be removed are reduced (Xia, 2016). This segregation often occurs between the values 0.0 and 1.0, with 1.0 representing the maximum stiffness and density, and 0.0 reflecting the smallest possible, which is the "removal" of material. By using this method, it is shown the most efficient distribution of material.

2.4.2 Lattice structures

Lattice structures with a regular geometric pattern that is repeated and fill a volume or a surface. They can be found in a wide range of materials because of their unique properties (Nagesha et al., 2020).

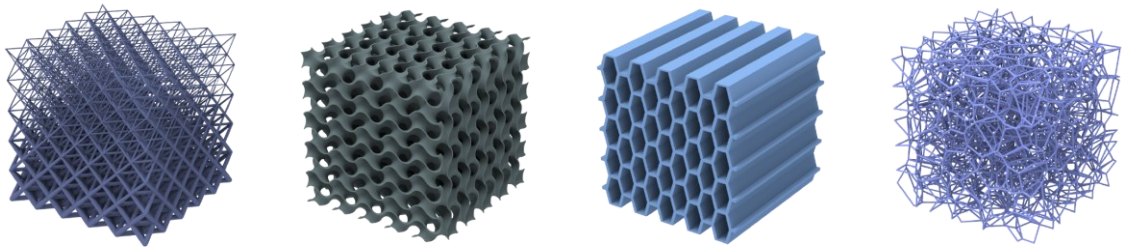

Figure 13. Lattice unit cell examples. (N Topology Website, 2022).

The most important characteristics of this type of structure are its high stiffness, surface area, elongation, energy absorption and porosity (Varotsis, 2022) (Figure 13). These properties can be analysed in detail to know which are the advantages and disadvantages of these structures.

The main advantage of this type of structure is the high strength-to-weight ratio. The repeating unit cells are designed to distribute loads uniformly through the structure, minimizing stress concentrations and reducing the risk of failure (Tao & Leu, 2016).

Another benefit is the high surface area-to-volume ratio. This makes them advantageous for processes like catalysis, filtration, and rapid energy transfers.

There are also some disadvantages of lattice structures. According to Mumtaz et al. (2011) the most important is the difficulty of their manufacturing because they have to be manufactured with high precision and consistently for all the volumes or surfaces.

Summarising, lattice structures have a special combination of features that make them appealing for a variety of applications, from energy storage and medicinal devices to aerospace and automotive engineering (Wang et al., 2018). Nevertheless, to guarantee the best performance and dependability, their design and production must be carefully thought out and analysed.

3 Materials and methodology

This section discusses general aspects to consider before starting to undertake the practical part of the project. A general methodological overview of the materials to use and the different workflows followed in each stage of the project is established for CAD design, topological optimisation, lattice making and printing preparation.

3.1 Original frame and bicycle components

The project is developed around the bicycle that has been purchased and is shown in the figure below (Figure 14). It is from the White Bike brand, and it is a mountain bike model XC Trainer Mns 22. As the aim is to build the whole bike and only the frame is designed and 3D printed, the remaining components such as wheels, handlebars or wiring among others are obtained from it.

Figure 14. Project reference bicycle. (White Bikes, 2020).

The designed frame must follow the similar measurements as the bought bicycle to make sure the final assembly of the frame with the components is correctly done. The angles between the tubes are important measures to take as the exact distance between the dropouts. The bottom bracket, seat tube and the head tube diameters are other relevant measures to consider.

3.2 Materials to be used

As said before, the technology used for the 3D printing is the Laser Powder Bed Fusion with the machine Prima Additive – Print Sharp 250 (see section *2.3 Laser powder bed fusion*). This machine can operate with a large range of metal powder types, but the one used in the Additive Manufacturing Laboratory of the University of Vaasa is Stainless Steel 316. Changing the printing material would mean reprogramming the machine and thorough cleaning.

Specifically, the used powder is MetcoAdd 316L-A from the brand Oerlikon. It is an austenitic steel powder with similar chemistry to the European Standard EN 1.4404. This powder is suitable for the Powder Bed Fusion process and has high resistance to corrosion (Oerlikon, 2020). To further information about this material, see *Appendix 1. Stainless Steel 316L Technical Datasheet*.

As regards the tubes, the decided material is aluminium 6060. For the first bicycle, the tubes used were carbon fibre, and it was determined that this type of tube does not have concentric inside and outside diameters, so a mechanical joint would be very difficult to make. As the tube composition is fibres glued together, the outer layer is reinforced not to peel. In the inner layer, the fibres are less reinforced, and the tube may crumble, which is what happened in the last design of the bicycle.

The selected diameter of the tubes were $\emptyset 30\ mm$ for the thick tubes and $\emptyset 16\ mm$ for the thin ones. The reason for the tubes to be that diameter is that, as the original bicycle's seat tube had this diameter with a wall thickness of $1.5mm$, using the same diameter with double wall thickness will also work for every large tube on the bike. As regards the thin tubes, this was the minimum diameter that was considered to be feasible to do a mechanical union, for thinner tubes, it would have been even harder and might not work

properly. Also, the tubes have a larger diameter and wall thickness than the original ones, so there will not be any problem regarding them.

The aluminium tubes used for this project have been bought in the store Hartman, and the technical datasheet for this material can be found *in Appendix 2. Aluminium 6060 Technical Datasheet*.

3.3 3D CAD design workflow

The first software to be used will be the 3D CAD, where different sketches of the parts will be done until the desired shape is obtained. In this part of the project, the software that have been used are CREO Parametric 9.0.0.0 and Solid Works 2019.

This is the first step in the process, where it is necessary to design the component itself, the partitions that will be used in during the topology optimisation and the joints.

A partition is a part of the component that has not to be optimised. They can be selected from the TO software itself or created in the CAD software and then imported. These parts have to be placed in a different file from the component, and in their exact position in space since they cannot be repositioned.

As the first component design is usually never final, there is a back-and-forth process between CAD and the optimisation software. So, this step will be present almost until the end of the project.

The following scheme shows the workflow followed or all the components of this thesis (Figure 15).

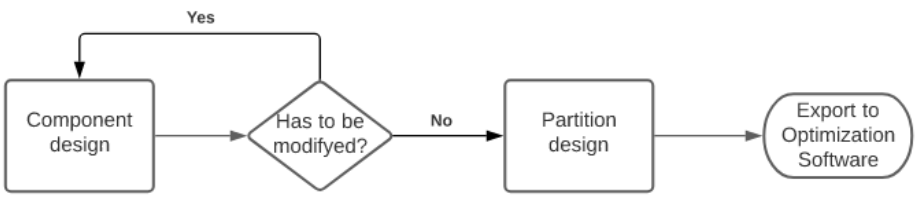

Figure 15. CAD design workflow. (Author's own).

As regards this part of the process, it can be considered finished and move on to the optimisation of the part.

3.4 Topology Optimisation workflow

After the design is made, the optimisation is undertaken with the software Altair Inspire 2022. In this part of the process, the loads that each component has to withstand, are applied in the corresponding direction and orientation. This program provides a topological optimisation taking into account the loads and the wall thickness desired.

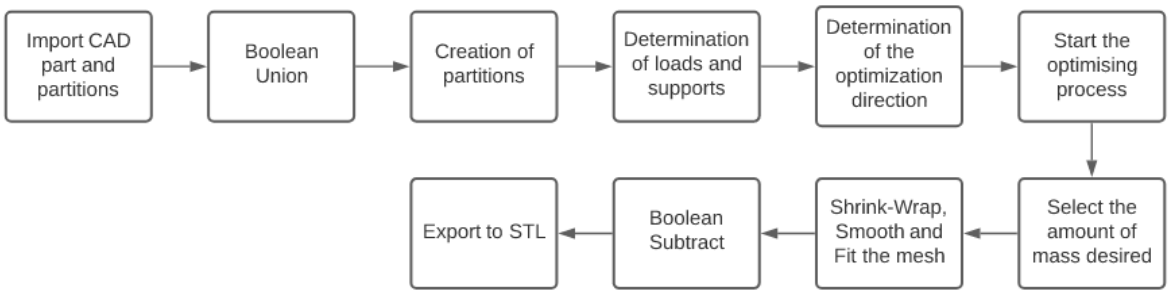

Figure 16. Optimisation process workflow. (Author's own).

As Figure 16 shows, the first step made in this program is to import the part and its partitions. With all the components in the working window, they have to be selected, marked as design space and determined the material, which is Stainless Steel 316 L. Then, the mesh of all the parts has to be merged, to do so it has to be used the Boolean Union operation. After this operation has been made, in the model tree there will only appear one component.

Once that has been checked that there is only one component, the partitions have to be indicated to the program which is done using the Partition Tool. The surface that has to become a partition has to be selected and then determined its thickness. The colour of the parts that have become a partition will change to a different colour from the rest of the component.

Then, the fixed part of the component and the applied loads have to be determined. The fixed part is where the component will be fixed in real life, and there may be more than one in the same component. As regards loads, they will be calculated in section *4. Stress analysis*, and each component will have their loads. As most of them are axil forces, they have to be concentric to the partitions of each joint.

At last, it has to be determined the optimisation direction, which will be the same as the printing one. This will make the program to consider the overhang and other parameters associated.

The overhang, for metal printers is 45º, which determines the maximum angle for a component to be tilted without the need of supports. It is highly desirable that the component has the minimum possible supports, because of the printing problems that they can cause and the post-processing work that will have to be carried out after printing.

To start the optimising process, the first parameter to be configured is the mass target, which for all the components has been set to be at least 30% of the original mass. The other parameter that has to be set is the wall thickness, it has been determined that the minimum will be 3mm for all the components, while the maximum will be determined automatically by the program.

Once the part has been optimised, there is a mass regulator that allows the user to determine how much mass is desired based on the appearance of the component. After the mass desired has been determined, some operations have to be made to the component to make the mesh smoother.

The first operation is Shrink-Wrap, which surrounds all the parts with a single iso-surface. According to Weinstein et al. (2005), an iso-surface is a 3D surface representation of points of equal value, which is the 3D equivalent for a contour line.

Next operation to be done is Smooth, which smoothens the mesh of the geometry.

And at last, the operation Fix. It generates a PolyNURBS part on top of the existing mesh geometry. A NURBS surface (Non-Uniform Rational B-Spline) is a two-parameter function that represents curves and surfaces in the space (Piegl & Tiller, 1995).

The last step before exporting the component is to remove the unwanted material that could have been generated during the last operations. A CAD component is exactly imported and placed in space where it has to be removed. After, a Boolean Subtract is made.

Finally, after the component is its final version, it has to be exported in Stereolithography (STL) to be able to work with it in the next software.

3.5 Lattice structure workflow

The other program for topological optimisation has been used also. It is called nTopology and allows to do the same as Altair Inspire with the advantage of making better lattice structures and Boolean operations (Figure 17).

The first step in this program is to import the CAD component of the part that is desired to add lattices. It is important that the part is in Standard for the Exchange of Product Data (STEP) format, otherwise, it could not be opened.

After the file is opened, to work with it, has to be converted into an implicit body. This is done by double-clicking on the part and selecting the option. Once the body to work is in implicit mode, other operations can begin.

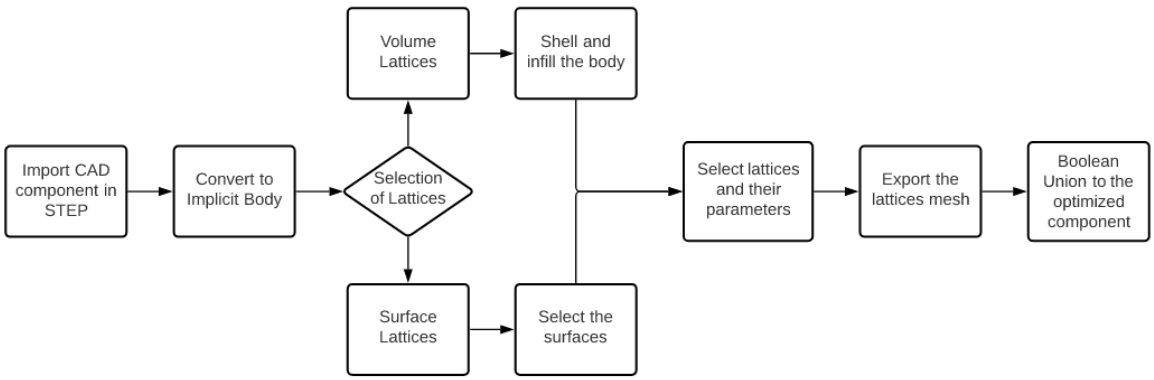

Figure 17. Lattice structure process workflow. (Author's own).

To create volume lattices, it has been used the operation "Merge Shell and Infill", where it shells the component imported with the desired wall thickness and infills the remaining volume with lattices. The parameters that have to be modified are the cell size in the 3-axis, the unit cell that will be used and the lattice thickness.

As regards surface lattices, it has been used the operation "Simple Conformal Lattice from Surface". This operation generates the lattices following the unit cell specified, the number of cells in all three spatial dimensions, how thick the lattice part needs to be and the thickness of the connecting bars between cells. The surfaces where are desired to have lattices must be selected and will be generated on them.

3.6 Printing preparation workflow

After the optimisation is finished, the obtained part is imported to Materialize Magics to prepare it for the printing process. There, all the mesh errors that the component could have, are fixed and the supports needed for printing are generated. Finally, the component is sliced into sheets of 0.03mm thickness and saved into a specific format to export it to the last software.

In the figure below (Figure 18) the diagram of workflow for the printing preparation shows all the steps needed.

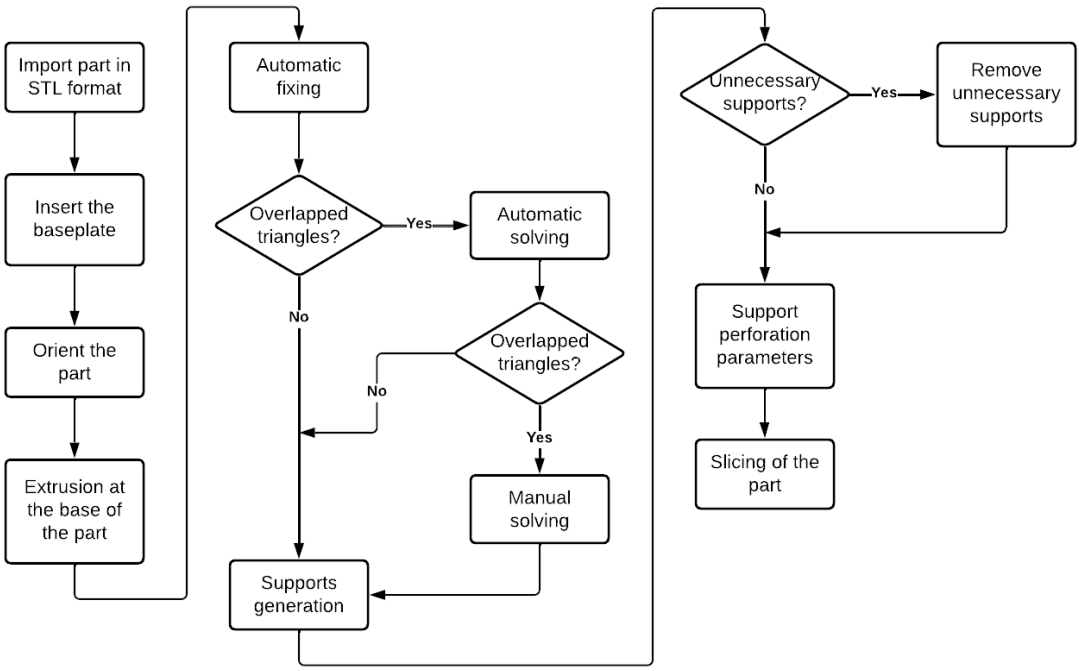

Figure 18. Printing preparation workflow with Materialize Magics. (Author's own).

The step *Insert baseplate* is the action of importing to the software the piece where the parts will be printed. In this case, it has to be the same as requires the printing machine Prima additive – Prima Sharp 250. Then, after having placed the part as desired, it is important to extrude 2mm at the base of the future-printed part. This extra material will be cut during the post-processing of the part when the parts are separated from the baseplate.

Then, the automatic fixing of the part analyses the possible mesh errors existing and informs the user if overlapping triangles have been detected. The software offers an option

which tries to reconstruct all the overlapping triangles. If not, it has to be done manually. Finally, the last steps are related to the support generation. Once generated, some of them are unnecessary and can be removed. In order to reduce the amount of material used, the perforation parameters are modified adding bigger holes on the support walls.

The slicing of the part is the final step of the process. It updates the part into a document format (CLI format) that converts it into layers for the printing machine. In this new file supports are also included.

The other software for printing preparation is EP Hatch and it is the last step before printing. It reads the sliced files and rewrites them in a way that the machine can understand and print. The following flow chart (Figure 19) shows how this simple process has to be carried out.

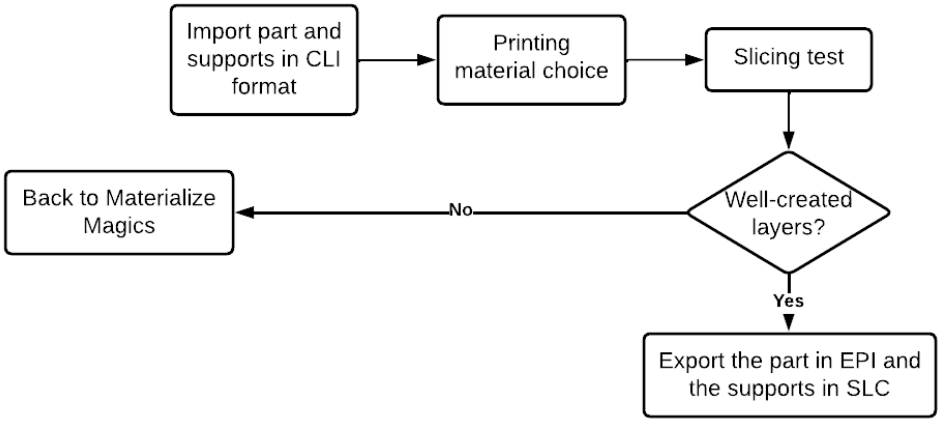

Figure 19. Printing preparation workflow with EP Hatch. (Author's own).

First, the Materialise Magics file is imported to the software. Then, the material of the printing has to be chosen and a rapid check of the layers created during the slicing process. If something is not as it should, the lines representing each layer will not be parallel to each other. Finally, this software generates two different files, one for the part in Encapsulated PostScript Interchange (EPI) format and another one for the support in Stereolithography Contour (SLC) format. Those two files are the ones introduced to the printer.

4 Stress analysis

This section analyses all loads applied to the bicycle frame. The main objective is finding the internal forces existing to design parts capable of withstanding the loads without

breaking. For this reason, it is needed to determine the value of the loads, where they are being applied and at what inclination they should be placed, to calculate the reactions on the bearing points. This will allow all internal forces to be calculated using the Analytical Stiffness Method for structural design.

As the main objective of this project is not to focus on the mathematical resolution process of the internal forces, the programme Barras V-2.00 Beta 14 has been used for this resolution. It was created for academic purposes by Francisco Javier Bradineras, professor specialising in the subject of Mechanics of Continuous Media and Theory of Structures at the University the Lleida.

4.1 Loads and reactions

To calculate the reactions generated at the supports of the bicycle, the parameters regarding the generic bicycle geometry have to be taken into account, which are the length of the tubes and the angle between them.

Table 2. Bike frame measurements

Distances	Angles
$l_1 = 600\ mm$	$\alpha = 36°$
$l_2 = 725\ mm$	$\beta = 88°$
$l_3 = 430\ mm$	$\gamma = 56°$
$l_4 = 465\ mm$	$\varphi = 58°$
$l_5 = 435\ mm$	$\lambda = 65°$
$x_1 = 591\ mm$	$\theta = 57°$
$x_2 = 924.85\ mm$	

(Author's own).

The measurement of the length of the tubes and the angles was taken from the original frame as a reference (Table 2), but they are slightly modified to fulfil the design needs.

The x_1 and x_2 measurements were taken from a sketch of the frame, done in CREO software.

For the analysis in Barras software, the structure is simplified as a 2D structure, not considering the two other bars that exist between the joints 2-4 and 3-4.

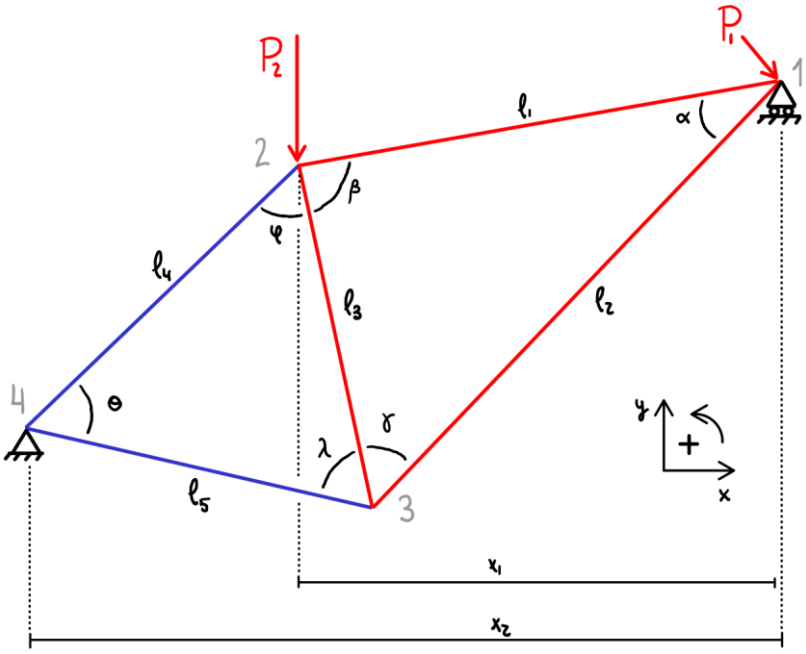

Figure 20. Graphic representation of the frame with applied loads and bearing points. (Author's own).

In Figure 20, there is a colour differentiation between the two types of aluminium tubes used. The red ones represent the tubes with a diameter of $30\ mm$ and wall thickness of $3\ mm$, while the blue ones are the diameter $16\ mm$ tubes with a wall thickness of $1.5\ mm$.

Considering the table and the drawing above, the reactions in the supports can be calculated.

They have to be calculated using the three Static Structure Equations:

$$\sum M = 0; \sum F_x = 0; \sum F_y = 0 \tag{1}$$

Since the calculations will be made in the original axis, which are X and Y, the force P_1 has to be decomposed in its vertical and horizontal components:

$$\boldsymbol{P_{1x}} = P_1 \cdot \cos 40 = \mathbf{368\ N}; \quad \boldsymbol{P_{2x}} = P_1 \cdot \sin 40 = \mathbf{309\ N}$$

The first to be calculated will be the summation of momentum in node 1.

$$\sum M_1 = 0 \rightarrow \ P_2 \cdot x_1 - R_{4y} \cdot x_2 = 0 \rightarrow \boldsymbol{R_{4y} = 1227\ N}$$

After the vertical reaction in node 4 is calculated, the sum of all vertical forces can be carried out:

$$\sum F_y = 0 \rightarrow R_{4y} - P_2 - P_{1y} + R_{1y} = 0 \rightarrow \boldsymbol{R_{1y} = 1002\ N}$$

Finally, the reaction of the horizontal axis. As node 1 is mobile in the X-axis, it will not have a reaction associated, so the equation is as follows:

$$\sum F_x = 0 \rightarrow P_{1x} - R_{4x} = 0 \rightarrow \boldsymbol{R_{4x} = 368\ N}$$

4.2 Analysis of deflections and internal forces

Once the reactions are calculated, the calculation of the internal forces of the tubes can begin. This analysis will bring out the deflection suffered by the structure and all the internal forces such as axial force, shear force and bending moment.

To do so a first important parameter is needed, which is the Young Module. The aluminium tubes, according to the supplier, are made out of Aluminium 6060. The Young Module, which Deshayes & Béchou (2016) state that is the parameter that relates the tension applied to the deformation of the material, is $E = 68000\ MPa$.

For structural design, the cross-section of the members used as well as the moment of inertia of the members are also required. These parameters be different for both types of tubes used.

The section and the inertia are calculated by the following formula respectively:

$$S = \pi\ (R^2 - r^2) \qquad (2) \qquad I = \frac{\pi}{2}(R^4 - r^4) \qquad (3)$$

For the Ø30 tubes, these parameters are: $S = 255\ mm^2$ and $I = 46950\ mm^4$.

For the Ø16 tubes, the parameters are: $S = 68\ mm^2$ and $I = 3630\ mm^4$.

Once these parameters have been calculated, they are entered into the Barras program to calculate their internal forces, deflections and the corresponding graphs, as demonstrates Table 3.

Table 3. Bar properties inserted to Barras, Young module (N/mm^2), inertia (mm^4), area (mm^2)

Name of the group	E (M.Young) N/...	I (Inertia) mm⁴	A (Area) mm²	Color
30 bars	68.000	46.950	255	
16 bars	68.000	3.630	68	

(Author's own).

The results obtained once the analysis is run, as far as the calculation of forces and moments is concerned, they are as follows in Table 4

Table 4. Numeric results for Barras' calculation of forces (N) and moments (Nmm)

Bar	Axial 'i' (N)	Shear forces 'i' (N)	Bending moments 'i...	Axial 'j' (N)	Shear forces 'j' (N)	Bending moments 'j...
[1-2]	-586,482	6,931	1.009,522	-586,482	6,931	-3.149,032
[1-3]	1.285,492	0,748	-1.009,522	1.285,492	0,748	-1.551,809
[2-3]	-1.223,416	-7,123	-2.198,724	-1.223,416	-7,123	866,113
[2-4]	-1.175,241	-2,281	-950,308	-1.175,241	-2,281	110,315
[3-4]	1.180,825	-1,323	-685,696	1.180,825	-1,323	-110,315

(Author's own).

A better option to figure out the numbers obtained is representing the previous results into graphics. The figure below (Figure 21) represents a force diagram for the axial forces.

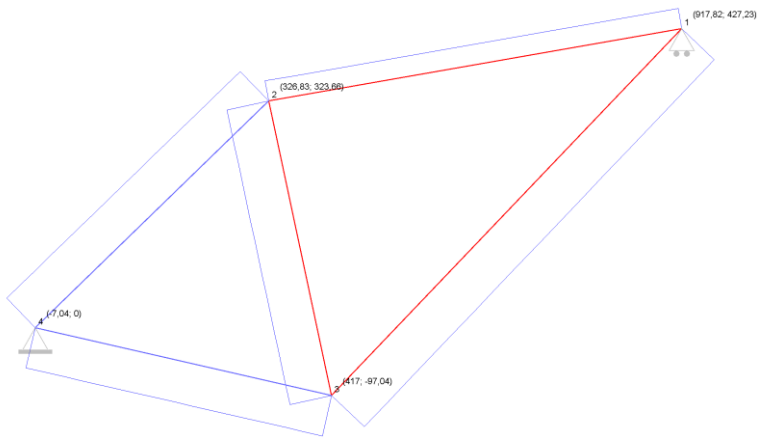

Figure 21. Axial forces diagram of the frame scaling 5 times the actual value. (Author's own).

The figure below (Figure 22) shows two different diagrams, for shear forces and bending moments on the structure. Comparing the axial forces to these others with the same scaling for all the diagrams is evidently the insignificance of the latter two. This will allow us to disregard the shear force and bending moment when optimising the parts, considering only the axial force.

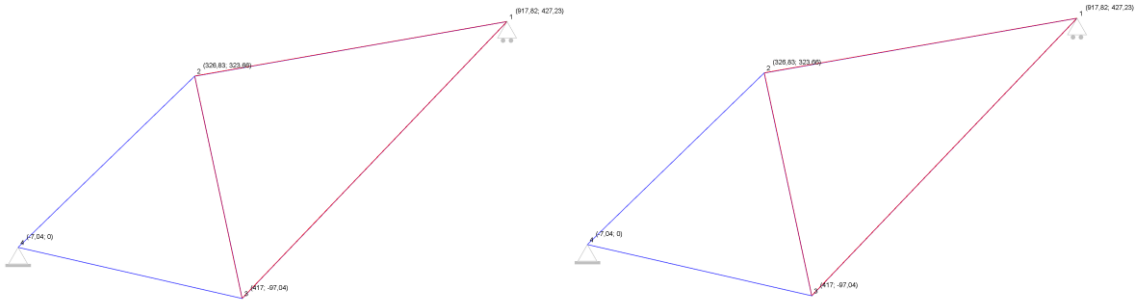

Figure 22. Shear forces and bending moment, respectively, scaling 5 the actual value. (Author's own).

The Barras software automatically generates another diagram which is not essential but helps to understand the behaviour of the frame under effect of the forces. This diagram is generated with the values in Table 5. There, it can be seen the displacement and rotation of every joint of the frame.

Table 5. Numeric results for the displacements ($\boldsymbol{mm}$) and rotation ($\boldsymbol{rad}$) of the joints.

Joint	Displac.'x'(mm)	Displac.'y'(m...	Rotation (rad)
1	-0,021	0	0,00039
2	0,036	-0,207	0,00019
3	0,076	-0,167	0,00010
4	0	0	-0,00060

(Author's own).

The figure below (Figure 23) shows these values in bigger scale to figure it out. Joints 1 and 4 do not experience major changes as they are support points of the structure. It can also be seen that with this oversized model some of the bars are slightly deformed by the loads.

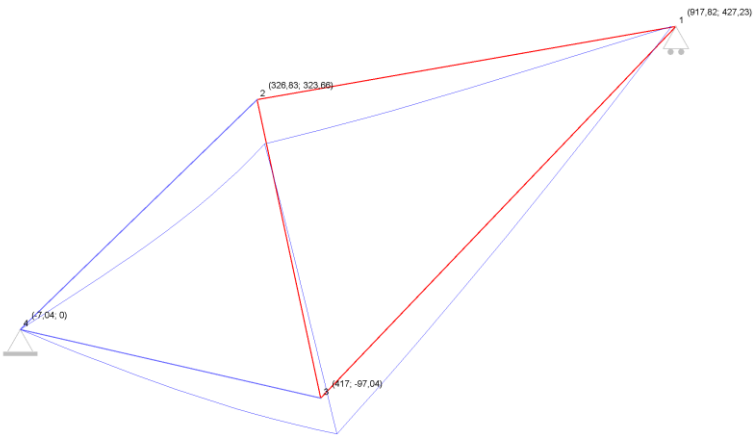

Figure 23. Deflection of the frame scaled 300 times larger. (Author's own).

This stress analysis is crucial for the future of the project. The values and diagrams obtained ensure the future resistance of the designed parts and a higher success rate of the project.

5 Assembly type analysis

An important aspect of this project that needs to be analysed is the assembly method of the joints with the aluminium tubes that will form the frame of the bicycle.

The most used way of joining metals is by welding or using a special type of glue. A requirement of the project stakeholders is for the joints to be mechanical and not use any welding. The joint also has to be as lightweight as possible and good-looking. For this reason, it has been decided that the printed part will be the male part of the joint and the aluminium tube the female part. In this way, printing larger pieces can be avoided, which make the process cheaper, while reducing the total weight of the piece.

The following sections show the options that were considered and their pros and cons.

5.1 Design option one

The sketch presented below (Figure 24) tries to simulate the first idea developed. This joint operates by friction between the male and the female.

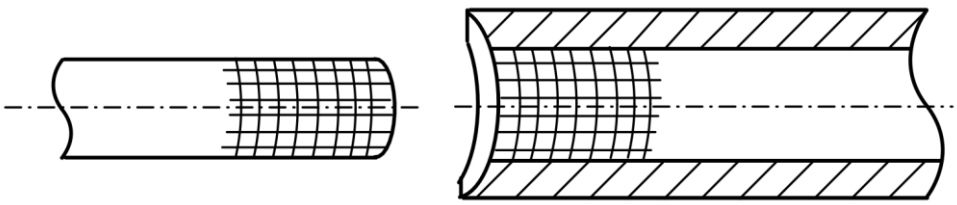

Figure 24. Sketch of the first option. (Author's own).

The section of the aluminium tube shows a series of grooves, also present on the outside of the male, which increase the friction between the two. If necessary, some type of glue should be used to fix them, although it is not a desirable scenario.

5.2 Design option two

The Figure 25 shows the sketch of another type of connection. The scheme represents a section of the tube and the part already united.

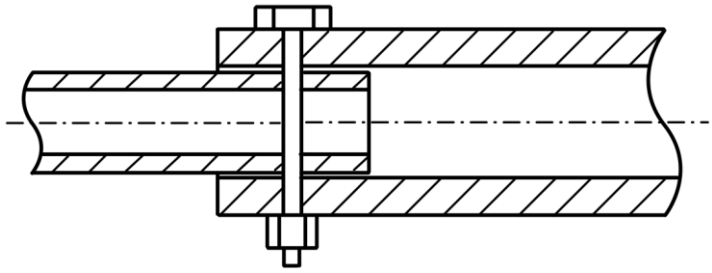

Figure 25. Sketch of the second option. (Author's own).

The union of the two parts is carried out by means of a bolt locked with a nut. The joint remains locked without any level of freedom as it cannot move nor rotate.

5.3 Design option three

The third option investigates another way to fix the tubes with the part. Figure 26 presents the sketch of it.

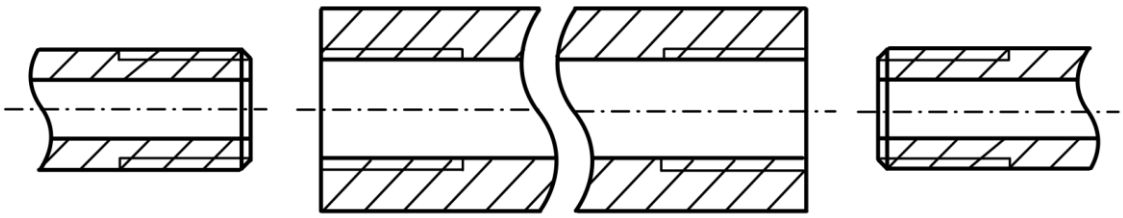

Figure 26. Sketch of the third option. (Author's own).

This system tries to connect the parts with the tubes by means of threads. The parts have the male thread while the tubes are the female. The important fact to consider is the direction of the threads in order to be able to assembly the frame. For this reason, a detailed study would be carried out to find which would be right-hand or left-hand thread. In other words, when the tube rotates, the two parts are being threaded at both ends of it.

5.4 Design option four

The Figure 27 represents another way to fix the joints of the frame. This one is more complex to try to make it understandable with only the sketch.

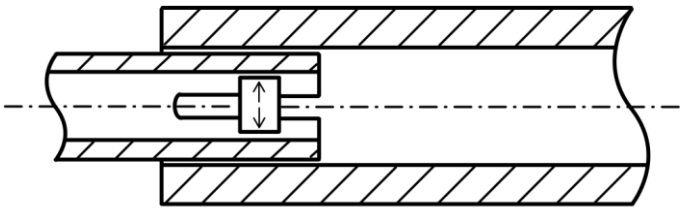

Figure 27. Sketch of the fourth option. (Author's own).

The basic operation of this type of connection needs some kind of mechanism to press the inner tube into the outer tube. This will increment the friction between the printed part and the tube fixing the joint. As it is not known whether the mechanism exists, the case should be designed and implemented in a way that fits the requirements of the union.

5.5 Design option five

The following sketch (Figure 28) represents another way to fix the joint. The male tube has a partial section in order to make it more understandable.

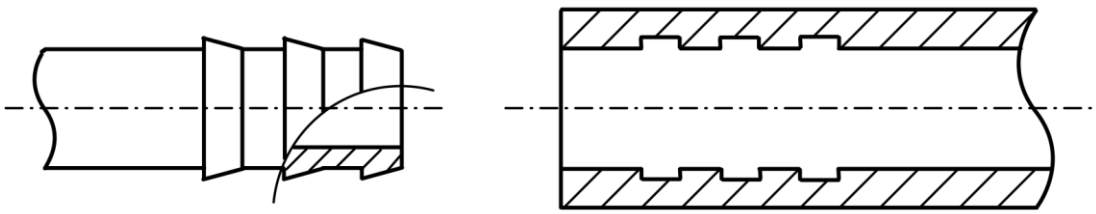

Figure 28. Sketch of the fifth option. (Author's own).

This connection works in a simple way. The male tube has to be introduced in the female tube. The protrusions on the inner tube fit into the holes on the outer tube (grooves), preventing the male from coming back out.

5.6 Design option six

The Figure 29 represents a similar way of connection to the previous one but with important modifications.

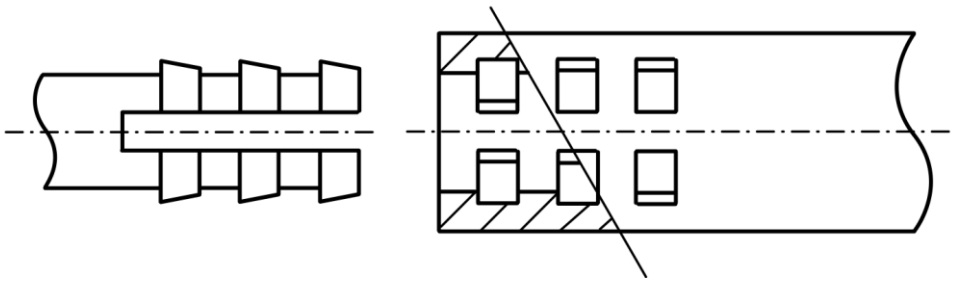

Figure 29. Sketch of the sixth option. (Author's own).

In this case the holes go all the way through the female tube and four of them in each of the three levels. The male tube has four sticks which fit in the holes with the same protrusions as in the previous option.

This option has the same mechanism as the one before, but with the difference of not having the lathe limitations for small diameter tubes, since the holes could be always done, no matter the diameter of the tube.

5.7 Design option seven

Finally, Figure 30 shows the sketch of the last option that has been engineered. The system differs from the others because the fixing mechanism is on the outside side of the female tube.

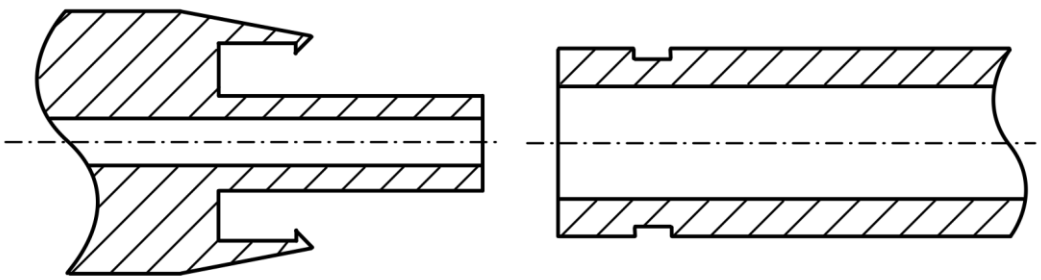

Figure 30. Sketch of the seventh option. (Author's own).

The outer tube has a groove where the small hook on the male tube part is fixed. The part that gives the strength to the joint is the male tube which is inserted inside the female tube. This allows it to withstand the loads and the moments.

6 3D design and optimisation of the parts

This section will discuss the design, optimisation, and printing preparation of the 3D components, also the workflow followed at each software and images of this process.

In order to have a reference on the geometry of the bicycle, the angles were used and measurements shown in section *3.1 Original frame and bicycle components*. From these measurements, the shape of the parts to be optimised was considered to make a first sketch.

The following sections show for each component the workflow that has been undergone.

6.1 Right dropout

The right dropout has been the first component to be manufactured. It has had several design modifications, including its general morphology and small details, to improve the impression.

The frame of the original bike was taken as a reference, to take measurements of distances, angles and circumference diameters. In the following figure (Figure 31), it can be seen the original shape.

Figure 31. Original right dropout. (Author's own).

Taking into account the previous geometry, a first model was designed, which tried to have a similar geometry, but with some modifications to give it a different approach and be more original.

Figure 32. Right dropout first design. (Author's own).

This second design (Figure 32) has a good appearance and was considered good until the left dropout was designed. The geometry of the dropout had to be changed slightly to avoid problems with the bicycle's general geometry. Therefore, with the corresponding modifications, the following design was obtained (Figure 33).

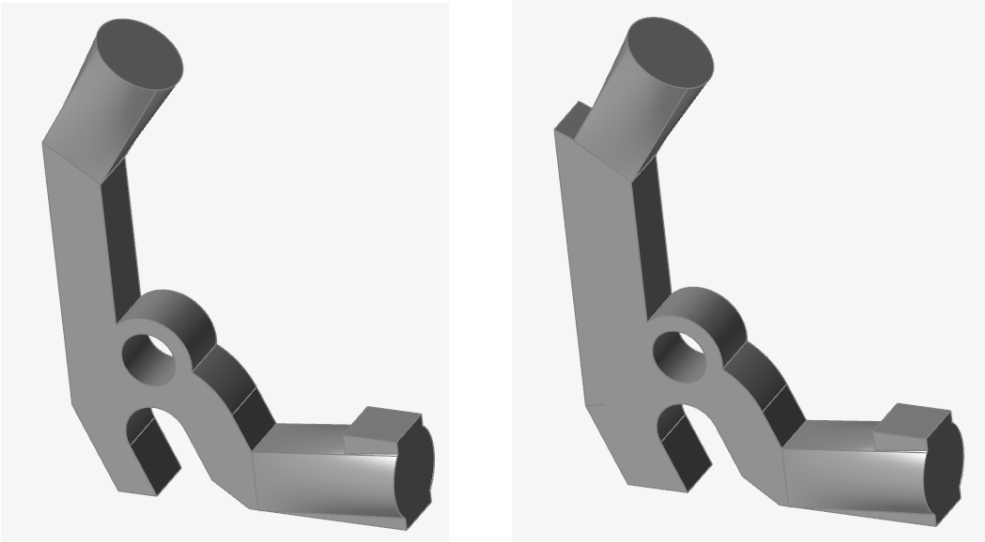

Figure 33. Right dropout second design and modification. (Author's own).

The modifications made were to reduce the hole in which the wheel axle is fitted and increase the length of the vertical part. In the next section, *6.2 Left dropout*, there will be further discussion about the last-mentioned distance.

As this design is quite similar to the last one and is aesthetically appealing, was also considered good. It was decided to put more material in the exterior area to make it able to withstand the stresses to which the part will be subjected. So, the piece has the same

shape as the previous version but with reinforcement in that area. In Figure 33 can be seen how the two pieces look compared to each other.

When it was believed that the design was completely closed and finished, and that this would be the final CAD shape of the right dropout, it was realized that the component had to have a notch in a specific place. The notch must have a specific shape to host the part shown below (Figure 34).

Figure 34. Derailleur support. (Author's own).

The figure on the left shows the visible side of the part, while the right side is the hidden side with the notch to be replicated.

As taking measurements of this part is very complicated, several plastic versions had to be printed, until the two important holes (wheel axis and component screw) and the notch shape coincided.

Figure 35. Rapid Prototyping of the notch for the derailleur. (Author's own).

The series of attempts shown above (Figure 35) is a clear example of RP, where small modifications were made to each last design, and were printed until the obtained piece matched the shape of the metallic component.

After having the final shape, it was implemented into the right dropout, obtaining the final design (Figure 36).

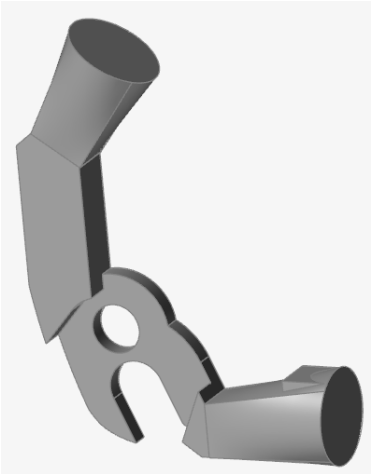

Figure 36. Right dropout third design. (Author's own).

To start the optimisation process, the partitions have been determined. In the case of this component, the partition is the union itself and the fixing area of the dropout with the wheel axis.

Figure 37. Right dropout partitions. (Author's own).

Figure 37 shows the partitions of the right dropout, which are the grey parts. All the other parts will be optimised and the mass reduced.

For this project, it has been determined that the easiest way to make partitions is to use only small rings for optimisation, and after optimising, import the joints. As the Altair program is very intuitive, it allows the creation of partitions in areas where no parts were imported.

Once the mesh of the component has been unified, the forces must be applied to it and its supports must be determined. The following image shows where they have been placed.

Lastly, after selecting the optimisation direction with the Overhang tool and adding the mass reduction and wall thickness parameters, the final optimised design with and without unions is as follows (Figure 38).

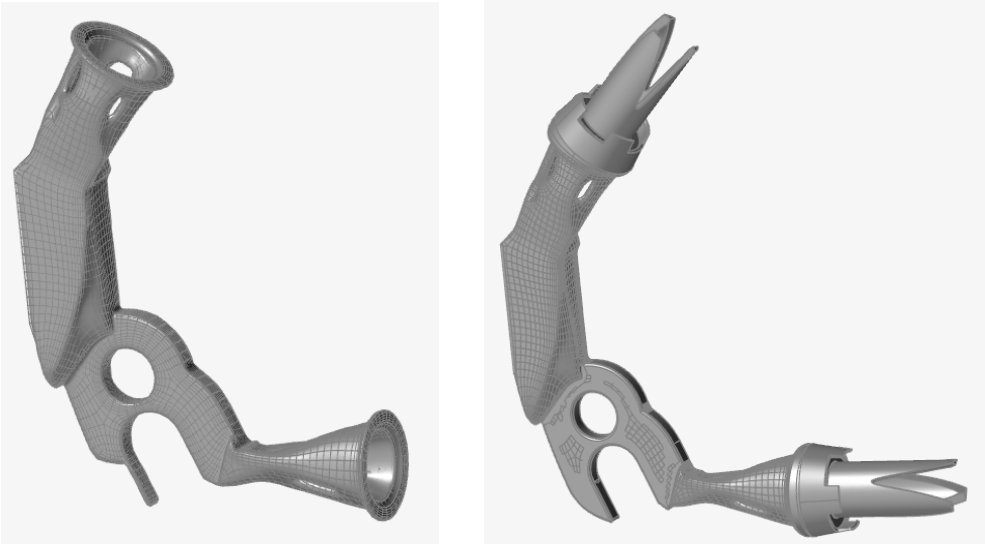

Figure 38. Optimised right dropout with and without unions. (Author's own).

Once the final component is obtained, it has to be imported to the program Materialize Magics to prepare it for printing. By following the already explained workflow, the process undertaken is shown picture by picture.

The first step in Magics is to import the component and add the baseplate to the workspace (Figure 39).

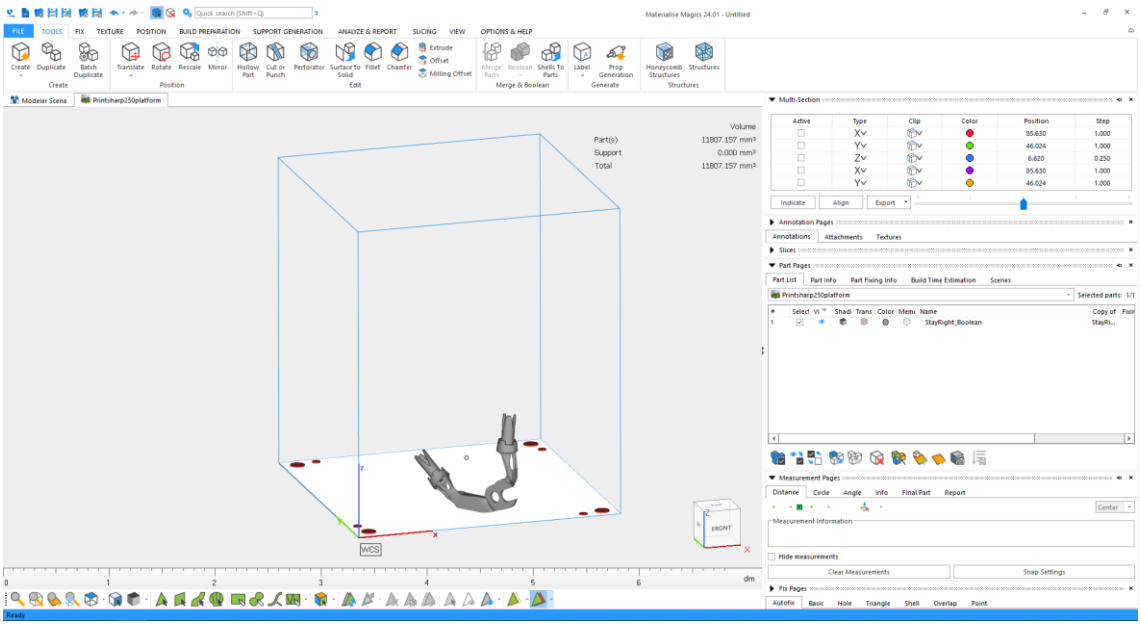

Figure 39. Component in Materialize Magics baseplate. (Author's own).

To fix the mesh errors, the tool Fix Wizard has to be used and the program will automatically fix as many problems as it can.

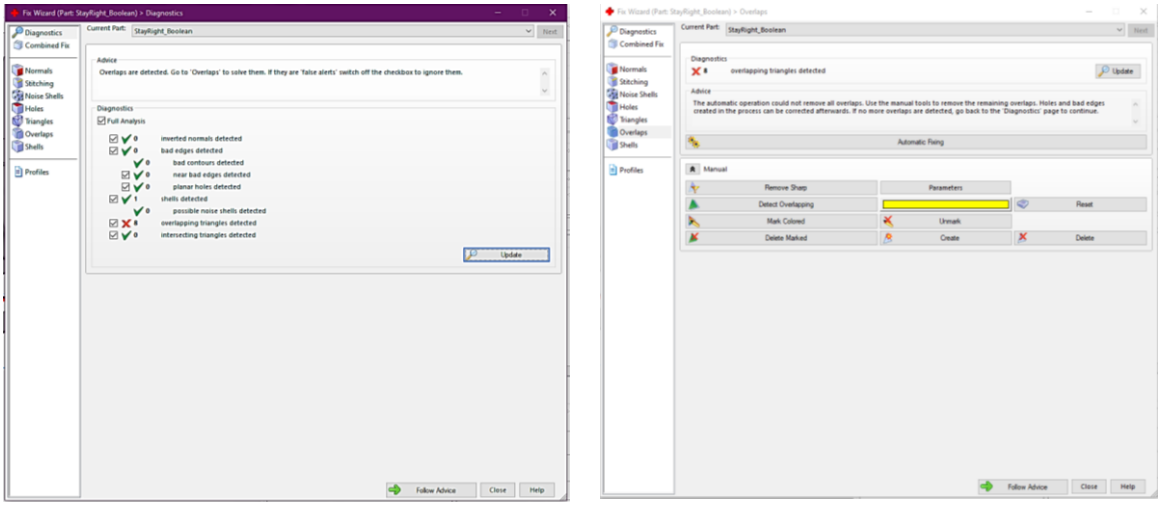

Figure 40. Materialize Magics fix wizard. (Author's own).

Figure 40 show the component's mesh errors, which using the automatic fixing were reduced to 8. Usually, the errors that appear are overlapping triangles and are caused by the Boolean union of two meshes, which are the partitions and the component itself.

All the remaining errors that have not been solved with the Wizard had to be fixed manually.

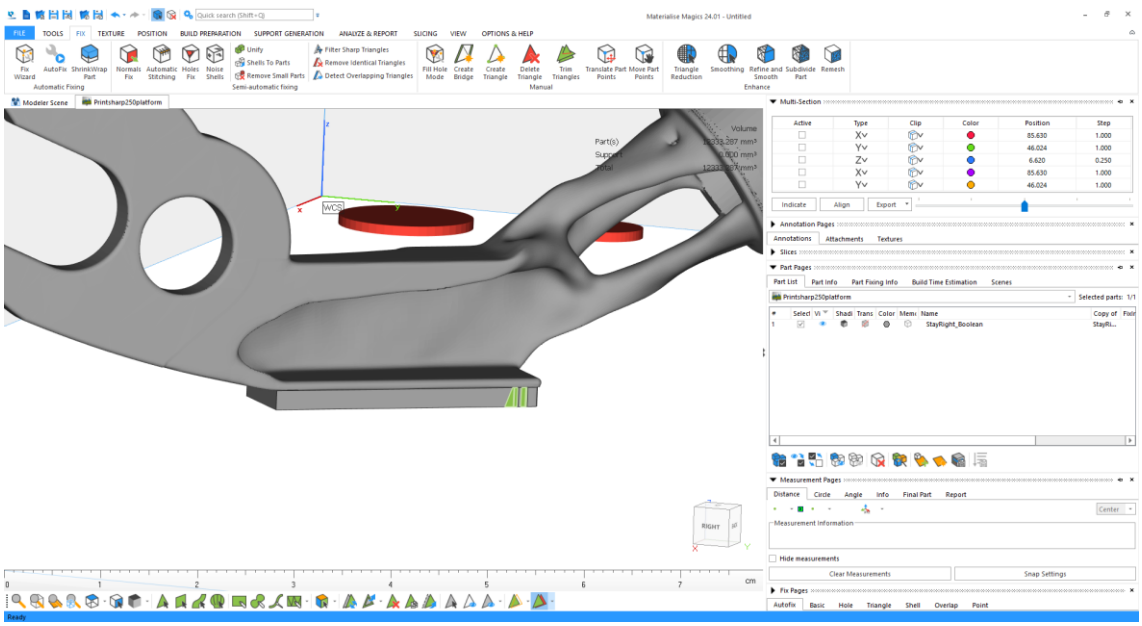

Figure 41. Mesh errors in the right dropout. (Author's own).

The green surface in Figure 41 are the triangles that have to be deleted and created once again. The figure below shows the process followed (Figure 42).

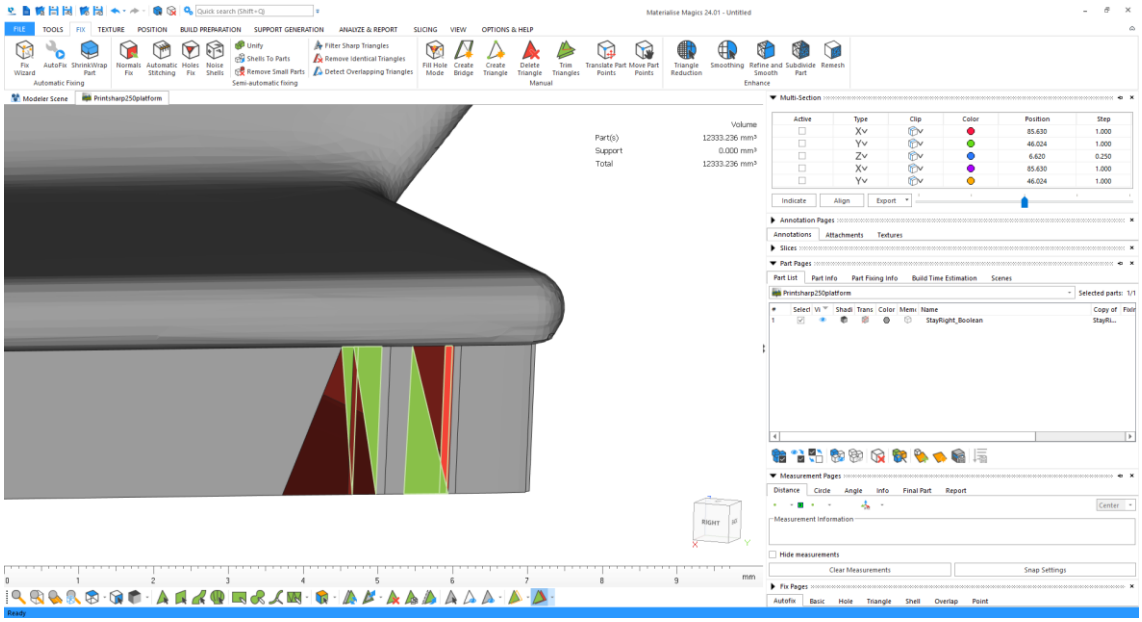

Figure 42. Mesh errors fixing process. (Author's own).

The green coloured triangles are the mesh errors, and the red ones are already deleted. New triangles are drawn on the area of the removed triangles. This process has to be repeated until all the errors are eliminated, or they have a very low value.

The supports can be solid or have perforations. To use less material and make the printing process faster, perforations have been put in all the supports. The perforation parameters used are the following (Figure 43).

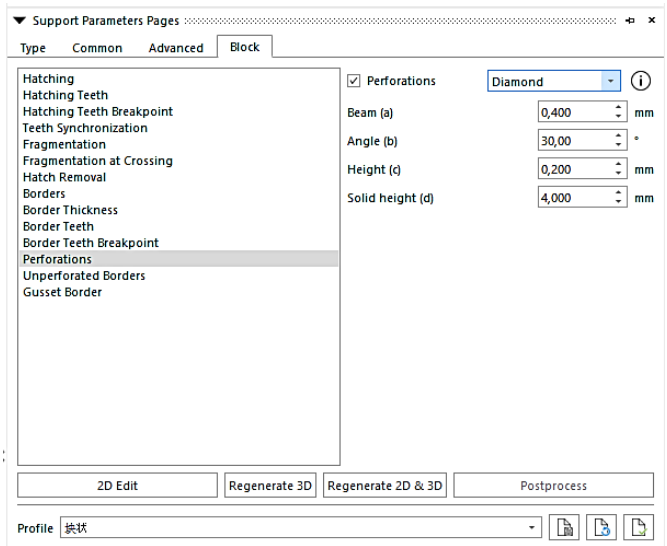

Figure 43. Support perforation parameters. (Author's own).

As regards the generated supports (Figure 44), they can all be checked to see which are really necessary and which, because of the component's geometry and taking into account the overhang, can be deleted.

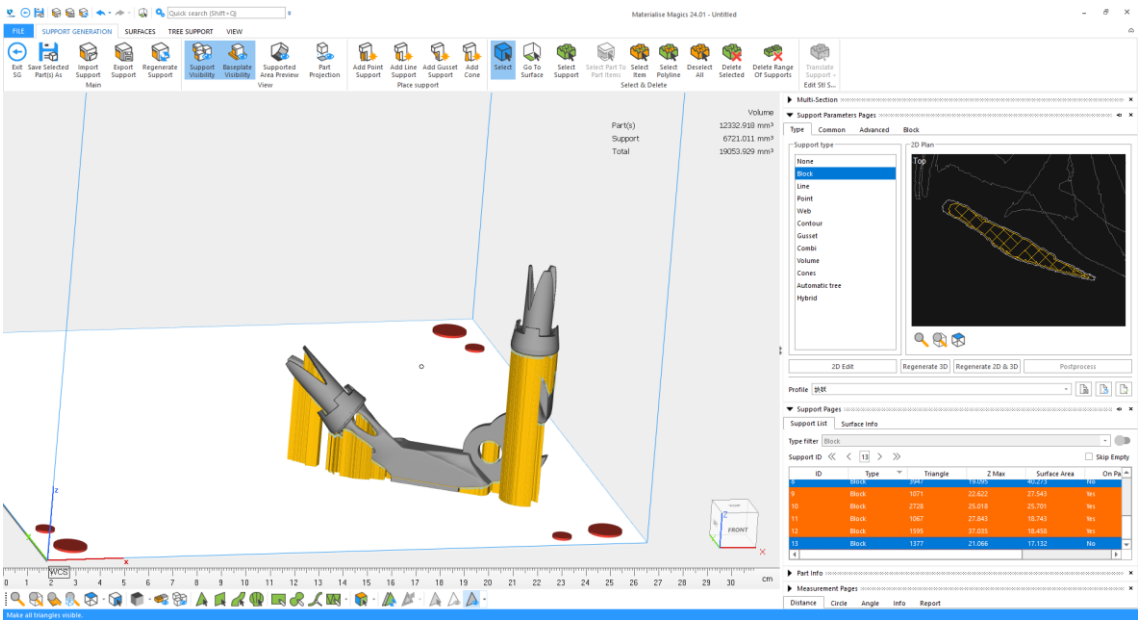

Figure 44. Generated support for right dropout. (Author's own).

With the support generated, the component has to be sliced into layers of 0.03mm. When slicing, the program generates two different files, one for the component and another for the supports.

The two files are then imported into the program EP Hatch. This program reads the imported files and rewrites them in a language understandable for the machine. These two files are the ones that will be used in the machine to print the component.

After having the files prepared for this design, a problem arose during the printing that forced it to the stop and modify the design of a part of the component to try to avoid supports. The applied modification is shown in Figure 45.

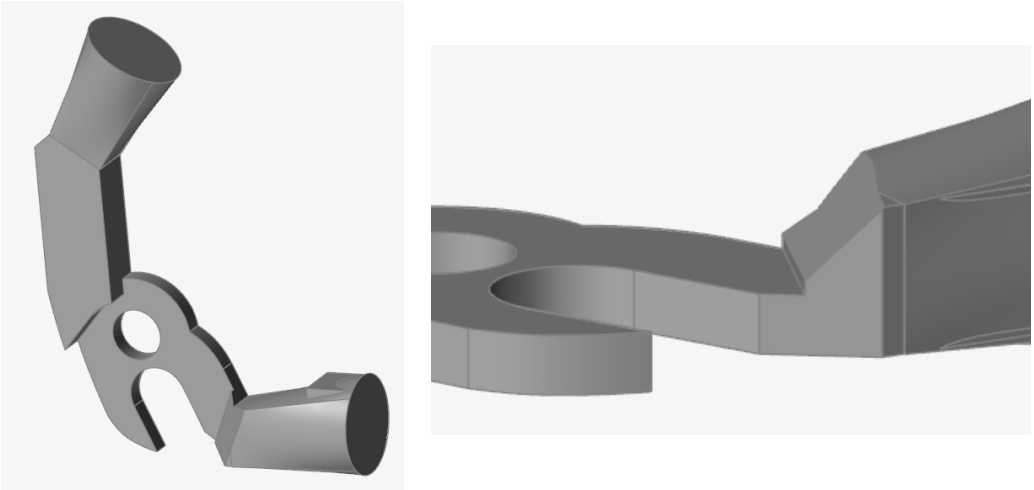

Figure 45. Right dropout final modification and close-up. (Author's own).

As can be seen in the close-up image, a 45° chamfer has been done, so there is no overhang in that area. After applying this modification, the final design to be printed is as follows in Figure 46.

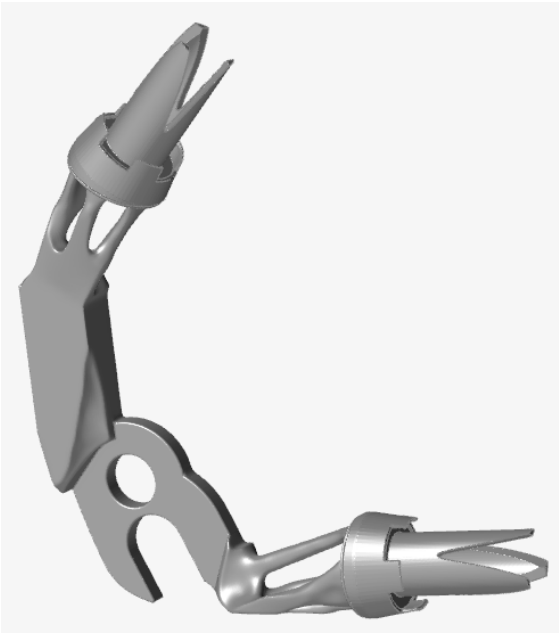

Figure 46. Right dropout final design and optimisation. (Author's own).

With this topology, the support generation is expected to improve. By checking them in Magics, the generated supports have been slightly reduced, but since there is a vertical support right in front of this part it cannot be seen.

Following the same procedure as in the first printing test, both files have to be sliced and then brought to the machine to be printed.

6.2 Left dropout

In contrast to the right, there have not been that many designs for this dropout. The right dropout was a reference design, so achieving the desired shape was easier. Also, the original design of the component was taken into account, which is the one of Figure 47.

Figure 47. Original left dropout. (Author's own).

Having these two reference images and the other dropout already designed, the first design of this part, which is shown below (Figure 48), was simpler and faster to do.

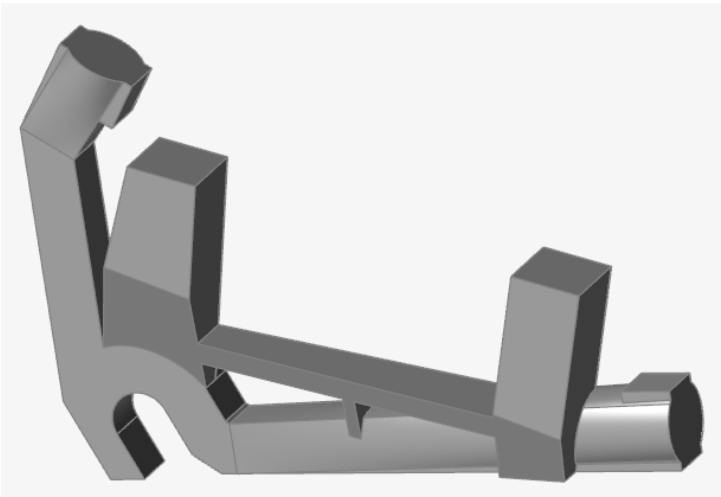

Figure 48. Left dropout first design. (Author's own).

This first design is very similar to the right dropout, as the left dropout needed to have the support for the disk brake, the height of the upper joint will have to increase. The right dropout was modified to have the same height to have symmetry in the rear part of the bicycle's geometry. The wheel axle attachment point height is also different so, for the same reason as above, the right dropout was modified.

For the second design of this component (Figure 49), the thickness of some walls was increased to better withstand the applied loads. Also, two holes were put where the actual

holes should go to attach the disk brake. These holes are of a smaller diameter than the bolt diameter so that the thread can be machined.

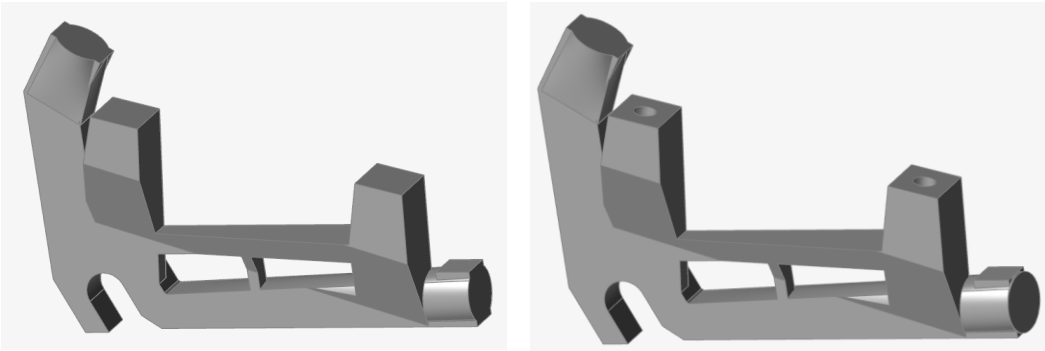

Figure 49. Left dropout second design and modification. (Author's own).

The right design was optimised, as it was believed to be the final design. The optimisation process followed is the same as that for the right dropout, so the partitions and loads had to be determined (Figure 50).

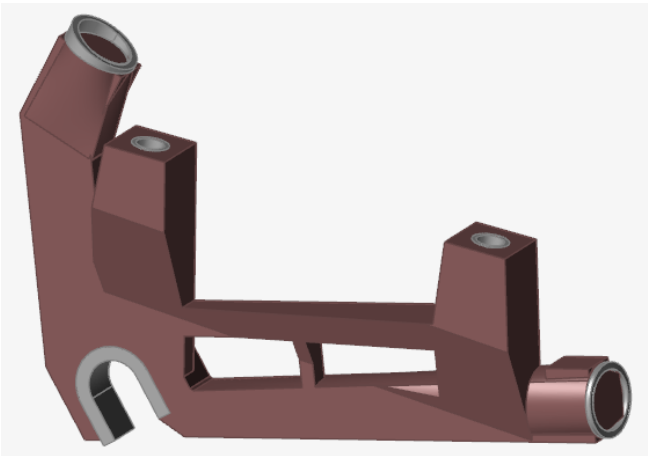

Figure 50. Left dropout partitions. (Author's own).

Once the loads and supports are determined and applied, the optimisation is carried out. The following figure shows the configuration obtained (Figure 51).

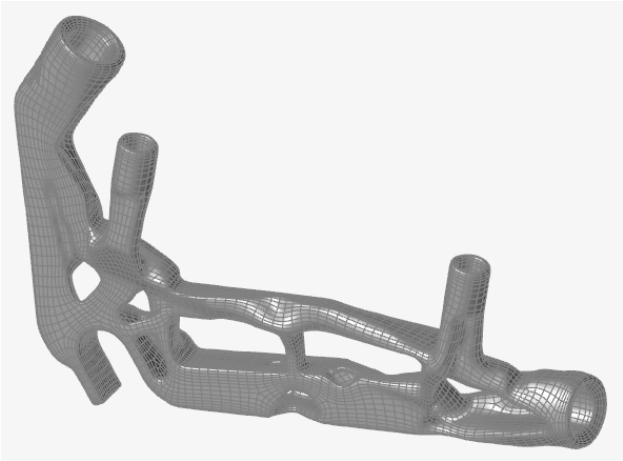

Figure 51. Left dropout first optimisation. (Author's own).

This component was printed in plastic to check if the brake disk supports were in the correct place (see section *7.3 Left dropout*), and also to see how the component would look physically and their dimensions.

It was determined that the support was too high, and the inclination was too low. To make the holes coincide, a new design had to be made (Figure 52).

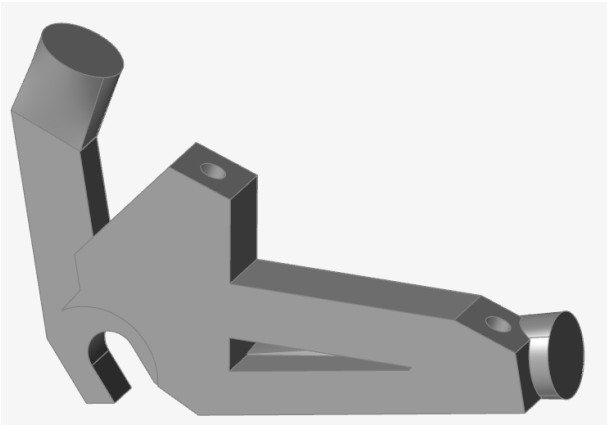

Figure 52. Left dropout final design. (Author's own).

This was the last design, where more material was left for Altair to be optimised. Also, the position of the holes can be noticed much closer to the position of the original frame and closer to the bottom part of the component.

After considering this design as the final, it was optimised following the same process as before. The same partitions and forces were used and the obtained result with the joints already assembled is the following (Figure 53).

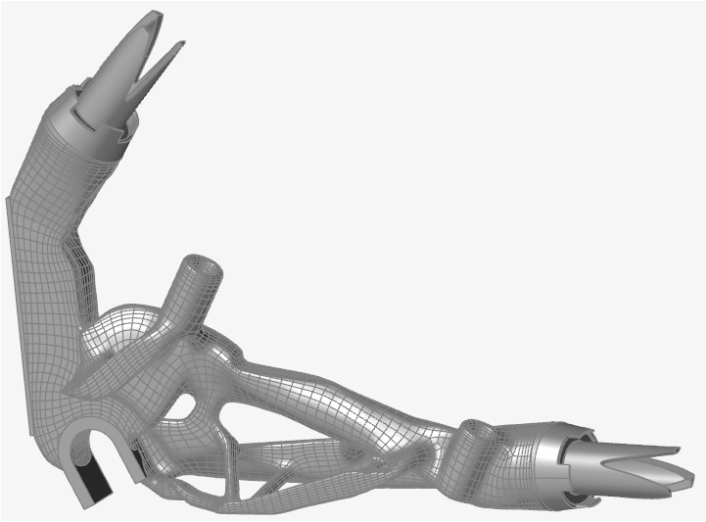

Figure 53. Left dropout final optimisation. (Author's own).

The geometry of the final component is quite similar to the one obtained before with some minor differences in the bottom geometry of the component.

After having the final optimised design, it was imported to Materialize Magics to prepare it for printing. Following the same process as for the right dropout, the component has to be imported into the baseplate. As both dropouts were expected to be printed at the same time, they used the same workspace (Figure 54).

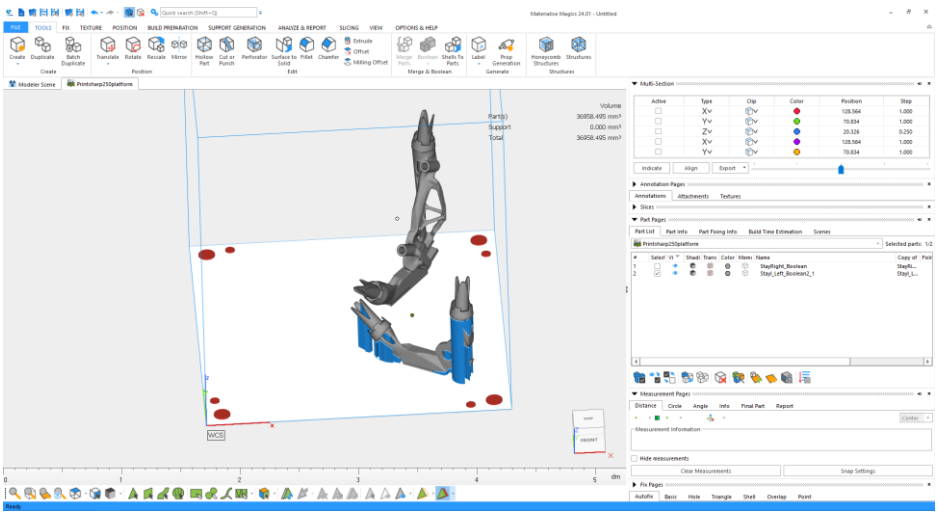

Figure 54. Left dropout Materialize Magics baseplate. (Author's own).

Once the component is imported, the mesh errors have to be checked. For this component, the obtained errors were 6.

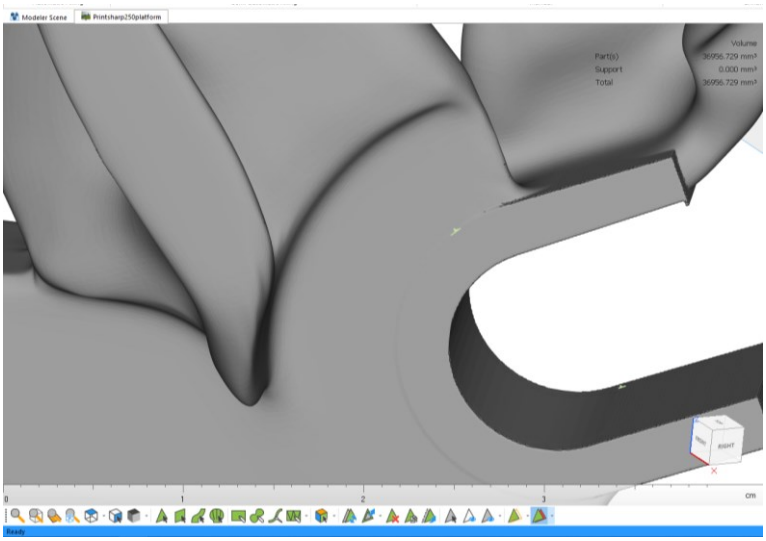

Figure 55. Mesh errors of the left dropout. (Author's own).

As can be seen in Figure 55, they are very small areas where a Boolean union has been made. To remove them, is followed the same process as for the right dropout.

As regards support generation (Figure 56), at first sight, this component seems to require a big amount of support, but as it was designed considering the overhang and they were highly reduced. The perforation parameters for the supports are the same as for the right dropout.

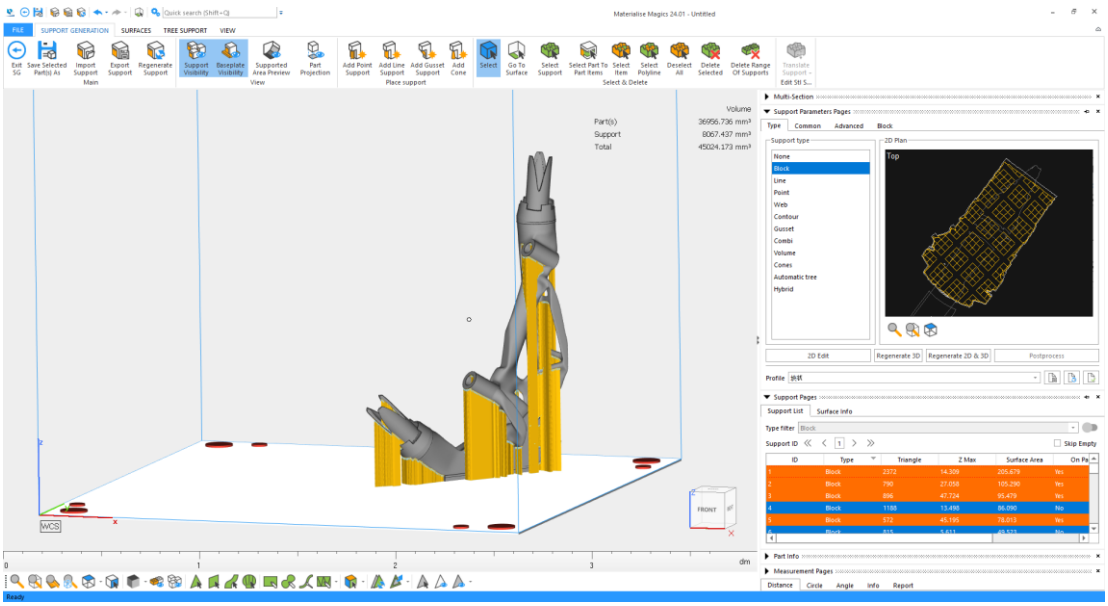

Figure 56. Support generation for the left dropout. (Author's own).

Most of the supports of the picture are very thin and easy to remove, and others meet the overhang, but the programme places them on anyway. That is why a few supports have been removed, which can be seen in the picture below (Figure 57).

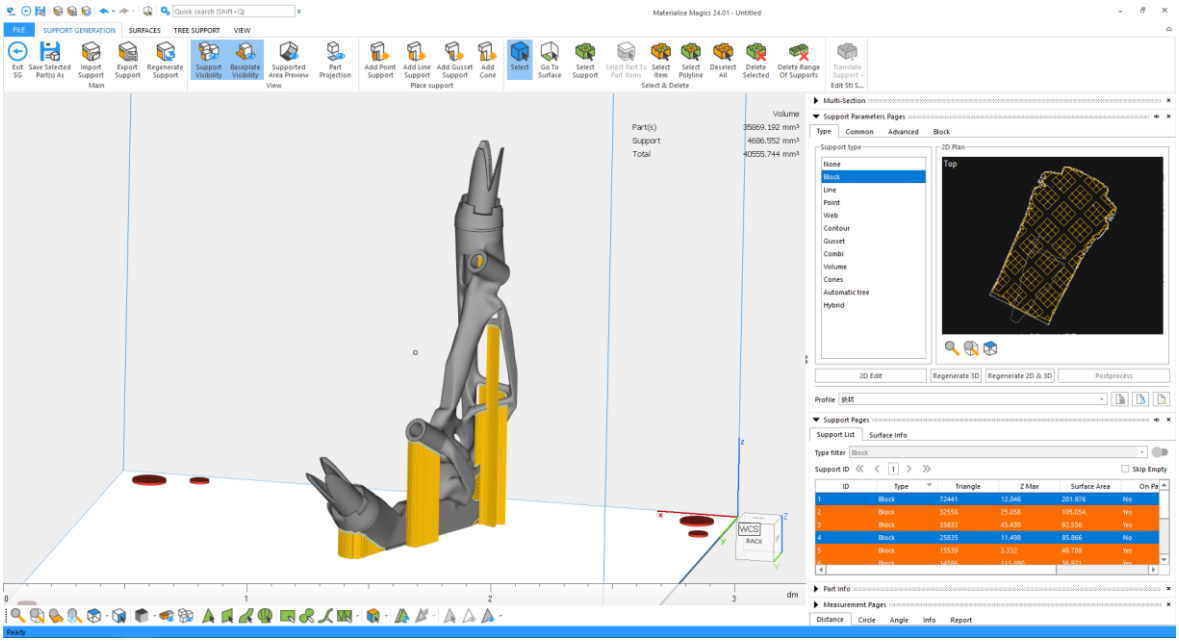

Figure 57. New support generation for the left dropout. (Author's own).

Because of one of the unions in this part, there was support generated inside the tube as can be seen in the following component section (Figure 58).

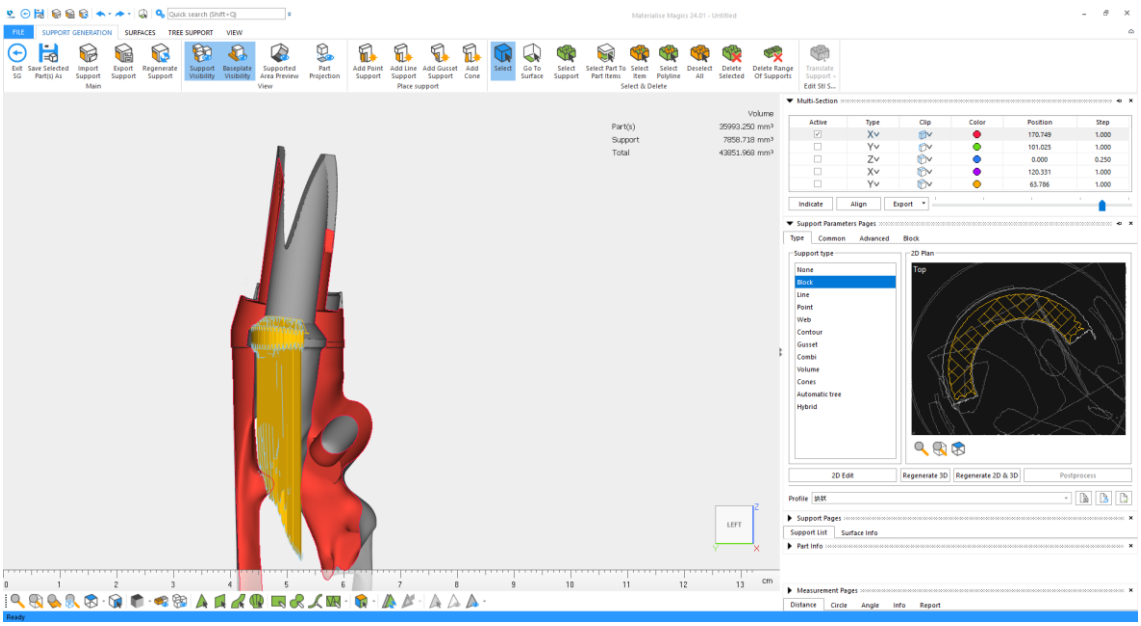

Figure 58. Internal support to fix left dropout. (Author's own).

It is not desirable to have supports inside the components because of the difficulties involved in removing them. The 3D design was modified to have an inclination of more than 45° so that no supports are required.

Finally, the stays were sliced into 0.03mm layers and exported to the program EP Hatch.

6.3 Head tube

This is probably the simplest component to design since it is a plain tube with two connections to the tubes that come from the frame (Figure 59). An internal thickness must be considered at a determined height because it is the part where the bearings are allocated and cannot be eliminated.

Figure 59. Original head tube. (Author's own).

The first design proposed ended up being the definitive shape for this component. Some modifications on one side were also made to modify the topology optimisation and get a better result. The designs are shown below (Figure 60).

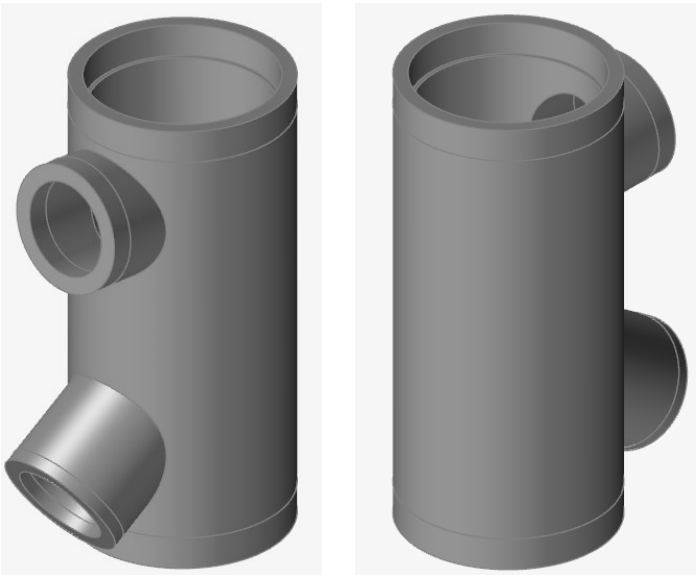

Figure 60. Head tube first design. (Author's own).

Notice the back of the component is completely flat, this is the side that has been modified with holes to obtain better optimisation results. The next figure shows the two modifications made (Figure 61).

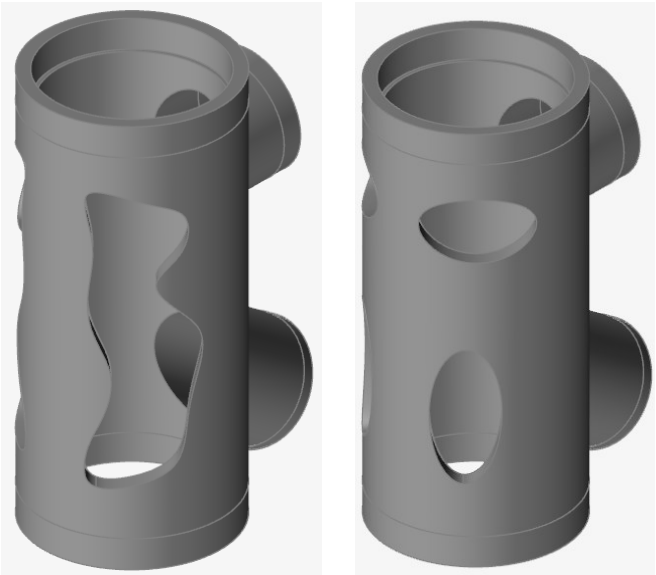

Figure 61. Head tube back modifications (Left: first design. Right: Second design). (Author's own).

These holes were expected to modify the optimisation obtained, but no major differences were obtained when testing the differences between designs.

The partitions used for this component are quite important, because of the reason stated before, the bearings needed to be allocated in a specific place, and without them the handlebars may not move smoothly. The following figure shows the partitions used (Figure 62).

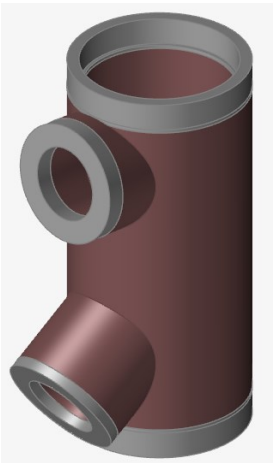

Figure 62. Head Tube partitions. (Author's own).

It can be noticed the smaller inner ring of the head tube where the bearings are placed. The rest of the component that has a dark-red colour will be optimised and its material reduced.

Below, in Figure 63, can be found the comparison between the optimisation made for all the designs stated before.

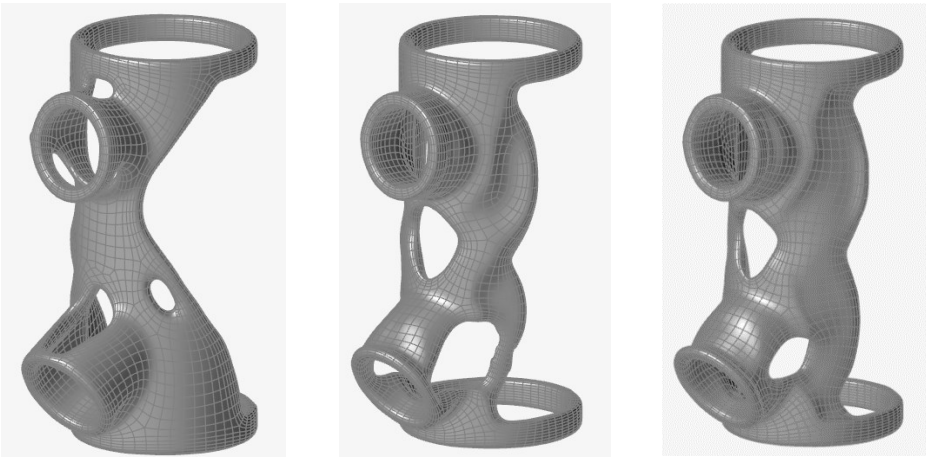

Figure 63. Topology optimisation of the head tube (From left to right; first design - first modification - second modification). (Author's own).

Although there are some small differences in the design obtained, all three optimisations have in common the open back part. It was determined that if it was desired to have a design in the back of the component it would have to be made manually.

As changing the shape of the component, did not affect much in its optimisation, the two modifications were discarded, and the first option was choosen.

Concerning the back design two options were considered. The first one was to make an organic design, which means that it looks at nature's shape to obtain a geometry that does not look artificial. The second option was to attach a lattice part to the main's component hole.

As regards the organic option the obtained shape was not as desired, below can be seen the design made (Figure 64).

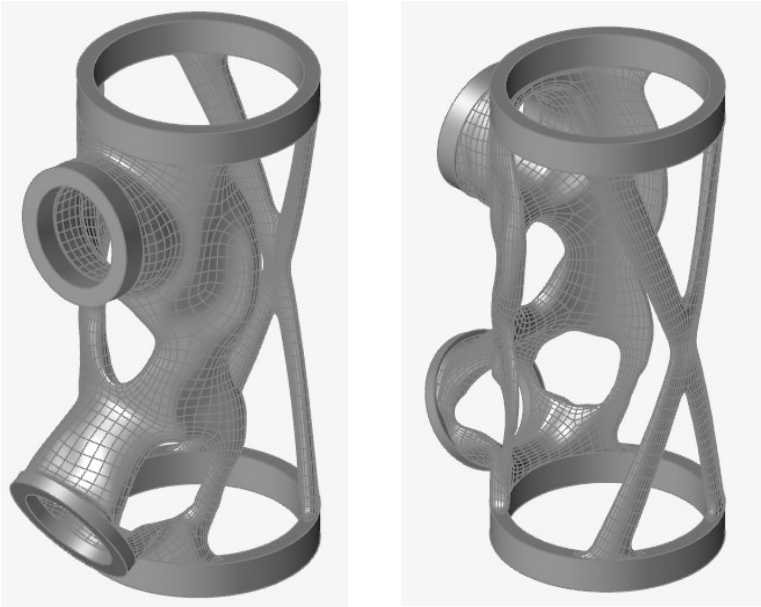

Figure 64. Head tube with back nerves. (Author's own).

After some attempts to make an organic design, this option was discarded because of its complexity and lattices were chosen instead. The lattices would fill the whole back hole with a triangle pattern. They are expected to give more support to the component and also reduce its weight. Below, in Figure 65, can be seen the component with the lattices attached.

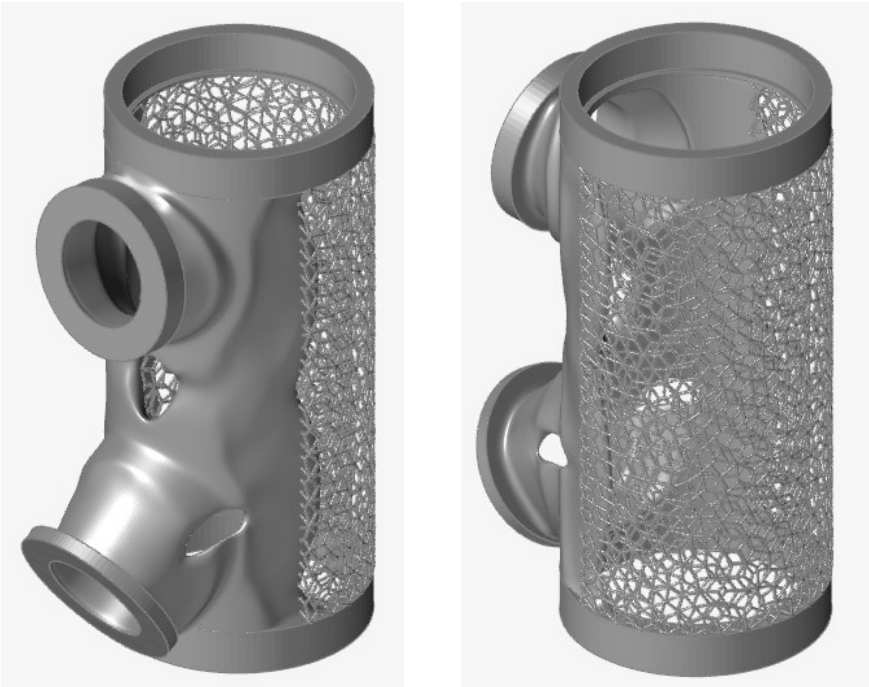

Figure 65. Head tube with lattices structure. (Author's own).

Comparing both designs, the lattice design is visually more attractive, but would provide less stability to the structure than the back nerves would. This is why the option of nerves was taken out again, but this time with lattices inside them to reduce mass.

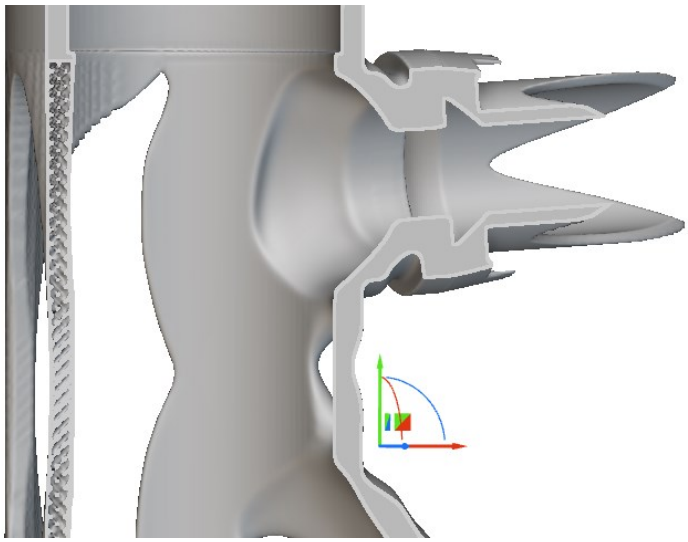

Figure 66. Back reinforcements with embedded lattices. (Author's own).

The figure above shows the last option of design considered (Figure 66). It represents a section of the Head Tube, where the back embedded lattices can be seen. They have been created with the operation "Merge Shell and Infill" which has already been discussed in section [3.5 Lattice Structure Workflow](#).

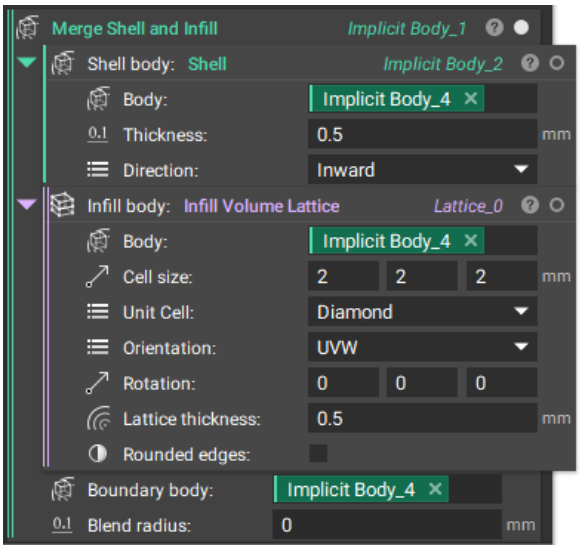

Figure 67. Embedded lattice parameters. (Author's own).

The figure above shows the parameters that have been used for these lattices (Figure 67). It has been selected the *Diamond Unit Cell* because of its self-supporting properties, meaning that there will not be any support during the printing of this component.

Lastly, before the component is prepared for being printed in metal the unions have to be assembled to the component and joined with the Boolean Union operation. After this, the final component is as follows (Figure 68).

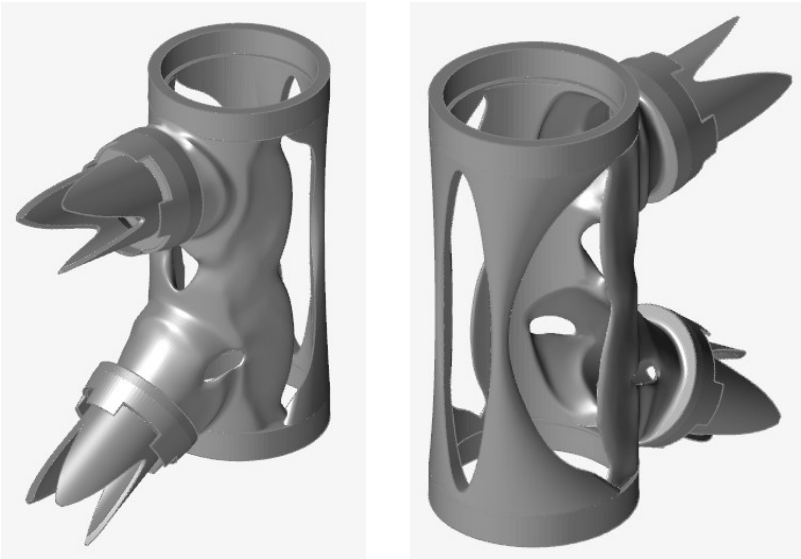

Figure 68. Final head tube with unions. (Author's own).

For the joint tubes, as their diameter changed, the design of the component had to be changed and make it fit with the desired one. The design shown for the head tube has already the diameters changed and can be noticed that is slightly bigger than the ones of the first designs.

Finally, the process followed in Materialize Magics is the same for the other components and it is shown below step by step with pictures.

First of all, import the component into the workspace, place it correctly and in the printing direction and check the mesh errors that it could have (Figure 69).

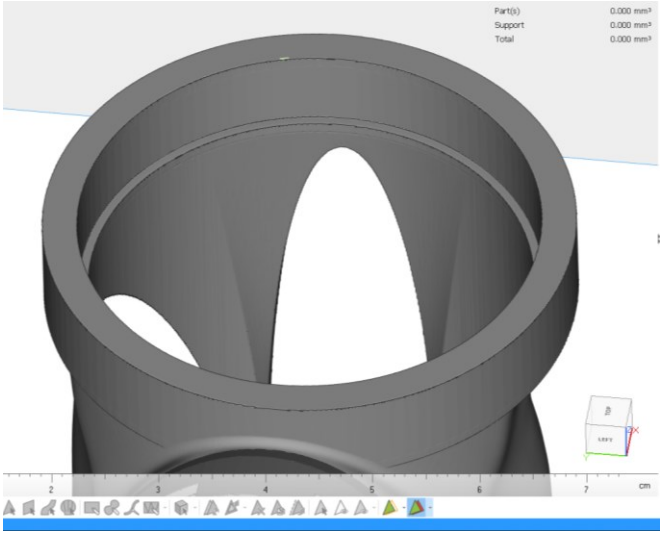

Figure 69. Mesh errors of the head tube. (Author's own).

After all the errors are checked and fixed, the supports have to be generated. It is expected that there will only be support where are the unions because the lattices are self-supporting. The generated supports are shown in Figure 70.

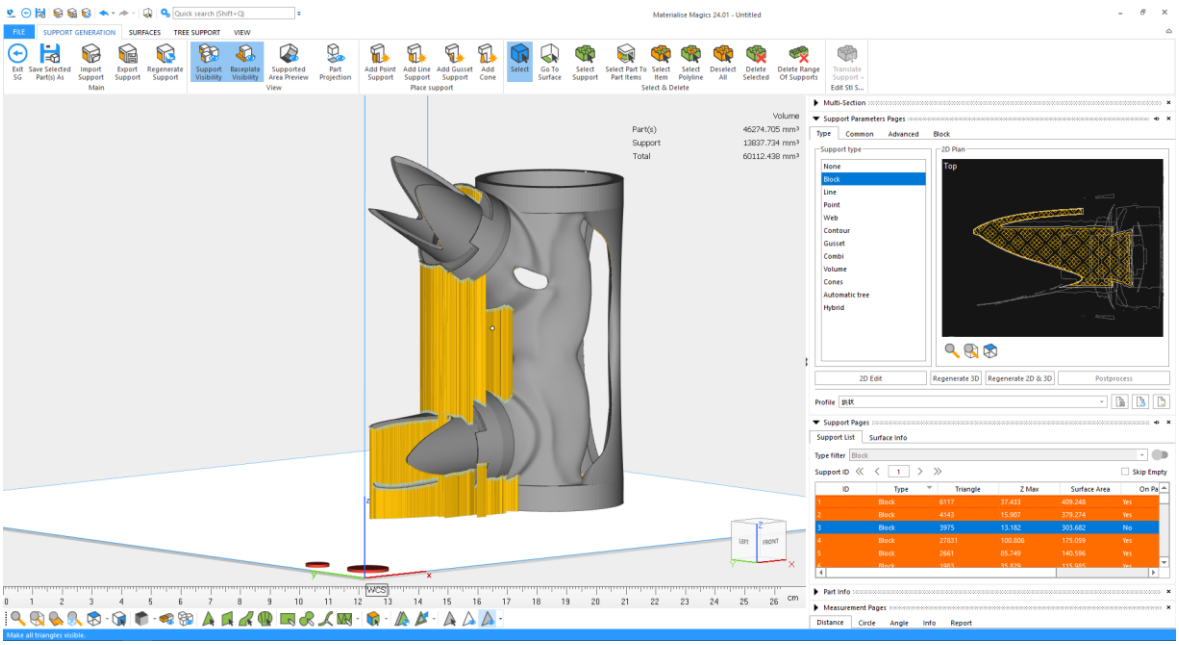

Figure 70. Support generation for the head tube. (Author's own).

Finally, the component and its supports have to be sliced into 0.03mm layers to prepare them for the EP Hatch program and its further printing.

6.4 Bottom bracket

This component has no major design complexities as the previous one. The part is created with simple extrudes and the Swept Blend tool as the main actions. Figure 71 shows what it looks like.

Figure 71. Original bottom bracket. (Author's own).

Figure 72 shows the CAD design of the bottom bracket. Although it looks simply it has its key aspects to consider. Below the figure there are the explanations of the most important aspects used to create the part.

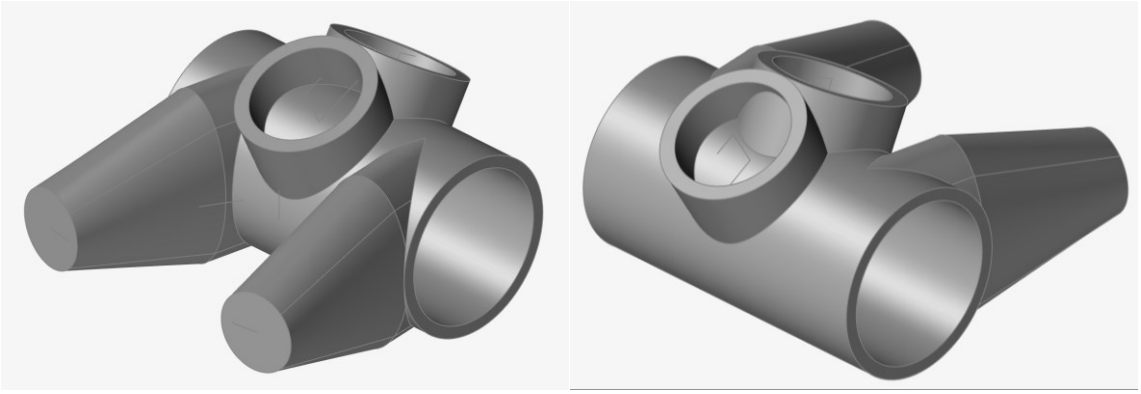

Figure 72. CAD design of the bottom bracket. (Author's own).

The internal diameter of the horizontal hole is important to be exactly measured. It has to allocate the bottom bracket itself (during the text the whole part is named bottom bracket although the mechanism inside it is the one that really has that name). Like in the original frame, a thread needs to be machined inside that hole to fix it.

Table 6. Table of measures for the rear part angles

Name	Value (mm)
a	50.0230
b	110.000
c	45.0100
d	47.7385
e	47.7385
f	432.680

(Author's own).

The other main aspects to consider designing this part are the angles of each of the tubes coming out. The ones of the $\emptyset 30\, mm$ tubes are simple angles obtained directly by measuring the already existing bicycle frame bought. The other angles have a complex way to find them. In Table 6 presents all the measures illustrated in Figure 73.

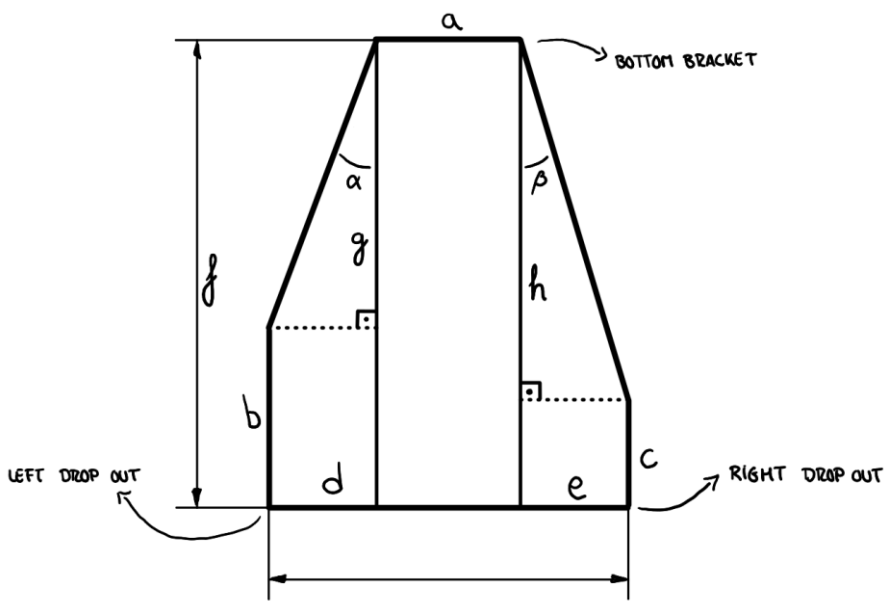

Figure 73. Geometry sketch of the rear part of the frame. (Author's own).

To find α and β, basic trigonometric relationships were used.

$$\alpha = atan\left(\frac{d}{g}\right) \quad (4) \qquad \beta = atan\left(\frac{e}{h}\right) \quad (5)$$

$$\alpha = atan\left(\frac{47{,}7385}{322{,}68}\right) \approx 8{,}4155° \qquad \beta = atan\left(\frac{47{,}7385}{387{,}67}\right) \approx 7{,}0202°$$

As the same process in the other parts, some rings were created to be the partitions. These partitions, grey coloured in Figure 74, remain untouched after the optimisation while the maroon area is modified by the software.

Figure 74. Bottom bracket partitions. (Author's own).

Figure 75 shows two different views of the optimised part after the optimisation is run in Altair. The disappearance of most of the material from the two rear horns was the main change in the shape of the piece.

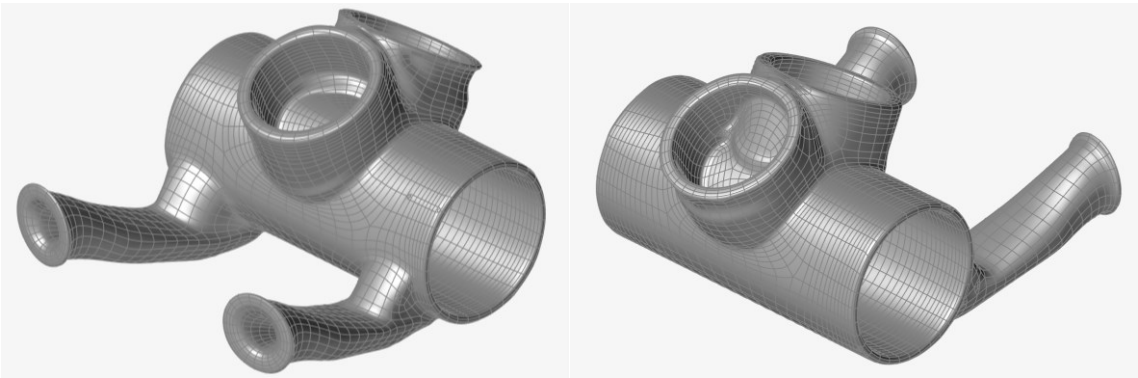

Figure 75. Different views of the bottom bracket optimised. (Author's own).

As the optimisation seemed to be great it was decided to be the definitive one. Then, the last step before having the part ready to print was the assembly of the connections. In this part there are two different joint diameters as the bigger ones are for the $\emptyset 30\ mm$ tubes and the smaller ones for the $\emptyset 16\ mm$ tubes. The figure below represents it (Figure 76).

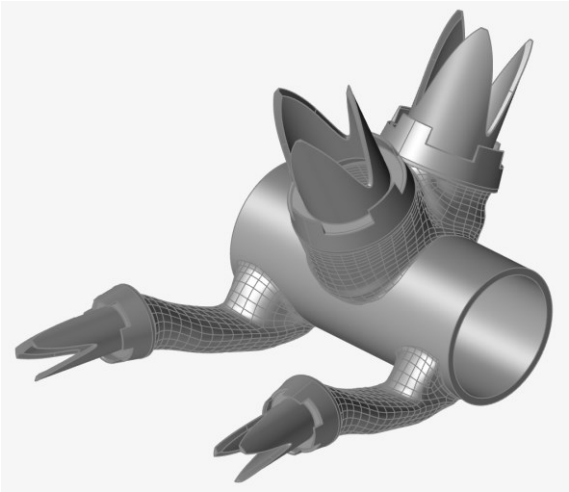

Figure 76. Bottom bracket optimised with unions. (Author's own).

After that, the addition of lattices with the nTopology software was the last step before preparing the part for printing. Surface lattices were the ones decided to add in that part as was the best decision to extract more material without compromising the strength of the part. The figure below shows how the part looked like (Figure 77).

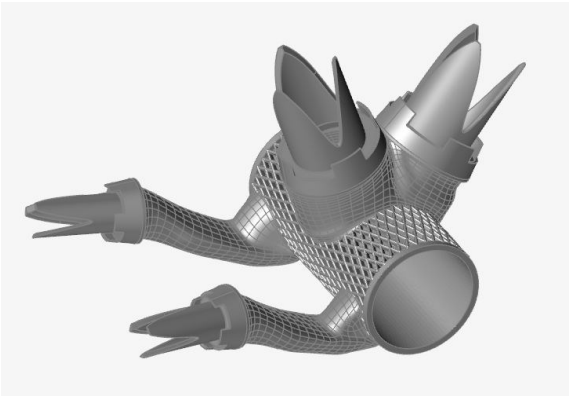

Figure 77. Lattices added to the bottom bracket perimeter. (Author's own).

Figure 78 shows the surface lattices type and parameters given. This option seemed to be the best as they were support-less and the ones which reduced the part mass the most.

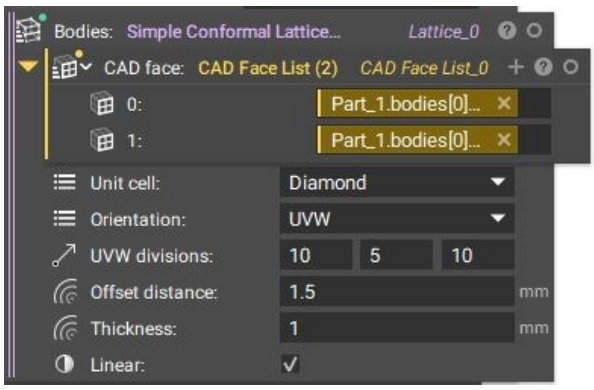

Figure 78. Surface lattices parameters. (Author's own).

Finally, the process followed in Materialize Magics is the same for the other components and it is shown below step by step with pictures. Import the component into the workspace first, then position it correctly and in the printing direction while checking for any potential mesh issues (Figure 79). The little green spot on the right side of the bottom bracket are the overlapped triangles automatically found by the software. Notice that they are located at the point where the lattice mesh merges with the outer ring.

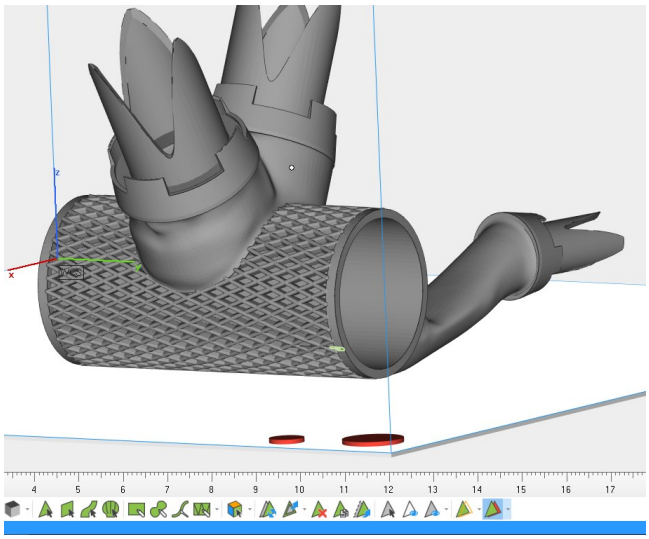

Figure 79. Mesh errors of the bottom bracket. (Author's own).

The supports must be generated once all errors have been verified and corrected. Given that the lattices are self-supporting; it is anticipated that there will only be support where there are unions. The figure below displays the created supports (Figure 80).

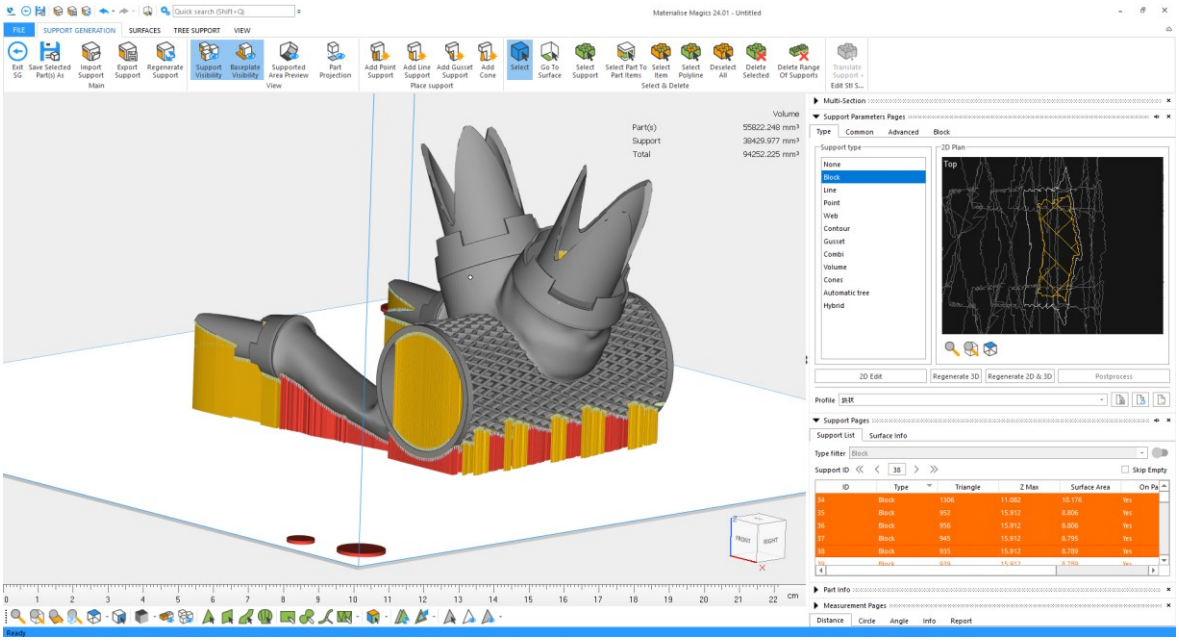

Figure 80. Support generation for the bottom bracket. (Author's own).

In order to get the component and its supports ready for the EP Hatch software and subsequent printing, they must finally be divided into 0.03mm layers.

6.5 Seat tube

This part was one of the most complicate to design. It had angles, distances, and technical issues to consider and that so more than one was tried to satisfy all of these.

Figure 81. Original seat tube. (Author's own).

The figure above is the original seat tube of the purchase bicycle. It helped to understand its shape and extract ideas about how it could be redesigned (Figure 81).

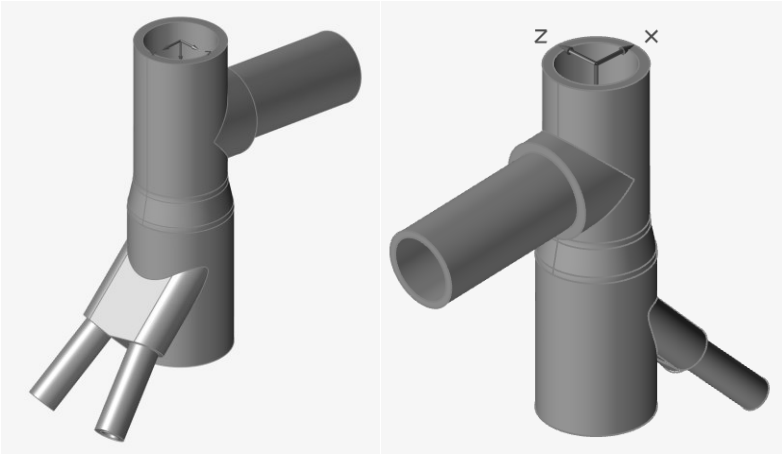

Figure 82. First CAD design of the seat tube. (Author's own).

The design on Figure 82 seemed to be good and without without exceeding too much the amount of material used. However, the two little connections where the stays go were not separated enough. The problem encountered is that the thickness of the wheel, being a mountain bike, was too large for this design.

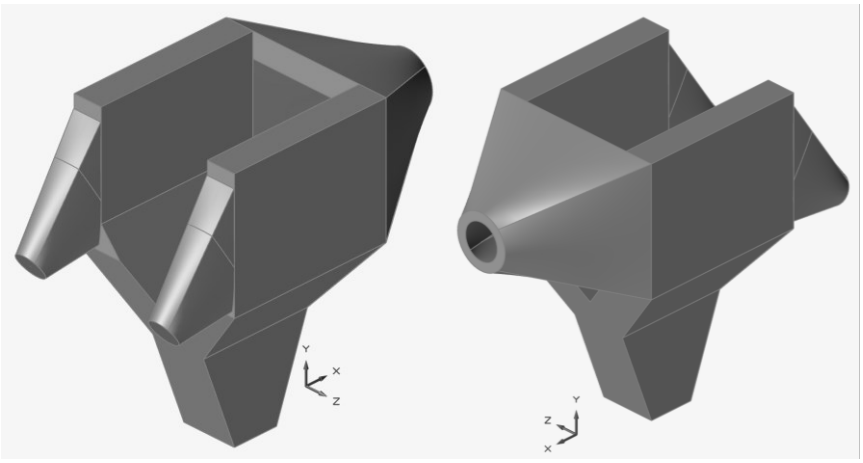

Figure 83. Second CAD design of the seat tube. (Author's own).

A second design was tried due to the insonsistencies of the first one. However, the shape of it did not seemed to be the desired one. As can be seen in Figure 83, it was difficult to design the part where the seat has to be fixed. Therefore, another design was made, presented in Figure 84.

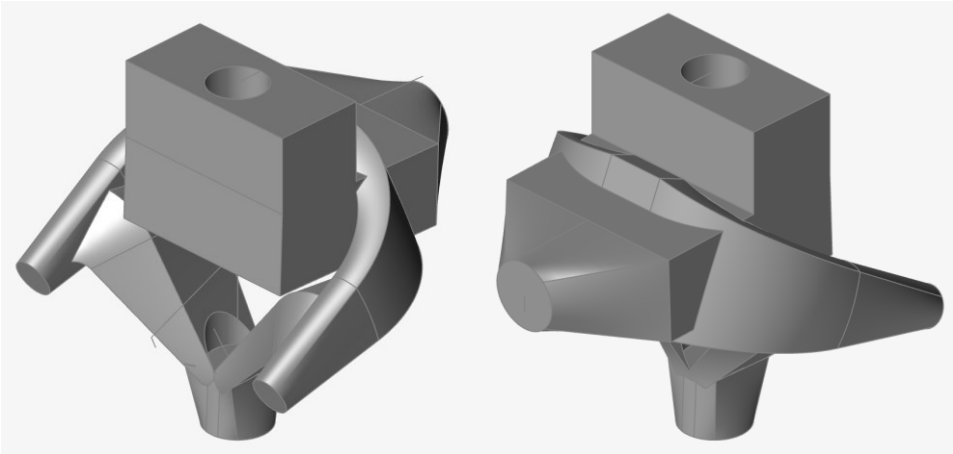

Figure 84. Third CAD design of the seat tube. (Author's own).

The design presented above is similar to the previous one but with important modifications. This one could hold the seat and also the distance between the two stay outlets is enough to let the wheel rotate without touching any post. For this reason, it was thought that it could be the final design.

The design is not the optimal in terms of amount of material used and the shape gave to it. This is not a problem because when optimised the software will remove all the unnecessary material. This ensures that there is enough material to spare during optimisation and the software can create the optimal shape.

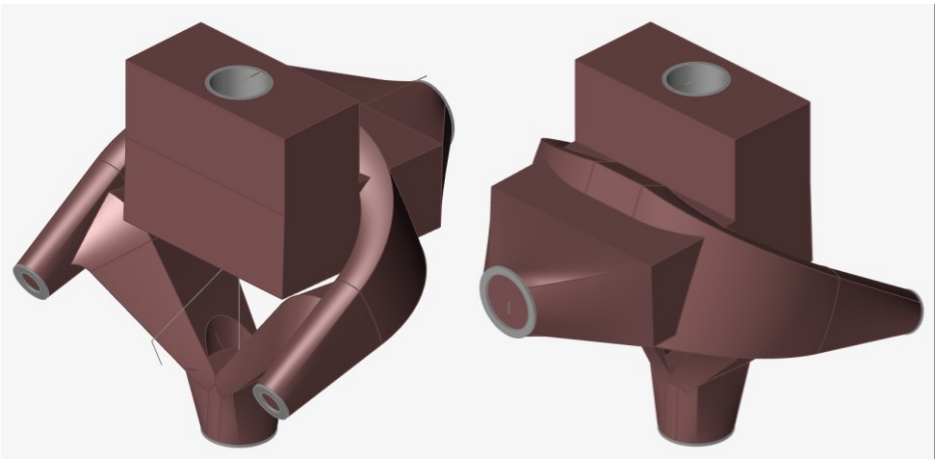

Figure 85. Seat tube partitions. (Author's own).

As the same process in the other parts, some rings were created to be the partitions and a longer cylinder to be the seat host. These partitions, grey coloured in Figure 85, remain untouched after the optimisation while the maroon area is modified by the software.

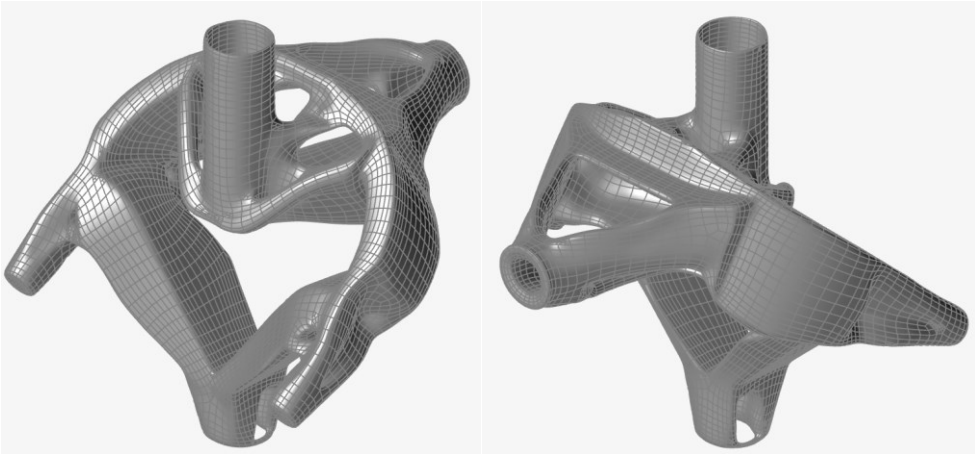

Figure 86. Different views of the first optimised seat tube. (Author's own).

Figure 86 shows two different views of the optimised part after the optimisation is run in Altair. The most curious shape created is that between the seat tube and the top tube outlet. The topology optimisation shapes try to make it the most organic looking, trying to represent shapes in nature as roots or in this case, like a human coccyx.

Although this optimisation looked good, a new one had to be made as an angle of the part had to be modified. In addition, it was found that the size of the part could be minimized. For this reason, a further design was still made. The following figure shows the results obtained (Figure 87).

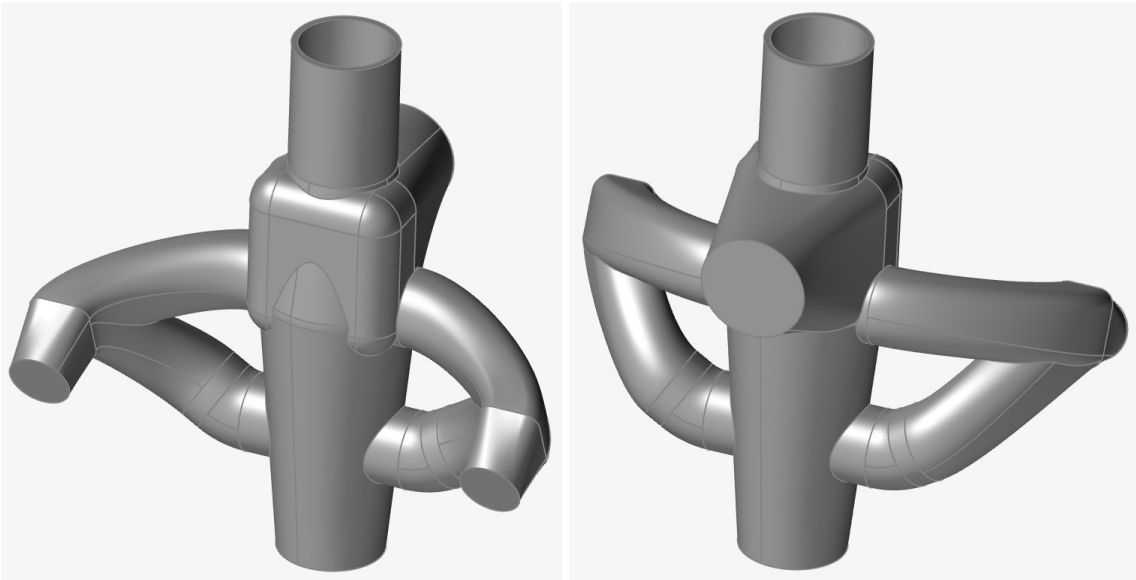

Figure 87. Fourth CAD design of the seat tube. (Author's own).

The new design looked good with the same basics of the previous CAD model, but the size reduced. The two links to the stays were shortened fixing them on the seat tube. The link to the top tube was also reduced and put more compact with the seat tube.

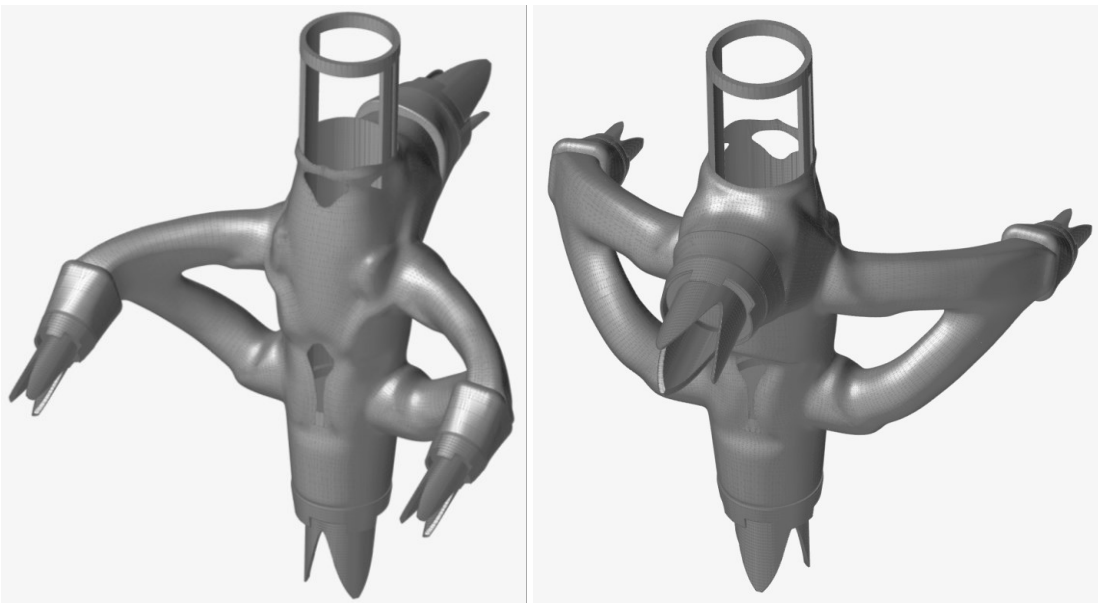

Figure 88. Final seat tube with unions. (Author's own).

Figure 88 shows the result of the seat tube part once the unions are added to the previously optimised part.

Finally, the steps taken in Materialise Magics are the same for the other components, and they are illustrated below. Before positioning the component appropriately and in the printing direction, it was imported it into the workspace and checked for any potential mesh errors (Figure 89).

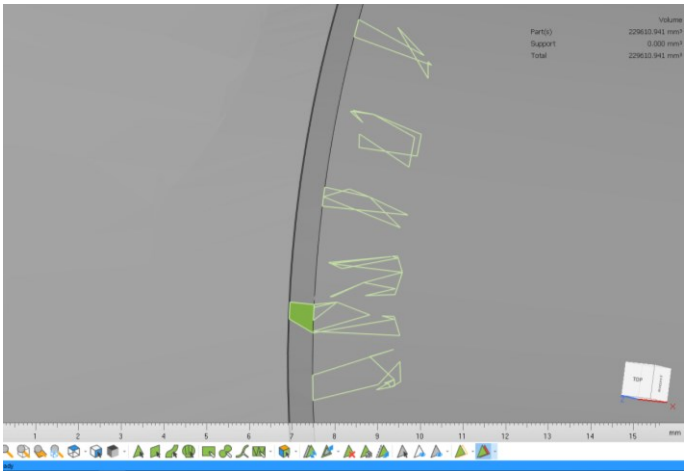

Figure 89. Mesh errors of the seat tube. (Author's own).

The mesh errors showed on Figure 89, were presented between the union and the part. That happens when the Boolean of the final component has some errors. In that case, they were fixed automatically, and then, the remaining ones manually.

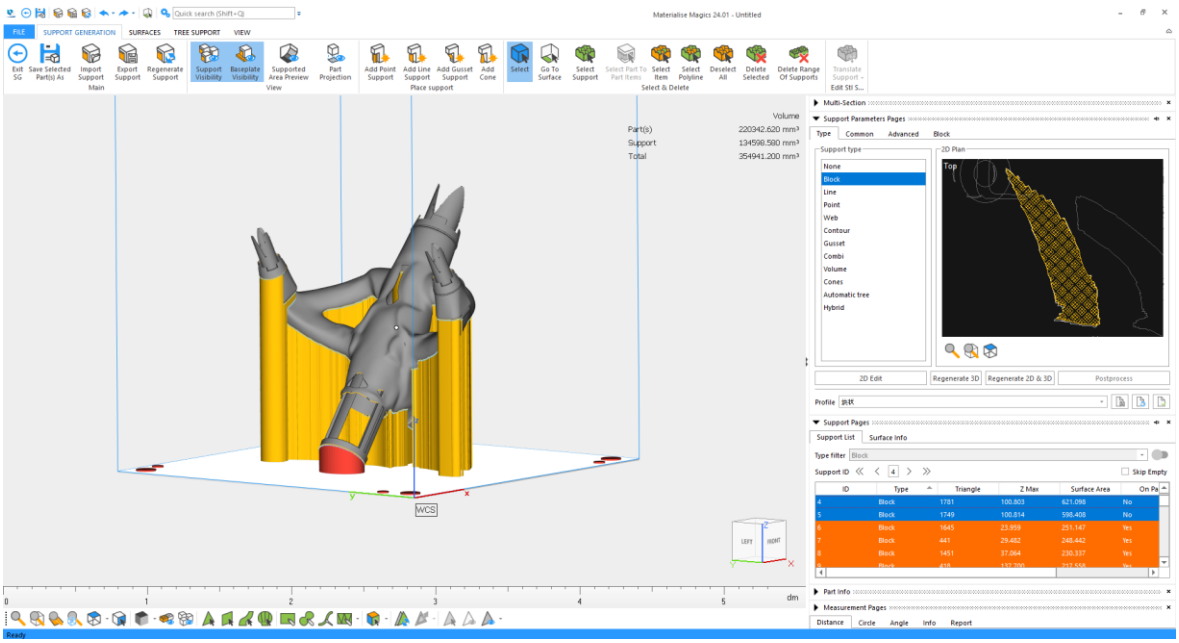

Figure 90. Support generation for the seat tube. (Author's own).

Finally, the supports were generated (Figure 90) and the part was sliced, ready for the EP Hatch software, the previous step before printing.

7 3D plastic printing

This section discusses all the printings made of plastic. Before printing in metal, all the components have been printed in plastic to check how would they look in real life and their magnitude.

The first thing to be printed were the joints, to check their functioning and if they had to be modified. After the joints were determined the rest of the components must be printed in plastic to check their geometry, appearance and if some modifications had to be made.

The printer models provided by the Additive Manufacturing Laboratory in Technobothnia are S5, 3, 3 Extended and S3 by UltiMaker. Each printer has different characteristics allowing the operator to choose depending on the needs of the part to be printed: velocity, accuracy, size or height.

The software used for these printers is Ultimaker CURA 4.12.1.. It allows configuring each printing for the desired needs stated before, changing the printer used and putting or not supports and adhesion to the baseplate.

7.1 Joints

As stated before, these are the first components to be printed in plastic. All the tests printed are not the final version as the type of joint has to be decided.

The parameters to consider when choosing the option which fits the better for the parts need to be set up. In this way, the final decision of the joint type needs its own reflection and analysis. Referring to chapter *5. Assembly type analysis*, this section presents all the tests done with some different type of joints and the final joint-type decided.

The best option would be that one able to fix the printed part with the aluminium tube more efficiently. That is, one that is as simple as possible and can successfully fix the two parts while minimising weight and the need for machining. The addition of other components as glue, bolts or a metal brace would not be desired.

Some of the design options for the joint were directly dismissed due to its weak consistency or its difficulty to implement them. For this reason, at first the one which seemed to be the best was the option five (see section *5.5 Design option five*).

Figure 91. Plastic tests of the fifth type joint. (Author's own).

Figure 91 presents some tests made with the plastic 3D printer of the design option five of the joint. The components include also those simulating the aluminium tubes with the grooves inside.

As it can be seen on the left of the figure, first it has been attempted to print only one female tube and try to assemble and disassemble with the two little holes at the top of the tubes. The male tubes had different diameters to find which one could fit better. However, it was impossible to take it out after the first assembled tube. For this reason, a female tube was created for each male. On the left of the figure, different diameters were printed at the same time the wall thickness was varied among them.

The joint once the right diameters and thicknesses were found, seemed to be an option that worked well. Nevertheless, the problem existing was in the machining of the aluminium tubes. The metal workshop that was commissioned to make these notches did not have the tools to do the job. For this reason, that option had to be discarded and find a new suitable design.

The modification done to option five was mainly to change the female part. Instead of having an internal groove, it would have a hole, making it easier to machine in the metal workshop.

The male part of the union had to change also. Rather than having the male split in half, four parts have been made independent of each other. Each part corresponds to one of the holes of the female and would fit completely.

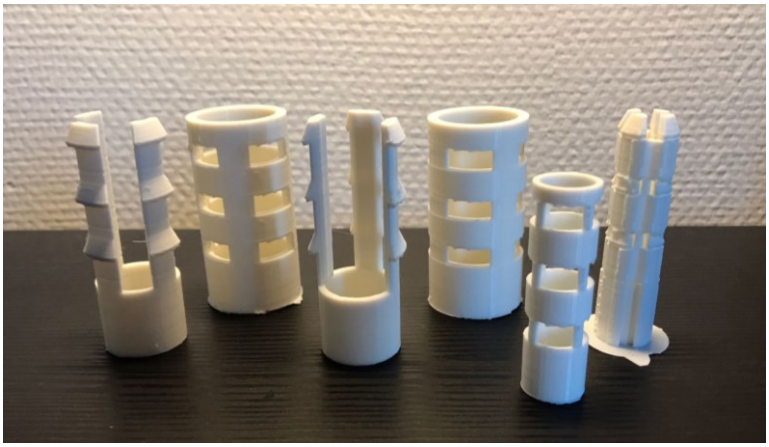

Figure 92. Plastic test of the sixth type joint. (Author's own).

It can be seen in Figure 92 some of the male parts are broken, this is due to the fragility of this modification. As for this project it is important that the joint is not fragile but strong and able to withstand stresses, this option has been discarded to avoid the possibility of its breakage.

The last printed option follows the same functioning as the others, a notch into which fits a thickening. The notch this time is at the outer part of the aluminium tube, so it does not create any difficulty in machining. As regards the male of the tube, it has three prongs that go inserted inside the aluminium tube to reinforce it and also a thickness that will fit to the notch done in the tube (Figure 93).

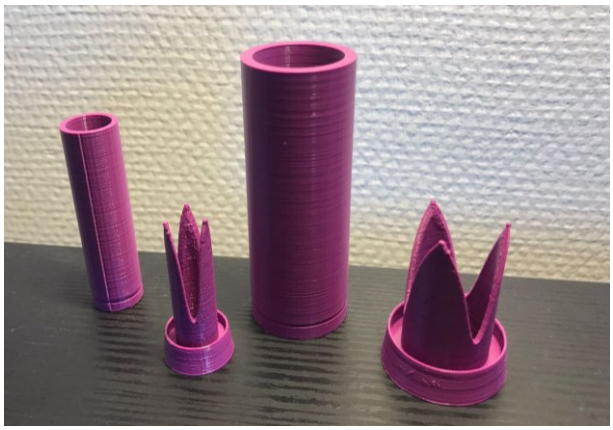

Figure 93. Plastic test of the seventh type joint. (Author's own).

Due to the limitations of the plastic 3D printer, the thickness was not print correctly, but the joint still worked properly. So as the metal 3D printer has a much higher resolution than the plastic one, it will be able to print it well and a strong connection will result.

7.2 Right dropout

This component and the left dropout were the first to be printed in plastic. The printing direction was the same as the one used in Altair for its optimisation. This first prototyping of the component aimed to see how it looked physically, the generated supports and its size.

Figure 94. First plastic printing of the right dropout. (Author's own).

Figure 94 was the first iteration of the right dropout before any modification was carried out. It was then modified the length of the joint that is closer to the ground because of the geometrical limitations explained in section *6.2 Right dropout*. This component was not printed again until the last version of the joints was decided, so the following printing was thought to be the last one.

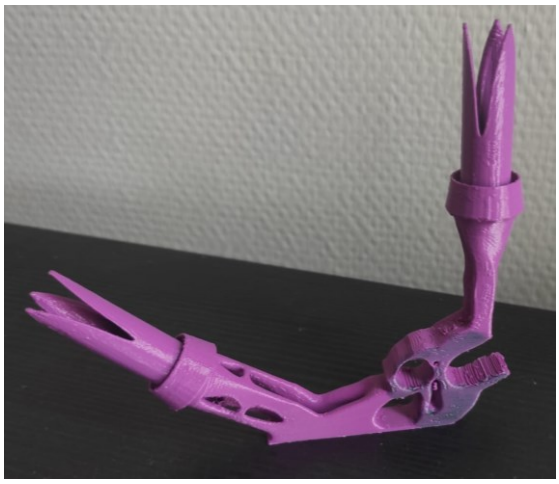

Figure 95. Second plastic printing right dropout. (Author's own).

It can be seen in Figure 95 that there is a dark mark in the place where the notch for the gear shift should be. It was done to ensure the side where it had to be done, and the component was also used to have a physical reference of where the material had to be reduced.

After the RP iterations to get the correct notch, the final right dropout obtained is the one shown in the figure below (Figure 96).

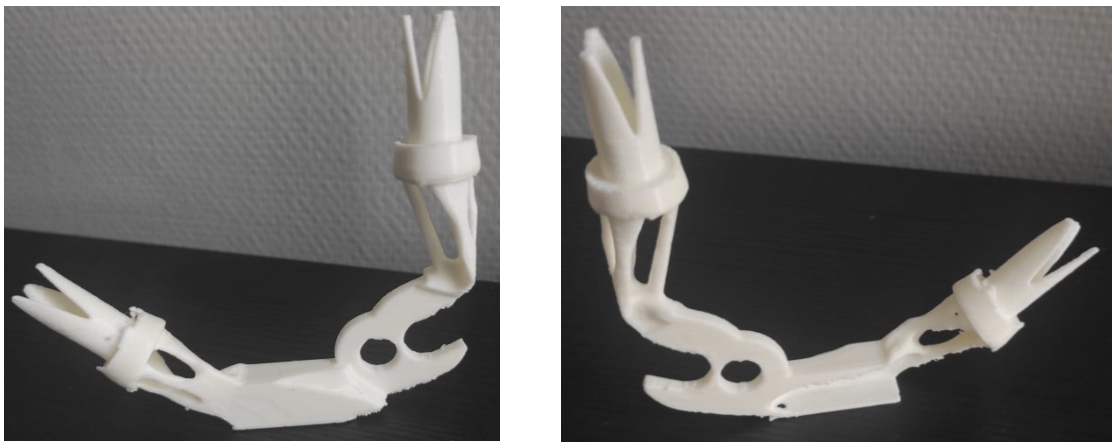

Figure 96. Final plastic printing of the right dropout. (Author's own).

Having this part completely designed and finished, it could be prepared and brought to the metal 3D printer to manufacture the final version.

When printing all the components, some support was needed, but most of them are different from the ones needed at the metal 3D printer. In the next section, *7.3 Left dropout*, will be seen Figure 101 where the supports generated by the CURA software for the two dropouts, since they were printed together.

7.3 Left dropout

For the left dropout, as mentioned above, it is one of the first components to be printed. In its case, it was printed in a different way to the direction marked in Altair because it was believed that it would generate less support, see Figure 97.

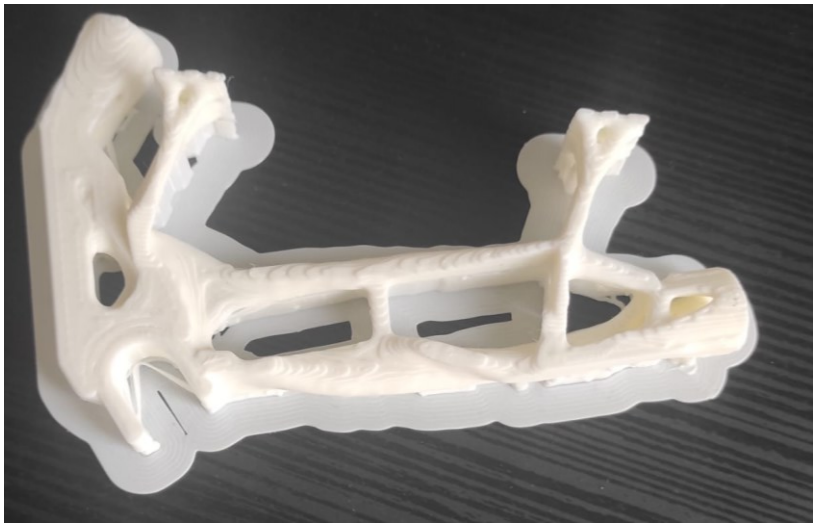

Figure 97. First plastic printing of the left dropout. (Author's own).

By using this configuration, less mass of supports was required than if the same direction as indicated in Altair had been used. The supports generated were clamped to the entire surface, making it nearly impossible to detach them without damaging the component.

The next printing was slightly different to this first one (Figure 98). The component had already attached the final unions, the holes for the brake were previously made and it was also a different optimisation.

Figure 98. Second plastic printing of the left dropout. (Author's own).

This was the first component used to check if the brake was in the correct place. As they were not properly positioned, another version of this component was printed. To check that the holes were in the correct position, the final version of this component was printed (Figure 99). The joints were not attached to save printing time and material.

Figure 99. Third plastic printing of the left dropout. (Author's own).

This component made possible to check that the holes were now in the correct position for the disc brake to fit into position. Finally, the final version of the joints was attached to this component and was printed to have the physical component (Figure 100).

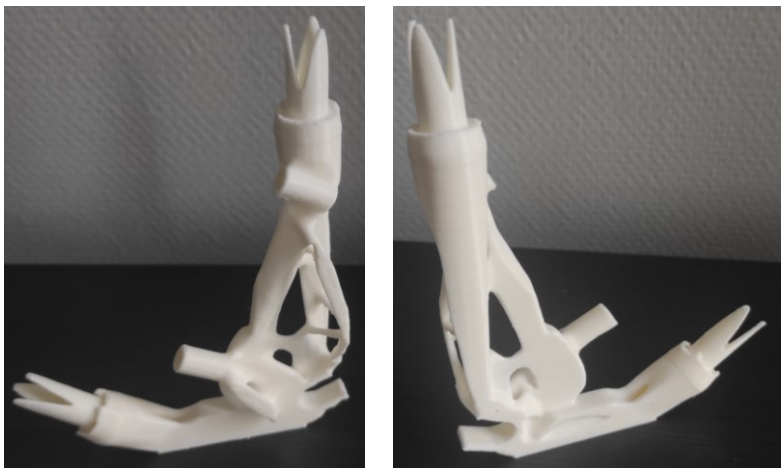

Figure 100. Final plastic printing of the left dropout. (Author's own).

The generated supports in the CURA software for this component and for the right dropout is shown in Figure 101.

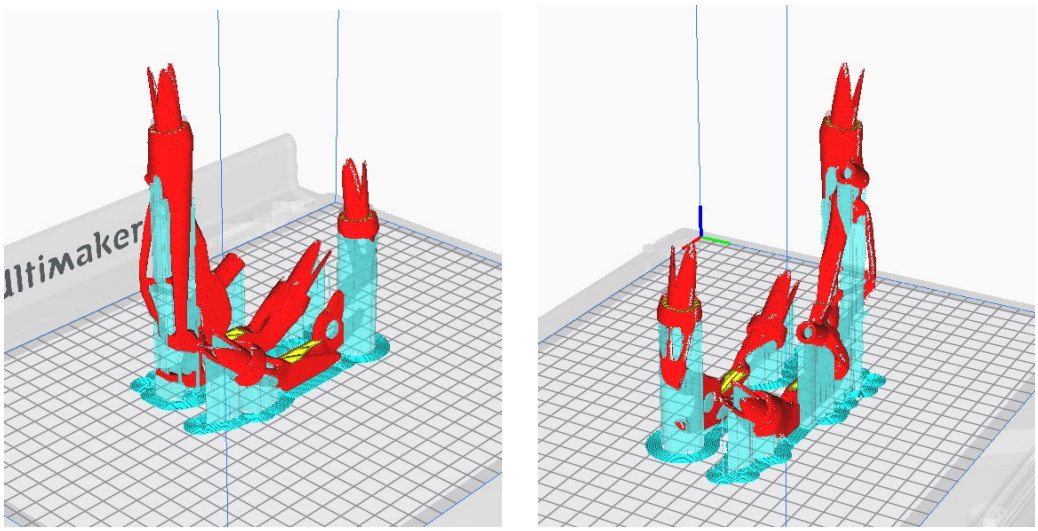

Figure 101. Generated support in the CURA software for both dropouts. (Author's own).

The generated supports are quite similar to the ones that Magics generates. The main difference is that the maximum overhang for the plastic printer is 60° instead of 45° that has the metal printer. This means that for angles that are less than 60° to the ground, there will be support, and thus the component will have more supports in general.

7.4 Head tube

There was only one printing for the head tube, since all the designs obtained never fulfilled the shape that was desired. This design corresponds to the last one, where there are embedded lattices in the back reinforcements.

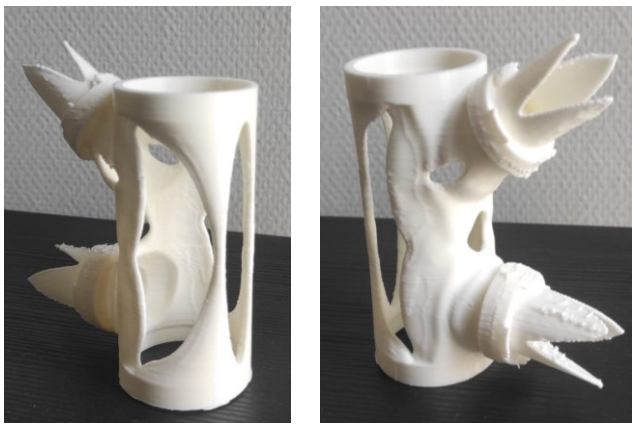

Figure 102. Plastic printed head tube. (Author's own).

Although Figure 102 is the final component, since the lattices are an internal part of the component, they will not be seen. For metal printing, there will be small windows to allow the dust trapped inside to escape, and therefore be visible.

As regards support generation, Figure 103 shows the supports generated for the plastic printing.

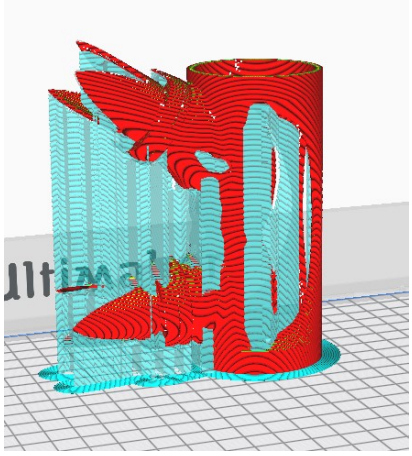

Figure 103. Generated support in the CURA software for the head tube. (Author's own).

Taking into account what has been said about the generation of supports in the dropouts, some of the supports generated in the figure above will not be generated for metal printing. Some of these unnecessary supports will be those inside the rear reinforcements, as they have been designed with the overhang in mind.

7.5 Bottom bracket

For the bottom bracket happened the same as for the head tube, there is only one design that met all the requirements. The figure (Figure 104) below shows the part in STL format filled into the CURA software representing the print preview with the support generation.

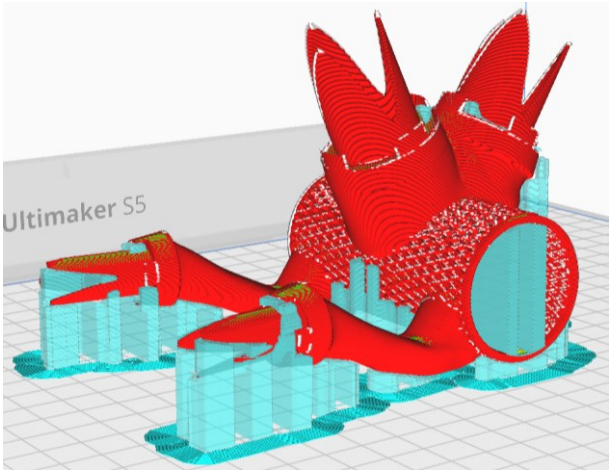

Figure 104. Generated support in the CURA software for the bottom bracket. (Author's own).

The positioning of the part on the print software is chosen to be the one with the less support generation. In addition, it should also be considered that the supports should be positioned in such a way that they are easy to remove.

The figure below (Figure 105) shows the result of the Bottom Bracket after being printed with the Ultimaker printer.

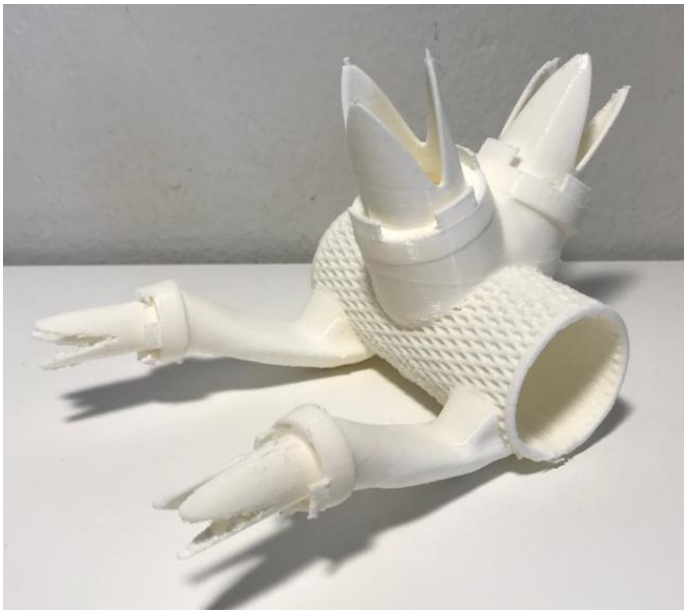

Figure 105. Plastic printed bottom bracket. (Author's own).

The lattices printed on the surface look good although the printing on plastic is not as accurate as it is on metal, where they will look better.

7.6 Seat tube

The seat tube was the last component to have ready to print in plastic due to the numerous modifications it suffered. The plastic printed versions obtained of the model helped to figure out the size of the part as it seemed that it was to be quite big.

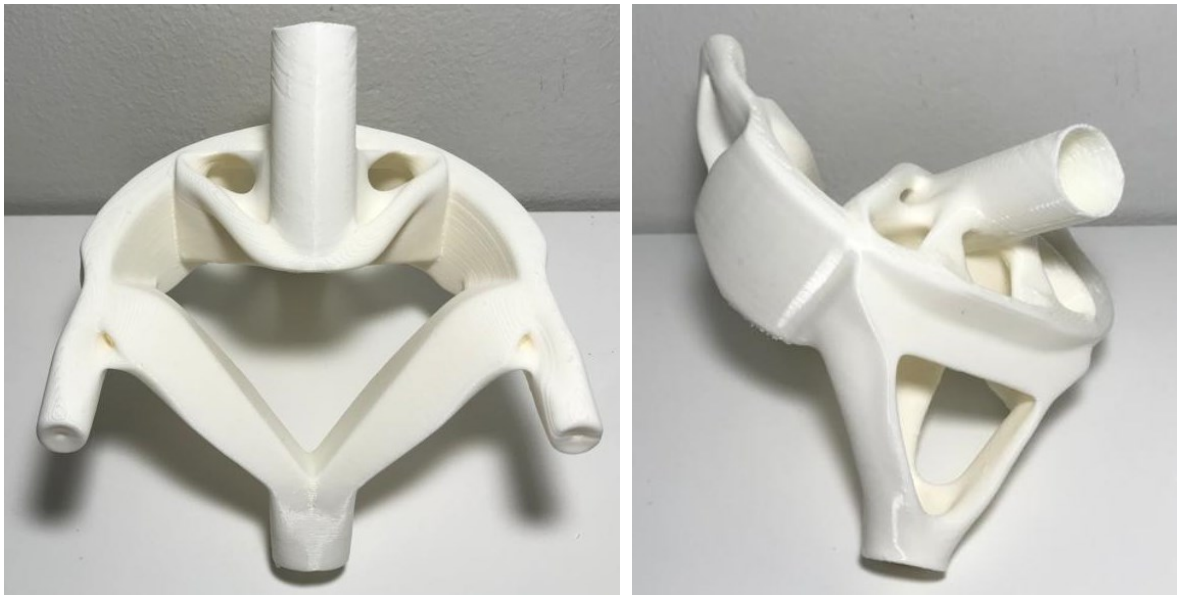

Figure 106. First plastic version of the seat tube. (Author's own).

The plastic printed part above resulted to be bigger than the desired size (Figure 106). The design made looked good on the software but not as good as wanted once printed. For this reason, and justified in Section *6.5 Seat tube*, another and definitive print in plastic was made.

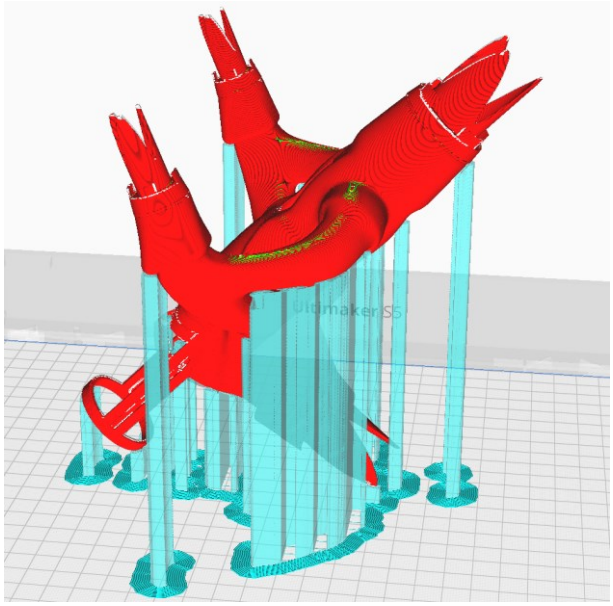

Figure 107. Generated support in the CURA software for the seat tube. (Author’s own).

The new seat tube designed was printed with the joints to check the new size and realise how it could be put in the metal 3D printer. The figure above shows the preparation of the part on CURA software (Figure 107).

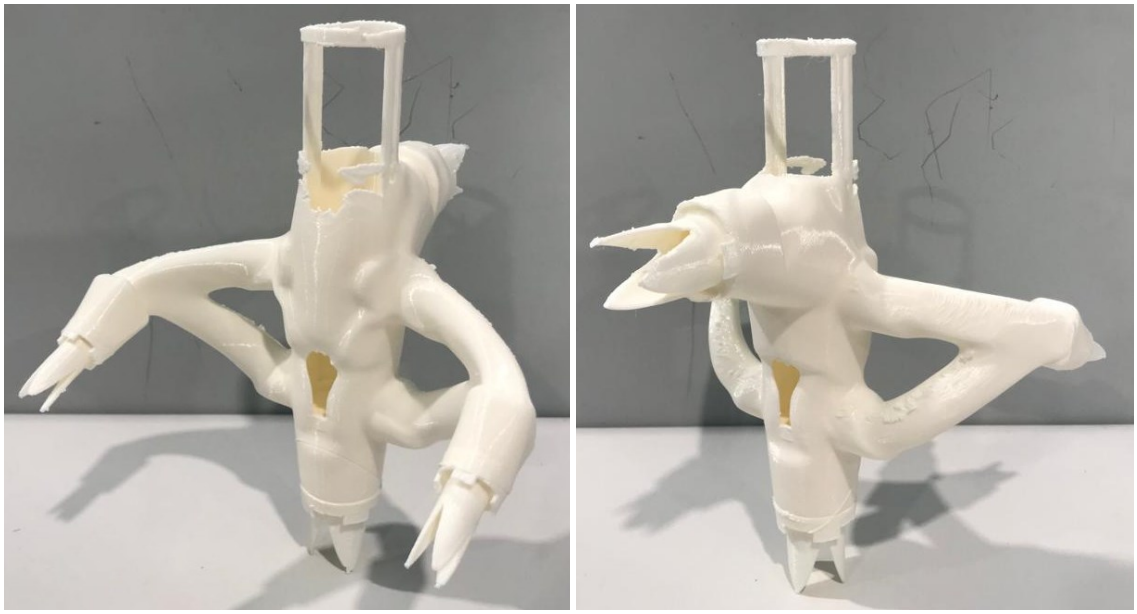

Figure 108. Definitive plastic parts of the seat tube. (Author's own).

Figure 108 shows the view of the final part with the joints. It is a part that fulfils the same requirements as the previous one but reducing its size and weight.

8 3D metal printing

This section will talk about the work carried out in the laboratory, as well as the process followed, and the activities done. It will be discussed the activities done during the printer preparation process, the supervision of the first's layers and finally the process after printing and the post processing.

8.1 Preparation process

The preparation process of all the needed for printing usually takes around two or three days. In these days, the powder is baked in the oven and then put in the machine, the baseplate calibrated, and the silicon blade placed.

The first step made was to put the powder on trays and place them in the oven (Figure 109), they had to stay there for approximately 7 hours at a temperature of 80°C and pressure of 0.8 bar.

Figure 109. Oven to bake the powder. (Author's own).

This is done to evaporate the excess water that the powder could have. The trays usually can carry up to 50kg of material, taking this into account, it has to be calculated how many trays will be needed. Once the powder is heated, it can be trespassed to the machine, where it is stored in the feeder and has to be put manually.

As regards the baseplate, it was milled within enough distance to remove the remains of the last printing but not so much as to reduce it by much. After this, it was polished with sandpaper and a file to remove any sharp edges and placed in the machine.

To fix the baseplate in the machine needs eight screws. Four of these screws are used to adjust the height of the corners of the baseplate, and the other four are to fix it into the machine. This initial step of the calibration has as its objective to level the baseplate with the fixed sides of the machine (Figure 110).

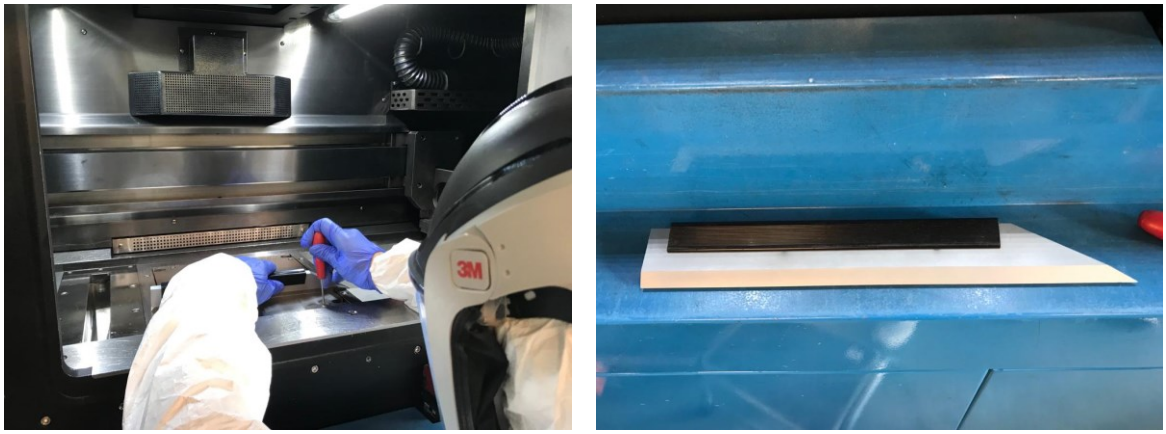

Figure 110. Baseplate calibration and control rule. (Author's own).

It is used a precision control rule, standardized by the norm DIN 874 300/0 284605, to visually check if there is light passing through any place.

The next part that was prepared and calibrated was the silicon blade, showed in Figure 111. Each time that a new print is started, a new one has to be put in.

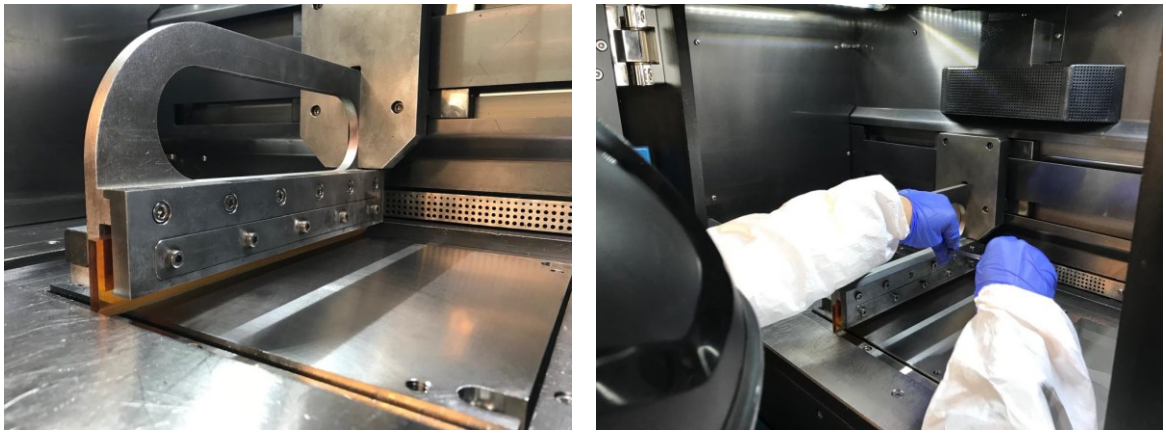

Figure 111. Silicon blade placement and fixing. (Author's own).

The blade was put in its support and lightly tightened the fastening screws. As the baseplate was already calibrated, this component was calibrated against it. After this, the blade holder was placed in the middle of the baseplate and the screws were loosened so that the blade touches against the baseplate. Finally, the screws were tightened to fix the blade in place.

The last verification of the calibration made is to pour a light coating of metal powder on the baseplate and see that it spreads evenly along the length of the baseplate (Figure 112). If the result is not as desired, the part motor has to be lowered until is achieved.

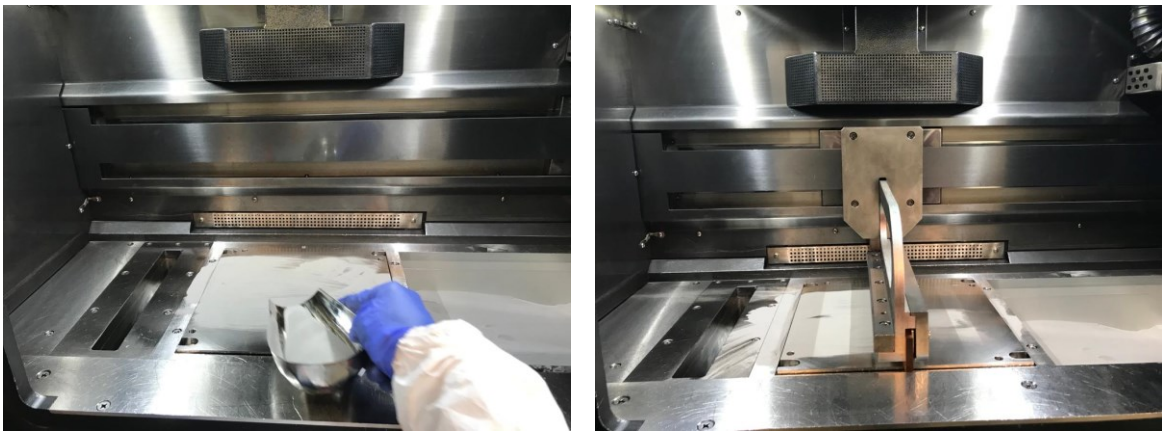

Figure 112. Silicon blade calibration. (Author's own).

One of the last steps taken was to fill all the holes that were around the baseplate with powder. In this same step, the feed motor was raised to the height where the powder is at the level of the baseplate so that an even layer of powder is left throughout the interior of the machine.

The lens of the laser was cleaned before printing. It was cleaned with a special wipe (Figure 113), doing circles and starting at the centre, going to extremes. This same process was repeated until the wipe did not have any metal powder.

Figure 113. Laser lens cleaning. (Author's own).

The last step before closing the gate to the printing chamber was to clean all the powder from the baseplate and place the part that vacuums the surplus nitrogen. Once this is done, the chamber can be closed.

Before starting to introduce nitrogen into the chamber was checked the correct functioning of the cooling system. If it works properly, it is turned ON approximately 15 minutes before opening the nitrogen flow.

The printer could not start unless some parameters are in a determined range. The next image shows which are these parameters and their ideal value for the printer (Figure 114).

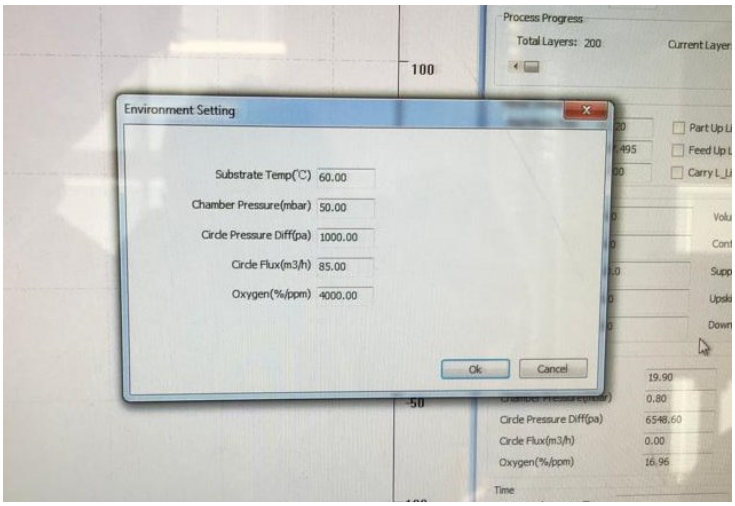

Figure 114. Environment Settings. (Author's own).

Once all the parameters are reached, the next and last step is to turn on the laser. To check if it is turned on, an orange light, which is placed below the computer, should be turned ON.

8.2 Printing supervision

The printer used for this project has some limitations in terms of complex structures, therefore the first layers of the print must be supervised.

Before starting the printing, a thin layer of metallic powder has to be spread all around the baseplate's surface. This first layer is put manually by activating the powder deposit and blade motors. Once the layer is spread, the laser auto-calibrates by drawing the outline of the first layer of the parts to be printed into the baseplate.

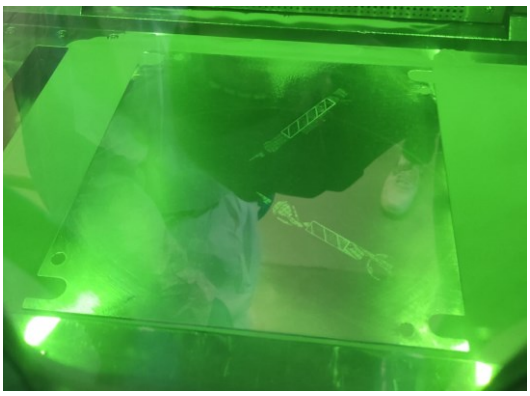

Figure 115. First layer drawing of the dropouts. (Author's own).

The last image is the printing of both dropouts. The first layer corresponds to the first layer to be printed, which can be checked in Figure 115.

After this calibration is done, the printing can start. The process is automatic and the only thing that has to be done there is to supervise if there are any errors during the printing. The most common error that can occur is that the powder is not spread all over the baseplate, leaving holes in the component surface.

These holes cause the laser to directly touch the component to be printed and melt it. If the laser comes into contact with steel that has already melted before, it re-melts and slowly creates a stalagmite. This stalagmite will gradually damage the blade making it unable to properly spread the powder on the baseplate.

In these cases, the best option for the security of the rest of the printing is to abort the component where are occurring the errors.

8.3 After-printing process

After the printing is completed, the baseplate has been lowered the same distance as the component's height and it is covered by layers of unused powder.

First, the nitrogen aspirator has to be removed to access the printing chamber. Before raising the baseplate, some of the powder has to be taken out by scooping it with a large spoon. After some scoops, the inside of the machine looks like the following figure (Figure 116).

Figure 116. Baseplate covered in metal powder. (Author's own).

After all the powder has been removed, the hoover is used to remove any remaining dust in the machine. When all the dust is cleaned, the baseplate is removed from the machine and starts the post-processing of the components.

Figure 117. Sifting machine. (Author's own).

As regards the scooped powder, it is stored in plastic containers for their later sieving. To sieve it, it has to be transferred from the plastic bottles into a special metal container which is then placed in the sifting machine (Figure 117). This machine passes the powder through different filters that remove the impurities from the metal powder, thus cleaning it.

8.4 Component post-processing

After the baseplate is taken out from the machine, the supports have to be removed from the components. It is done before cutting the parts out of the baseplate because it gives more control when applying force.

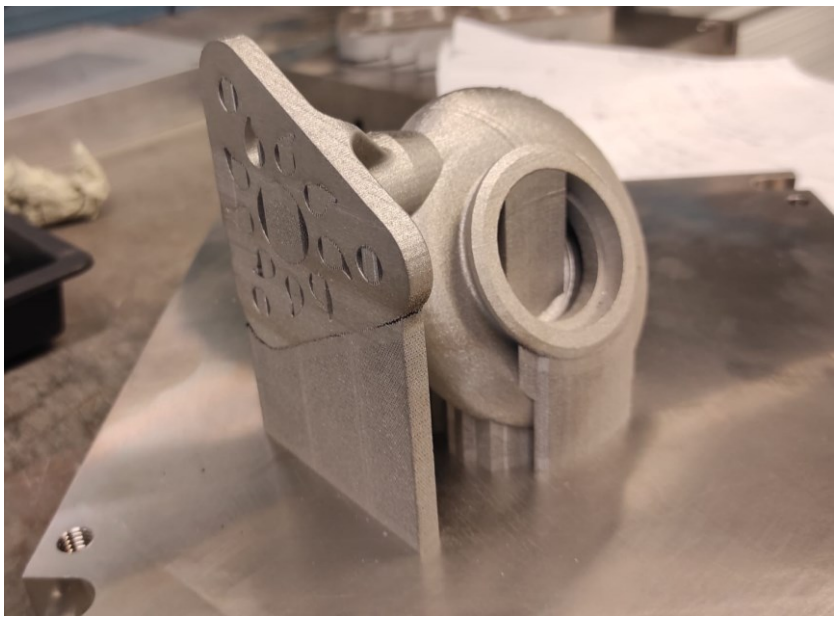

Figure 118. Example of a component with supports. (Author's own).

The removal of the supports is a process that has to be completed manually before the component is detached from the baseplate (Figure 118). It is usually done using pliers or a hammer and chisel. Care must be taken as any error in the process can damage the part and force it to be reprinted.

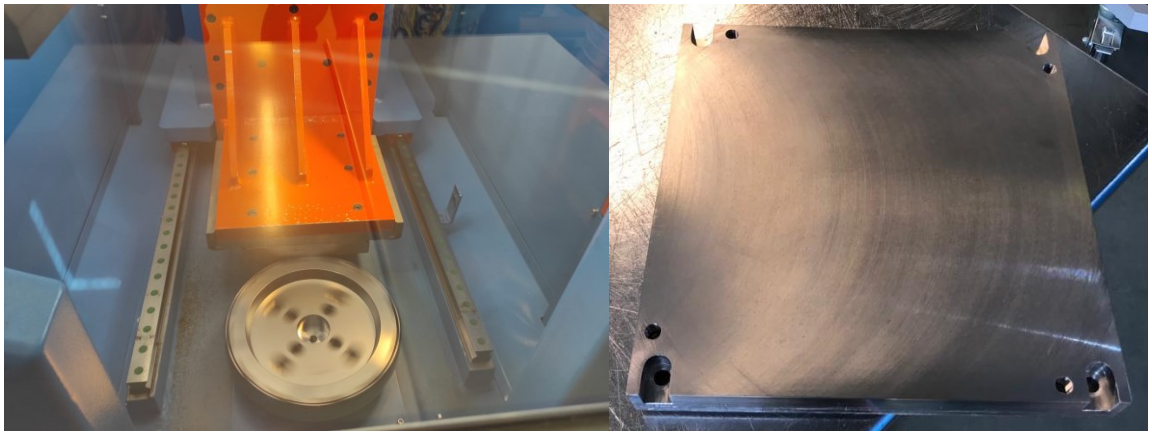

Figure 119. Baseplate being milled (left) and the baseplate result (right). (Author's own).

Figure 119 shows the process when the baseplate is filed after having cut the printed parts. The radial polisher goes through the baseplate multiple times taking lowly layer by layer the protrusions there are. After that, the baseplate is given a final finish with hand polishing.

The whole process to undertake when post-processing a printed part is described in detail on section *2.3.2 Post-processing*. As it was not possible to print any own part, the procedure explained above and carried out in the laboratory is not completed.

9 Results

In this section, the results obtained during the project development are presented. The result of the connection as well as all the final parts printed in plastic and metal are the main items discussed. In addition, a short analysis of the costs involved in carrying out the metal printing of the designed parts is also added.

9.1 Joints

The final joint decided to take for the final designs of the parts is the one presented on the figure below (Figure 120).

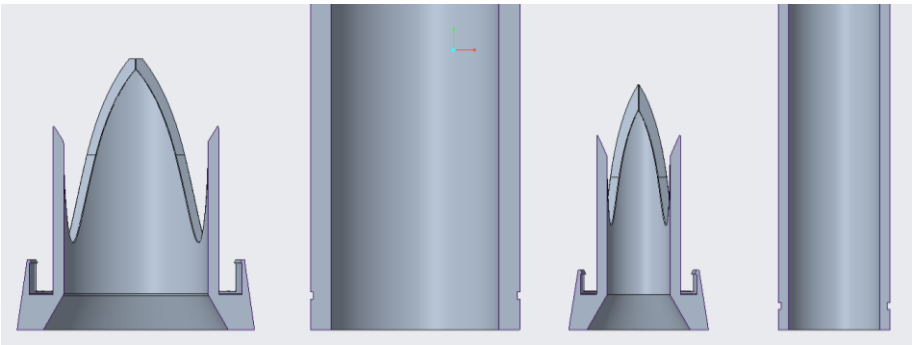

Figure 120. Section view of the two different diameters of the final joint. (Author's own).

The results obtained in plastic, after trying different diameters to set the right tolerance between the inner and the outer tube, worked well with the requirements established in the chapter *5. Assembly type analysis*. The joints were as simple as possible, and they were able to fix the tube preventing them from separating again once united. Figure 121 shows the definitive joints in plastic.

Figure 121. Definitive plastic joints. (Author's own).

After the joint was checked to work in plastic, the figure below (Figure 122) shows the joints printed again, this time in metal, and the joint connected to a piece of aluminium tube.

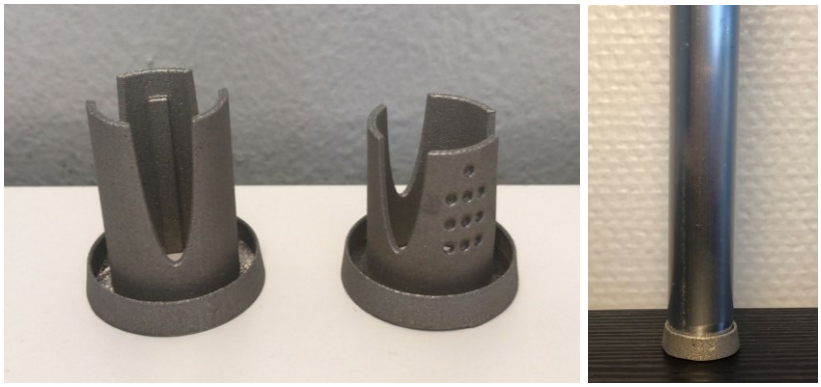

Figure 122. Printed metal joints. (Author's own).

The rib in the left joint and the holes through the joint on the right side were different tries to test the resistance of them. Both details were discarded as it was strong enough and the amount of material could be reduced thinning the top of the walls.

To check the correct functioning of the mechanism a piece of an aluminium tube was cut to assemble it with the printed metal joints (right side of Figure 122). It worked well although there was still some clearance between the two tubes. That was useful to be able to modify the joints for the end pieces and put the correct measurements there.

The last modification that was decided to add was the reduction of the perimeter that locks the tube. Instead of being an entire circumference it was replaced by four flanges with the same inner shape (see Figure 120). This reduces the amount of material but still holds the workpiece in place.

9.2 Plastic parts

All components were optimised and printed in plastic in order to have them physically, to get an idea of their dimensions and to compare them with those of the first prototype. Table 7 shows all the components that were printed and the comparison with those of the first prototype.

Table 7. Summary of the printed parts compared with the first bicycle prototype

Left Dropout	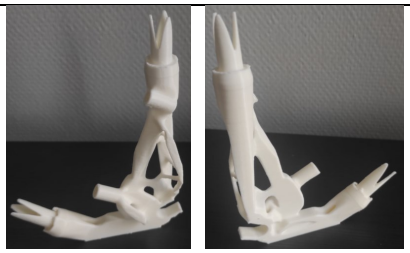	
Right Dropout	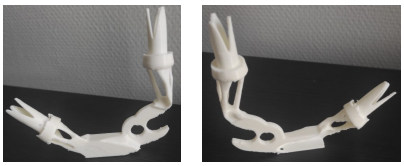	
Heat Tube	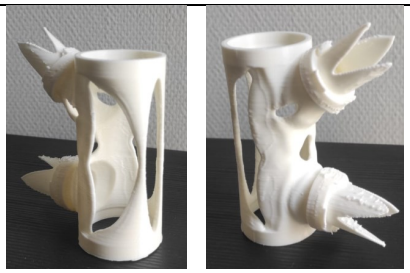	
Seat Tube		
Bottom Bracket	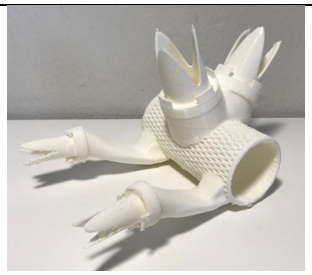	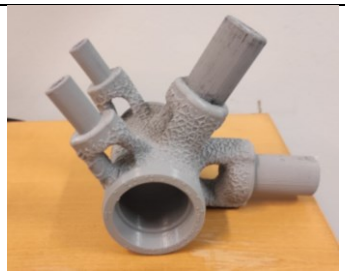

(Author's own).

The plastic printing did not cause any problems. All the printers worked well, and they were all available at almost any time.

As regards the visual aspect of the components, because of the optimisations applied and the lattice structures, the new designed components have a more futuristic and organic design. It is subjective whether a piece is visually appealing or not, but it has been considered that the overall appearance has been improved.

9.3 Metal parts

After some attempts of printing the components with the metal printer, their complex geometry always caused some error to appear. Left side of Figure 123 shows how it looks like when the printing is not going as it should. The two shiny, silver parts of the tips are areas where the printed part is starting to be damaged. On the other side there is the result of an aborted printing once extracted from the printer.

Figure 123. Metal printing error on the left and aborted printing result on the right. (Author's own).

Although none of the component were physically obtained, the Altair software allows to do a calculation of the component's mass. Table 8 shows the weight of all the components for their different versions.

Table 8. Component's mass analysis

Component	Original mass (kg)	Optimised mass (kg)	1st prototype mass (kg)	Mass reduction percentage (%)
Left dropout	0.660	0.287	0.320	10.31
Right dropout	0.201	0.094	0.320	76.35
Head tube	0.748	0.370	1.963	81.15
Seat tube	2.558	1.681	1.185	- 27.96
Bottom bracket	0.989	0.443	1.260	64.84

(Author's own).

It is important to consider the original mass since the main objective of topological optimisation is to reduce the total mass of the component. Also is worth looking at the 1st prototype mass to really see if the optimisation has been useful.

Concerning the mass, for all the components designed except the seat tube, there has been a mass reduction regarding the first prototype. The most important reduction has been in the head tube where the reduction is nearly the 80%, followed by the Right Dropout, where the reduction is slightly higher than 75%.

The reason why the new seat tube is a 27.96% heavier than the first prototype is because the previous version did not consider that the tube that holds the seat has to be inserted into the frame. If this had been taken into account, the diameter of the previous seat tube would have been larger and the component even longer. Only by making these modifications, the weight would have been closer to this latest design.

Table 9. Parts metal printing time

Left dropout	Right dropout	Head tube	Seat tube	Bottom bracket	Total time
26h 29min	21h 44min	34h 23min	82h 30min	36h 21min	**201h 27min**

(Author's own).

Metal printing is a relatively low process, as can be seen on the table above (Table 9). These long times slow down the printing process, as the entire make-ready and post-processing work, as well as the maintenance and cleaning of the press, must also be considered. For all those reasons, it is not possible to do more than one printing process per week.

In *Appendix 3. Metal printing times*, will be shown the screenshots from the machine, where appear the printing time and other parameters such as the height of powder needed or the oxygen present in the chamber.

9.4 Cost analysis

Metal 3D printing is not a cheap process because of its still limited research and the high elevate prices of the materials used. For this reason, it is a good practice try to estimate the total cost of the printed metal parts. The online software used for this estimation is SelectAM.

Once the part is imported in STL format, the material of printing and how much post-processing is needed has to be chosen. The software automatically determines the part complexity and how it affects to the cost of it. See *Appendix 4. Estimated cost of the parts* for further details.

Table 10. Estimated price of the metal 3D printed parts

Part	Estimated price
Right dropout	333.58 €
Left dropout	2018.51 €
Head tube	1340.09 €
Bottom bracket	5783.09 €
Seat tube	6326.46 €
Total price	**15801.73 €**

(Author's own).

On Table 10 the estimated price of each part is stated. The software calculates it approximately. Therefore, this numbers are just to figure out the estimated cost of the printing parts in metal and to help understand why it is not yet a competitive technology in the manufacture industry.

10 Discussion

This section goes through the discussion of the results obtained related to the aim and objectives established at the beginning of the project. In addition, the limitations faced during the thesis development and some inconsistencies found within the project are also reviewed. Finally, future work is proposed suggesting possible assessment improvements.

10.1 Aim and objectives

The aim of this thesis was to design, and 3D metal print the joints of a bicycle. The design part has been satisfactorily achieved, notably reducing component weights and achieving complex visual appearances. Concerning metal printing, it has been tried several times to print some components, but there were always errors during the printing process which forced it to stop.

In terms of objectives, it has been possible to design a mechanical assembly system that is simple, efficient, and robust. This system could be printed on metal to test its operation and proved to be satisfactory, both in terms of its strength and its effective attachment to the aluminium connecting tube.

Regarding the improvement of the first prototype components, it can be said that they have all been improved. Concerning the visual aspect, all the components have a more intricate design, with futuristic forms, implementation of lattices and topological optimisation and a more organic aspect. On the other hand, the mass of almost all the components has been reduced in great percentages, meaning that the new designs and modifications have worked as expected. However, although the weight of the seat tube is slightly higher this is not a major problem since, unlike the first prototype, this new version is a functional and feasible design.

As far as the production of the optimised parts is concerned, it has been possible to print them all in plastic so that they can be seen physically, but not in metal for the reason explained above in this section.

The last objective of this project was to conduct a performance test with the whole bicycle already assembled, to check if all the components really can withstand the weight of a person and if the unions remain assembled under that pressure. As the components could not be printed in metal, this test was done to the joints. It was tried to pull the joint apart of the tube with laboratory tools, and the result was satisfactory, a single joint could handle the weight of a person.

10.2 Limitations

This project has had some limitations regarding the metal printing part. The Additive Manufacturing Laboratory has a high volume of projects, making it challenging to print parts quickly. It must also be considered that all the processes followed by the machine, which are the preparation, printing and post-processing, are very time-consuming and slow. Usually, the whole process takes around one week, and if the printing results in failure, the baseplate has to be post-processed anyway and requires time to leave it completely flat.

The machine used, despite being relatively new and using new technologies, has presented severe difficulties in printing components with complex designs. It was known in advance that the designs would be complex, but it was never considered that they could not be printed.

Another significant limitation of this project is the weight of the component files. Optimised files or files with lattices are very heavy and difficult to work with, as a high-performance computer is needed. For the execution of this project, the computers used were not as powerful as they should be. Optimising the components took more time than initially thought and complicated the correct development of the work.

10.3 Inconsistencies within the assessment's results

Despite the important limitations discussed above, this project does not seem to have substantial inconsistencies. The methodology was strictly followed during the development.

However, during the optimisations, some complementary forces were added to those precisely necessary. This was done to avoid the complete disappearance of material from some parts where it was required, even if no partition was needed. This means that forces have been applied that the component does not really have to withstand.

In addition, another inconsistency was found during the printing process. The dose factor of the printing machine is manually controlled by the operator. This parameter, which determines the quantity of powder spread on the baseplate, is changed during the print without knowing how it affects the piece's chance of success. It is believed that increasing it helps to ensure a positive outcome. Nevertheless, there have been situations where this has not happened, and it is not known why.

10.4 Suggestions for assessment improvements

At the beginning of the project a scheduling was made to time all the steps of this project (see *Appendix 5. Project scheduler*). With hindsight, it can be said that the time allocated to printing was insufficient. It was not considered that printing errors could delay the whole

process so much. Therefore, a better understanding, knowledge and foresight of the printing process and its contingencies is vital in order to achieve the planned objectives.

The non-reduction of seat tube mass is another area for improvement. To avoid making it so wide, and thus reduce its size and weight, the design of the "horns" that join the stays could be modified. This could be achieved by joining them together and adding an angle of aperture.

A change of the material used could be implemented. Using Stainless Steel for the design of a bicycle is not the best option in terms of weight. Other possibilities such as aluminium, titanium or even carbon fibre could be explored. In addition, these materials could have better behaviours with the geometries designed while printing.

Not having been able to print any metal components, leads to the suspicion that this machine is not suitable for printing the very complex designs that are generated by applying DfAM techniques. Hence, trying a different type of machine might be good for the result.

11 Conclusion

The project commissioned by the Additive Manufacturing Laboratory of University of Vaasa enables students to introduce in this rapid developing industry. Because of the advantages Additive Manufacturing provide, its role in industry is growing against traditional manufacturing. Therefore, the project has carried out a development in the bicycle industry by bringing to the sector the implementation of Additive Manufacturing techniques.

As this is a relatively new sector, validation of techniques and methods is very important. Hence the significance of creating complex designs, to be able to see which aspects are lacking and to identify areas for improvement.

The topological optimisation of the components was undertaken using the software Altair Inspire, while the nTopology software was used to create the lattices and merge the meshes. Using these techniques, the mass of the components has been reduced.

The left dropout connector was the component which experienced the smallest weight reduction compared to the first prototype of the bike, which was 10.31%. In contrast, the

component with the highest mass reduction was the head tube, achieving a mass decrease of 81.15%. The other components also experienced a significant decrement in weight, averaging more than 50%. The seat tube is the only component whose weight could not be reduced. It was increased by a 27.96% due to design considerations that, unlike the current design, were not taken into account in the first prototype of this component. Nevertheless, it is clear from the above data that one of the main objectives, which was to reduce the weight of the components, has been successfully achieved.

As for the visual design of the parts, the results obtained are also satisfactory. Initial validation proofing was conducted using PLA printed components in the Ultimaker S5 machine. The resulting components have suitable organic shapes, achieved by using the aforementioned topological optimisation and lattice optimisation software.

Concerning the joints, their design is adequate. The mechanical system meets the requirements and can withstand the loads it will be subjected to during normal use without collapsing.

The metal 3D printing part, done with the machine Prima Additive – Print Sharp 250 could not be completed because of the limitations of the machine and the high demand of the equipment used, which led to limited printing sessions. The more than 200 hours of printing were another limiting factor for the manufacturing of the components. For those reason, the two last objectives of manufacturing and testing the performance of the 3D printed components were not executed.

Regarding the cost of the components, can be said that it is an expensive technology. The estimation of 15,800€, confirms what has been said above. It should also be borne in mind that these prices mean that the printing process must be very careful in order to be successful.

The non-achieved work of this project is not a failure but a new opportunity to try. The errors and difficulties faced during the process sets a precedent and gives experience for those who want to restart or continue this project.

Using Stainless Steel 316L for this project is not optimal in terms of achieving the minor weight. The bicycle industry uses other materials such as aluminium, titanium or carbon

fibre to manufacture its frames. This modification could provide solutions to the difficult printing on Stainless Steel 316L with the Prima Sharp 250 machine. There is a possibility that other materials with this printer or another machine will behave differently with the geometries of the designed parts.

12 References

Abbey, T. (2018, April 2). What Is Topology Optimisation and Why Is It Useful? PTC. https://www.ptc.com/en/blogs/cad/what-is-topology-optimisation

Attaran, M. (2017). The rise of 3-D printing: The advantages of Additive Manufacturing over traditional manufacturing. *Business Horizons*, *60*(5), 677–688. https://doi.org/10.1016/j.bushor.2017.05.011

Ahn, D.-G. (2021). Directed Energy Deposition (DED) Process: State of the Art. *International Journal of Precision Engineering and Manufacturing-Green Technology*, *8*(2), 703–742. https://doi.org/10.1007/s40684-020-00302-7

Al Rashid, A., Ahmed, W., Khalid, M. Y., & Koç, M. (2021). Vat photopolymerization of polymers and polymer composites: Processes and applications. *Additive Manufacturing*, *47*, 102279. https://doi.org/10.1016/j.addma.2021.102279

Alfattni, R. (2022). Comprehensive Study on Materials used in Different Types of Additive Manufacturing and their Applications. *International Journal of Mathematical, Engineering and Management Sciences*, *7*(1), 92–114. https://doi.org/10.33889/ijmems.2022.7.1.007

AM Power. (2019, September 27). *Laser Beam Powder Bed Fusion.* https://additive-manufacturing-report.com/technology/metal/laser-beam-powder-bed-fusion/

Arnold, K. (2022, June 21). AM 101: What Is Binder Jetting? Additive Manufacturing. https://www.additivemanufacturing.media/articles/am-101-binder-jetting

Bandyopadhyay, A., & Bose, S. (2016). *Additive Manufacturing (1st ed.).* CRC Press.

Bandyopadhyay, A., Traxel, K. D., Lang, M., Juhasz, M., Eliaz, N., & Bose, S. (2022). Alloy design via Additive Manufacturing: Advantages, challenges, applications and perspectives. *Materials Today*, *52*, 207–224. https://doi.org/10.1016/j.mattod.2021.11.026

Bendsøe, M.P., & Sigmund, O. (2013). *Topology Optimisation: Theory, Methods and Applications.* (2nd ed.). Springer.

Bhatia, A., & Sehgal, A. K. (2021). Additive Manufacturing materials, methods and applications: A review. *Materials Today: Proceedings*. https://doi.org/10.1016/j.matpr.2021.04.379

Bigrep. (2018, August 6). Guide to post-processing 3d printed parts: 16 methods. https://bigrep.com/post-processing/

Bourell, D., Kruth, J. P., Leu, M., Levy, G., Rosen, D., Beese, A. M., & Clare, A. (2017). Materials for Additive Manufacturing. *CIRP Annals*, *66*(2), 659–681. https://doi.org/10.1016/j.cirp.2017.05.009

Braconnier, D. J., Jensen, R. E., & Peterson, A. M. (2020). Processing parameter correlations in material extrusion Additive Manufacturing. *Additive Manufacturing*, *31*, 100924. https://doi.org/10.1016/j.addma.2019.100924

Brennan, M. C., Keist, J. S., & Palmer, T. A. (2021). Defects in Metal Additive Manufacturing Processes. *Journal of Materials Engineering and Performance*, *30*(7), 4808–4818. https://doi.org/10.1007/s11665-021-05919-6

Carlota V., (2019, April 15). AREVO creates the first 3D printed carbon fiber unibody bike frame. 3Dnatives. https://www.3dnatives.com/en/arevo-bike-frame-150420194/#!

Century Cycles. (2023). Tech Talk: Bike Components for Beginners. https://www.centurycycles.com/tips/tech-talk-bike-components-for-beginners-pg1269.htm

Cerniglia, D., & Montinaro, N. (2018). Defect Detection in Additively Manufactured Components: Laser Ultrasound and Laser Thermography Comparison. *Procedia Structural Integrity*, *8*, 154–162. https://doi.org/10.1016/j.prostr.2017.12.016

Chen, Y., Peng, X., Kong, L., Dong, G., Remani, A., & Leach, R. (2021). Defect inspection technologies for Additive Manufacturing. *International Journal of Extreme Manufacturing*, *3*(2), 022002. https://doi.org/10.1088/2631-7990/abe0d0

Das, S., Bourell, D. L., & Babu, S. S. (2016). Metallic materials for 3D printing. *MRS Bulletin*, *41*(10), 729–741. https://doi.org/10.1557/mrs.2016.217

Demir, A. G., & Previtali, B. (2017). Investigation of remelting and preheating in SLM of 18Ni300 maraging steel as corrective and preventive measures for porosity

reduction. *The International Journal of Advanced Manufacturing Technology*, *93*(5-8), 2697–2709. https://doi.org/10.1007/s00170-017-0697-z

Deshayes, Y., & Béchou, L. (2016). Methodologies of Reliability Analysis. *Reliability, Robustness and Failure Mechanisms of LED Devices*, 117–160. https://doi.org/10.1016/b978-1-78548-152-9.50004-3

Dev Singh, D., Mahender, T., & Raji Reddy, A. (2021). Powder bed fusion process: A brief review. *Materials Today: Proceedings*, *46*, 350–355. https://doi.org/10.1016/j.matpr.2020.08.415

Dilberoglu, U. M., Gharehpapagh, B., Yaman, U., & Dolen, M. (2017). The Role of Additive Manufacturing in the Era of Industry 4.0. *Procedia Manufacturing*, *11*, 545–554. https://doi.org/10.1016/j.promfg.2017.07.148

Du, W., Ren, X., Pei, Z., & Ma, C. (2020). Ceramic Binder Jetting Additive Manufacturing: A Literature Review on Density. *Journal of Manufacturing Science and Engineering*, *142*(4). https://doi.org/10.1115/1.4046248

Duda, T., & Raghavan, L. V. (2016). 3D Metal Printing Technology. *IFAC-PapersOnLine*, *49*(29), 103–110. https://doi.org/10.1016/j.ifacol.2016.11.111

Elkaseer, A., Chen, K. J., Janhsen, J. C., Refle, O., Hagenmeyer, V., & Scholz, S. G. (2022). Material jetting for advanced applications: A state-of-the-art review, gaps and future directions. *Additive Manufacturing*, *60*, 103270. https://doi.org/10.1016/j.addma.2022.103270

Ford, S., & Despeisse, M. (2016). Additive Manufacturing and sustainability: an exploratory study of the advantages and challenges. *Journal of Cleaner Production*, *137*, 1573–1587. https://doi.org/10.1016/j.jclepro.2016.04.150

Formlabs (2023). Topology Optimisation 101: How to Use Algorithmic Models to Create Lightweight Design. https://formlabs.com/blog/topology-optimisation/

Fotheringham, A. (2022, October 25). *Ganna: Hour Record finale so painful "I wanted to fall off or puncture.* Cyclingnews. https://www.cyclingnews.com/news/ganna-hour-record-finale-so-painful-i-wanted-to-fall-off-or-puncture/

Gadagi, B., & Lekurwale, R. (2021). A review on advances in 3D metal printing. *Materials Today: Proceedings*, *45*, 277–283. https://doi.org/10.1016/j.matpr.2020.10.436

Gibson, I., Rosen, D., Stucker, B., & Khorasani, M. (2020). Sheet Lamination. *Additive Manufacturing Technologies*, 253–283. https://doi.org/10.1007/978-3-030-56127-7_9

Ginsberg, N. (2017, August 9). James Novak - World's First 3D Printed Bicycle. Bicycles Create Change. https://www.bicyclescreatechange.com/james-novak-worlds-first-3d-printed-bicycle/

Graf, S., Thakkar, D., Hansa, I., Muthuswamy Pandian, S., & Adel, S. M. (2023). 3D Metal Printing in Orthodontics: Current trends, Biomaterials, Workflows and Clinical Implications. *Seminars in Orthodontics*. https://doi.org/10.1053/j.sodo.2023.01.001

Gülcan, O., Günaydın, K., & Tamer, A. (2021). The State of the Art of Material Jetting—A Critical Review. *Polymers*, *13*(16), 2829. https://doi.org/10.3390/polym13162829

Valmistajat.fi. (2017, September 18). *Haponkestävä teräs EN – 1.4404 (ASTM – 316L)*. https://valmistajat.fi/materiaalit/en-1-4404

Hendrixson, S. (2021, October 11). What Is Laser Powder Bed Fusion (LPBF)? Additive Manufacturing. https://www.additivemanufacturing.media/articles/video-what-is-laser-powder-bed-fusion-lpbf

Hiles, D. (2015, June 23). 58 Milestones from Bicycle History You Must Know. Icebike. https://www.icebike.org/58-milestones-from-bicycle-history-you-must-know/

Hossain, M. S., Gonzalez, J. A., Hernandez, R. M., Shuvo, M. A. I., Mireles, J., Choudhuri, A., Lin, Y., & Wicker, R. B. (2016). Fabrication of smart parts using powder bed fusion Additive Manufacturing technology. *Additive Manufacturing*, *10*, 58–66. https://doi.org/10.1016/j.addma.2016.01.001

Hussein, A., Hao, L., Yan, C., Everson, R., & Young, P. (2013). Advanced lattice support structures for metal Additive Manufacturing. *Journal of Materials Processing Technology*, *213*(7), 1019–1026. https://doi.org/10.1016/j.jmatprotec.2013.01.020

Iacopo, B., Valerio, D. P., Tommaso, M., Massimiliano, P., & Alessio, V. (2022). Environmental impacts assessment of Bound Metal Deposition 3D printing process for stainless steel. *Procedia CIRP*, *105*, 386–391. https://doi.org/10.1016/j.procir.2022.02.064

Jiang, J., Xu, X., & Stringer, J. (2018). Support Structures for Additive Manufacturing: A Review. *Journal of Manufacturing and Materials Processing*, *2*(4), 64. https://doi.org/10.3390/jmmp2040064

Jin, Y., He, Y., & Fu, J. (2015). Support generation for Additive Manufacturing based on sliced data. *The International Journal of Advanced Manufacturing Technology*, *80*(9-12), 2041–2052. https://doi.org/10.1007/s00170-015-7190-3

Kauppila, I. (2023, March 29). *The Best Metal 3D Printers in 2023*. All3DP. https://all3dp.com/1/3d-metal-3d-printer-metal-3d-printing/

Kim, D. B., Witherell, P., Lipman, R., & Feng, S. C. (2015). Streamlining the Additive Manufacturing digital spectrum: A systems approach. https://doi.org/10.1016/j.addma.2014.10.004

Klahn, C., Leutenecker, B., & Meboldt, M. (2015). Design Strategies for the Process of Additive Manufacturing. *Procedia CIRP*, *36*, 230–235. https://doi.org/10.1016/j.procir.2015.01.082

Kotturkar, S. (2018). *How Does Post Processing Work in Metal 3D Printing?* Rapid DMLS Inc. https://www.rapiddmls.com/resources/

Kumar, M. B., & Sathiya, P. (2021). Methods and materials for additive manufacturing: A critical review on advancements and challenges. *Thin-Walled Structures*, *159*, 107228. https://doi.org/10.1016/j.tws.2020.107228

Loughborough University. (2023). *The 7 Categories of Additive Manufacturing.* https://www.lboro.ac.uk/research/amrg/about/the7categoriesofadditivemanufacturing/

Markforged. (2023). Post-Processing Metal 3D Printed Parts. https://markforged.com/es/resources/learn/design-for-additive-manufacturing-metals/3d-printing-strategies-for-metal/post-processing-metal-3d-printed-parts

McDonough, J. R. (2020). A perspective on the current and future roles of Additive Manufacturing in process engineering, with an emphasis on heat transfer. *Thermal Science and Engineering Progress*, *19*, 100594. https://doi.org/10.1016/j.tsep.2020.100594

Miller, M. (2016, February 9). Check Out The World's First 3-D Printed Metal Bike. Fast Company. https://www.fastcompany.com/3056353/check-out-the-worlds-first-3-d-printed-metal-bike

Mirzababaei, S., & Pasebani, S. (2019). A Review on Binder Jet Additive Manufacturing of 316L Stainless Steel. *Journal of Manufacturing and Materials Processing*, *3*(3), 82. https://doi.org/10.3390/jmmp3030082

MYTHOS (2014). *Born from Success.* https://www.mythos.bike/story

Mondal, K., & Tripathy, P. K. (2021). Preparation of Smart Materials by Additive Manufacturing Technologies: A Review. *Materials*, *14*(21), 6442. https://doi.org/10.3390/ma14216442

Mumtaz, K., Vora, P., & Hopkinson, N. (2011). A Method to Eliminate Anchors/Supports from Directly Laser Melted Metal Powder Bed Processes. *Utexas.edu*. https://hdl.handle.net/2152/88338

Nagesha B.K., Dhinakaran V., Shree M. V., Kumar K. S., Chalawadi D., & Sathish T. (2020). *Review on characterization and impacts of the lattice structure in additive manufacturing*. *21*, 916–919. https://doi.org/10.1016/j.matpr.2019.08.158

Naramore, C. (2019, December 16). Post Processing, The Biggest Hurdle for Metal AM. 3D Printing.com. https://3dprinting.com/metal/post-processing-the-biggest-hurdle-for-metal-am/

Oerlikon. (2020). *MetcoAdd 316L-A.* https://mymetco-europe.oerlikon.com/en-us/product/metcoadd316la

Pagac, M., Hajnys, J., Ma, Q.-P., Jancar, L., Jansa, J., Stefek, P., & Mesicek, J. (2021). A Review of Vat Photopolymerization Technology: Materials, Applications, Challenges, and Future Trends of 3D Printing. *Polymers*, *13*(4), 598. https://doi.org/10.3390/polym13040598

Pérez, M., Carou, D., Rubio, E. M., & Teti, R. (2020). Current advances in Additive Manufacturing. *Procedia CIRP*, *88*, 439–444. https://doi.org/10.1016/j.procir.2020.05.076

Piegl, L., & Tiller, W. (2023). The NURBS Book. *SpringerLink*. https://doi.org/10.1007-978-3-642-97385-7

Piscopo, G., & Iuliano, L. (2022). Current research and industrial application of laser powder directed energy deposition. *The International Journal of Advanced Manufacturing Technology*, *119*(11-12), 6893–6917. https://doi.org/10.1007/s00170-021-08596-w

Prima Additive. (2021). *Print Sharp 250.* https://www.primaadditive.com/en/technologies/powder-bed-fusion/print-sharp-250

Prima Additive. (2023a). *Prima Industrie.* https://www.primaindustrie.com/en/business-units/business-units/prima-additive

Prima Additive. (2023b). *Technologies*. https://www.primaadditive.com/en/technologies

Product Designer. (2021, December 18). *What is Topology optimisation? How does topology optimisation work?* https://engineeringproductdesign.com/knowledge-base/topology-optimisation/#How_does_topology_optimisation_work

Protolabs. (2020). *Understanding Powder Bed Fusion Additive Manufacturing.* https://www.protolabs.com/resources/design-tips/powder-bed-fusion/

Protolabs. (2023). *Post-processing for metal 3D printing.* https://www.protolabs.com/resources/design-tips/post-processing-for-metal-3d-printing/

Rontescu, C., D, Cicic T., Amasa C. G., Chivu, O., & Dobrotă, D. (2015). Choosing the optimum material for making a bicycle frame. *Metalurgija*, *54*(4), 679–682. https://hrcak.srce.hr/138286

Rosinha, I. P., Gernaey, K. V., Woodley, J. M., & Krühne, U. (2015). Topology optimisation for biocatalytic microreactor configurations. *12th International Symposium on Process Systems Engineering and 25th European Symposium on Computer Aided Process Engineering*, 1463–1468. https://doi.org/10.1016/b978-0-444-63577-8.50089-9

Sabzi, H. E., & Rivera-Díaz-del-Castillo, P. E. J. (2022). Microscopy Techniques for Additive Manufacturing. *Encyclopedia of Materials: Metals and Alloys*, 703–715. https://doi.org/10.1016/b978-0-12-819726-4.00071-5

Singh, R., & Davim, J. P. (2019). *Additive Manufacturing: Applications and Innovations (1st ed.).* CRC Press.

Snow, Z., Nassar, A. R., & Reutzel, E. W. (2020). Invited Review Article: Review of the formation and impact of flaws in powder bed fusion Additive Manufacturing. *Additive Manufacturing*, *36*, 101457. https://doi.org/10.1016/j.addma.2020.101457

Structuralia. (2022). *La historia de la impresión 3D y cómo está transformando al mundo*. https://blog.structuralia.com/historia-de-la-imprension-3d#:~:text=La%20historia%20de%20la%20impresi%C3%B3n%203D%20comenz%C3%B3%20en%20la%20d%C3%A9cada,aumento%20en%20los%20%C3%BAltimos%20a%C3%B1os.

Tao, W., & Leu, M. C. (2016). Design of lattice structure for Additive Manufacturing. *2016 International Symposium on Flexible Automation (ISFA)*. https://doi.org/10.1109/isfa.2016.7790182

Thompson, M. K., Moroni, G., Vaneker, T., Fadel, G., Campbell, R. I., Gibson, I., Bernard, A., Schulz, J., Graf, P., Ahuja, B., & Martina, F. (2016). Design for Additive Manufacturing: Trends, opportunities, considerations, and constraints. *CIRP Annals*, *65*(2), 737–760. https://doi.org/10.1016/j.cirp.2016.05.004

Torosian, M. (2023). *What is Design for Additive Manufacturing?* Jabil. https://www.jabil.com/blog/design-for-additive-manufacturing.html

Travitzky, N., Bonet, A., Dermeik, B., Fey, T., Filbert-Demut, I., Schlier, L., Schlordt, T., & Greil, P. (2014). Additive Manufacturing of Ceramic-Based Materials. *Advanced Engineering Materials*, *16*(6), 729–754. https://doi.org/10.1002/adem.201400097

TWI Global (A Complete Guide). (2023). *What is Material Extrusion?* https://www.twi-global.com/technical-knowledge/faqs/what-is-material-extrusion

Varotsis, A. B. (2022, April 28). Guide to lattice structures in Additive Manufacturing. NTop. https://www.ntop.com/resources/blog/guide-to-lattice-structures-in-additive-manufacturing/#what-are-lattice-structures

Wang, S., Ning, J., Zhu, L., Yang, Z., Yan, W., Dun, Y., Xue, P., Xu, P., Bose, S., & Bandyopadhyay, A. (2022). *Role of porosity defects in metal 3D printing: Formation*

mechanisms, impacts on properties and mitigation strategies. *59*, 133–160. https://doi.org/10.1016/j.mattod.2022.08.014

Wang, Y., Zhang, L., Daynes, S., Zhang, H., Feih, S., & Wang, M. Y. (2018). Design of graded lattice structure with optimised mesostructures for Additive Manufacturing. *Materials & Design*, *142*, 114–123. https://doi.org/10.1016/j.matdes.2018.01.011

Weinstein, D. M., Parker, S., Simpson, J., Zimmerman, K., & Jones G. M. (2005). Visualization in the SCIRun Problem-Solving Environment. *Visualization Handbook*, 615–632. https://doi.org/10.1016/b978-012387582-2/50033-2

White Bikes. (2020). *XC Trainer Mns 22.* https://whitebikes.com/xc-trainer-mns-22/b/3365/#tab

Wong, K. V., & Hernandez, A. (2012). A Review of Additive Manufacturing. *ISRN Mechanical Engineering*, *2012*, 1–10. https://doi.org/10.5402/2012/208760

Wu, B., Pan, Z., Ding, D., Cuiuri, D., Li, H., Xu, J., & Norrish, J. (2018). A review of the wire arc Additive Manufacturing of metals: properties, defects and quality improvement. *Journal of Manufacturing Processes*, *35*, 127–139. https://doi.org/10.1016/j.jmapro.2018.08.001

Xia, L. (2016). *Multiscale Structural Topology Optimisation*. https://www.elsevier.com/books/multiscale-structural-topology-optimisation/xia/978-1-78548-100-0

Yadav, A., Srivastav, A., Singh, A., Mushtaque, M. D., Khan, S. A., Kumar, H., & Arora, P. K. (2021). Investigation on the materials used in Additive Manufacturing: A study. *Materials Today: Proceedings*, *43*, 154–157. https://doi.org/10.1016/j.matpr.2020.10.975

Yao, B., Imani, F., Sakpal, A. S., Reutzel, E. W., & Yang, H. (2018). Multifractal Analysis of Image Profiles for the Characterization and Detection of Defects in Additive Manufacturing. *Journal of Manufacturing Science and Engineering*, *140*(3). https://doi.org/10.1115/1.4037891

Zhang, Y., Wu, L., Guo, X., Kane, S., Deng, Y., Jung, Y.-G., Lee, J.-H., & Zhang, J. (2017). Additive Manufacturing of Metallic Materials: A Review. *Journal of Materials*

Engineering and Performance, *27*(1), 1–13. https://doi.org/10.1007/s11665-017-2747-y

Appendix 1. Stainless Steel 316L Technical Datasheet

2 pages

2683 KB

[Oerlikon Official Website]

oerlikon
am

Additive Manufacturing
316L Stainless Steel

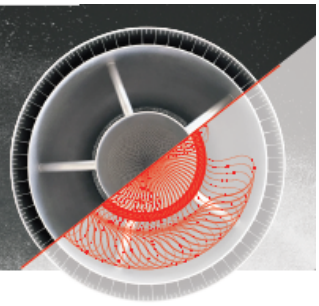

Designed for Processing in Laser Powder Bed Fusion (PBF-LB), Electron Beam Powder Bed Fusion (PBF-EB) or Directed Energy Deposition (DED) Systems

MetcoAdd™ 316L is a family of austenitic steel powders with chemistry similar to EN 1.4404 and UNS S316603

Room temperature static properties of PBF-LB processed, as-built, material coupons have been shown to be comparable to those of AMS 5424.

For reference purposes Oerlikon has processed MetcoAdd 316L-A using fixed parameters and 40 µm layer thickness to provide data below. Additional testing has been performed by an extensive network of consortia and customer partners on a broader range of machine types. Properties may be optimized based on application specific requirements.

Applications

- Aerospace: Clamping elements and heat exchangers
- Medical: Surgical tools and orthopedic implants
- Transport: Maritime components
- Tooling: Pressure injection dies and molds
- Consumer: Jewelry and watch components

Typical As-built Properties (316L-A) [1] [2] [3]

	Concept Laser M2 Cusing	EOS M290	Test Method
Ultimate Tensile Strength (MPa), XY/Z	670±2 / 635±9	677±7 / 609±2	ASTM E8
Yield Strength (MPa), XY/Z	548±15 / 491±4	562±12 / 500±3	
Elongation at break %, XY/Z	45±2 / 44±8	45±3 / 59±1	
Hardness (VHN_{300g})	216±23	228±6	ASTM E384-17
Relative Density %	>99.6%	>99.8%	Internal Spec.

[1] Disclaimer: All data published in this datasheet has been shared for reference purposes only and is not sufficient to design or certify parts. No warranty or guarantee is made against these results.
[2] Bounds are based on one standard deviation of each population with ten samples per orientation and machine. Test specimens were 6.35 mm diameter round bars machined from coupons (75x75x13mm). Direction XY data is an average of both X and Y horizontal build orientations.
[3] The process parameters and heat treatments of AM builds produced with other powder cuts (316L-D) and or AM processes (DED and PBF-EB) may be optimized based on application specific requirements.

As-built Microstructure (x 20 magnification, Vertical Build Direction)

	Concept Laser M2 Cusing	EOS M290
MetcoAdd 316L-A	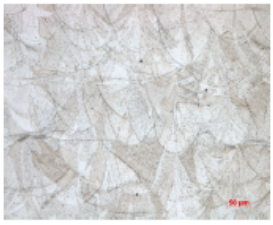	

Appendix 2. Aluminium 6060 Technical Datasheet

1 page

193 KB

[Nedal Aluminium]

Nedal
ALUMINIUM

Nedal Aluminium BV
Groenewoudsedijk 1
3528 BG Utrecht

P.O. Box 2020
3500 GA Utrecht
The Netherlands

+31 (0)30 292 57 11
info@nedal.com
www.nedal.com

ALLOY DATA SHEET
EN-AW 6060[AlMgSi]
(Type: General extrusion alloy)

The alloy EN AW-6060 is a widely used extrusion alloy, suitable for applications where no special strength properties are required. Parts can be produced with a very good surface quality, suitable for many coating operations. Typical application fields are furniture, finishing materials, windows and doors, carbody finishing, façade construction, lighting columns and flagpoles, architecture, and food industry.

Chemical composition according to EN573-3 (weight%, remainder Al)

Si	Fe	Cu	Mn	Mg	Cr	Zn	Ti	remarks	others	
									each	total
0.30-0.6	0.10-0.30	max. 0.10	max. 0.10	0.35-0.6	max. 0.05	max. 0.15	max. 0.10		max. 0.05	max. 0.15

Mechanical properties according to EN755-2

Temper*	Wallthickness e*** [mm]	Yield stress $Rp_{0.2}$ [MPa]	Tensile strength Rm [MPa]	Elongation A [%]	Elongation A_{50} [%]	Hardness** HB
T4	≤ 25	60	120	16	14	45
T5	≤ 5	120	160	8	6	55
	5 < e ≤ 25	100	140	8	6	50
T6	≤ 5	150	190	8	6	65
	5 < e ≤ 25	140	170	8	6	60
T66	≤ 5	160	215	8	6	70
	5 < e ≤ 25	150	195	8	6	65

*Temper designation according to EN515: T4-Naturally aged to a stable condition, T5-cooled from an elevated temperature forming operation and artificially aged, T6-Solution heat treated, quenched and artificially aged, T66-cooled from an elevated temperature forming operation and artificially aged to a condition with higher mechanical properties through special control of manufacturing processes. (T6/T66 properties can be achieved by press quenching)
** Hardness values are for indication only
***For different wall thicknesses within one profile, the lowest specified properties shall be considered as valid for the whole profile cross section

Physical properties (approximate values, 20°C)

Density [kg/m³]	Melting range [°C]	Electrical Conductivity [MS/m]	Thermal Conductivity [W/m.K]	Co-efficient of thermal Expansion 10^{-6}/K	Modulus of Elasticity [GPa]
2700	585-650	28-34	200-220	23.4	~70

Weldability[1]
Gas: 3 TIG: 2 MIG: 2
Typical filler materials (EN ISO18273): SG-AlMg5Cr(A) or AlSi5, and AlMg3 when the product has to be anodised. Due to the heat input during welding the mechanical properties will be reduced by approximately 50% (ref. EN1999-1).

Machining characteristics[1]
T4 temper: 3 T5 and T6 temper: 2

Coating properties[1]
Hard protecting anodising: 1
Decorative/bright/colour anodising: 1

Corrosion resistance[1]
General: 1 Marine: 2

[1]Relative qualification ranging from 1-very good to 6 unsuitable

November 2017
Rev. 01

a HunterDouglas company

Extrusion & Lighting columns

Appendix 3. Metal printing times

This appendix shows the printing times for each of the components. The times have been calculated in the machine itself, and allow to have an idea of how time-consuming is this process.

- Head tube

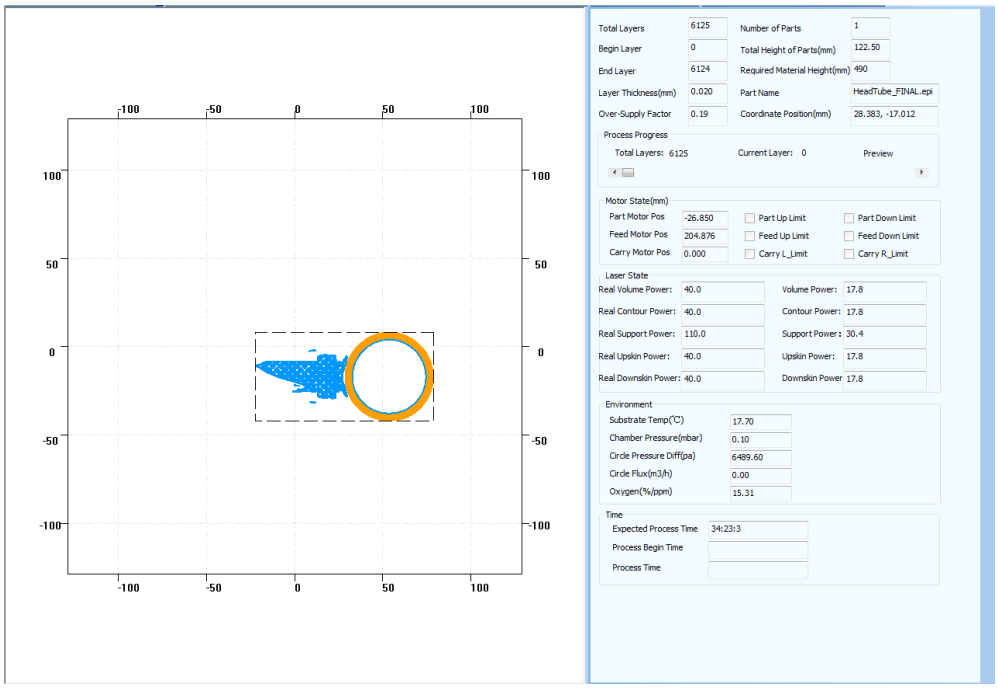

- Bottom bracket

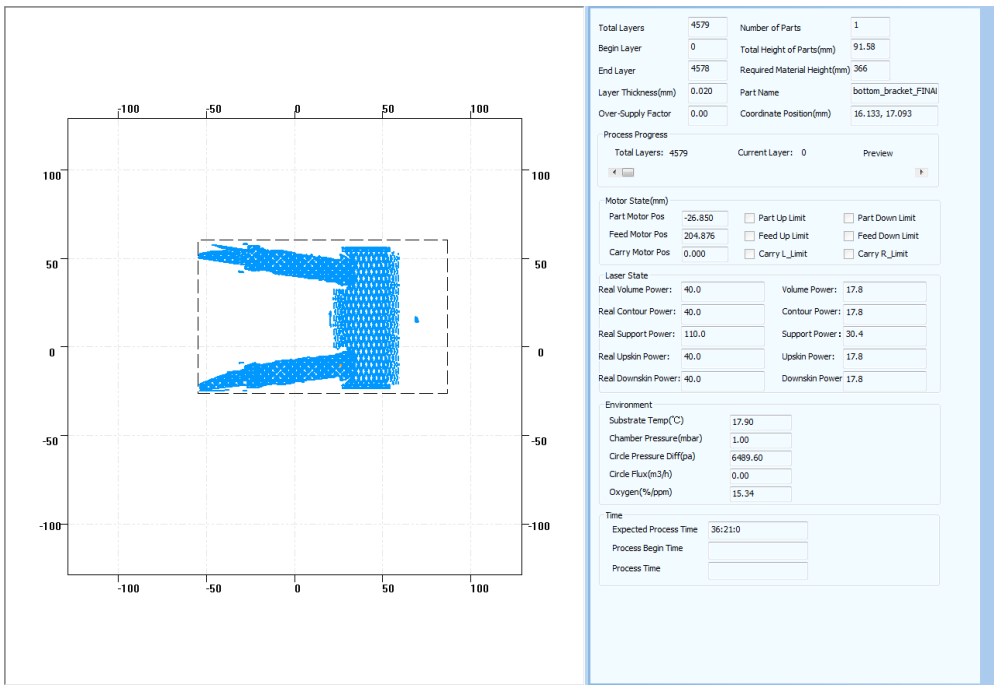

- Seat tube

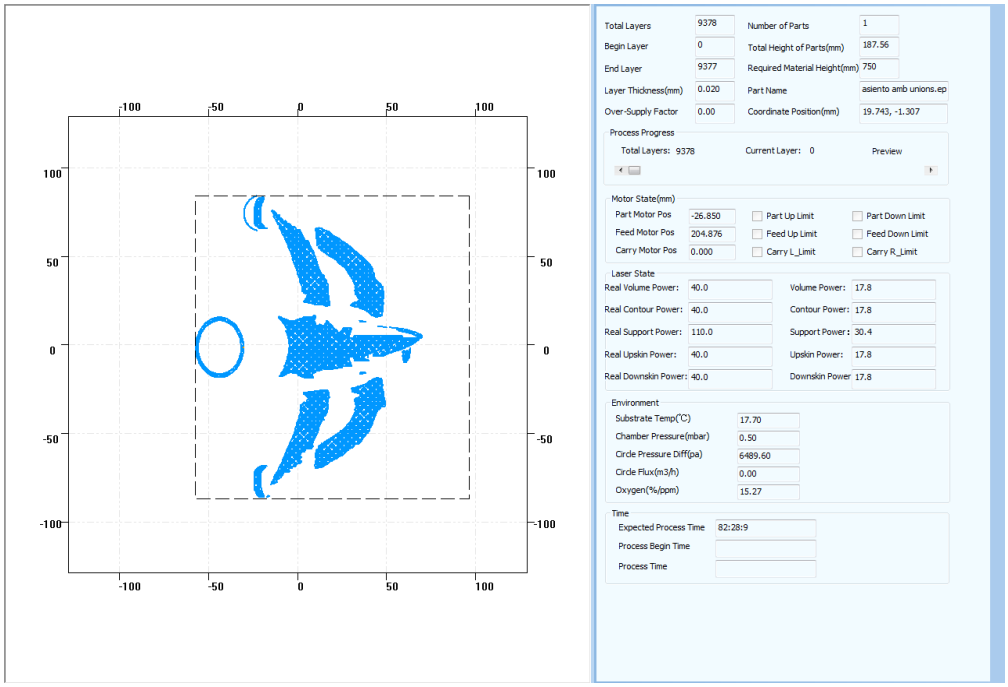

- Right dropout

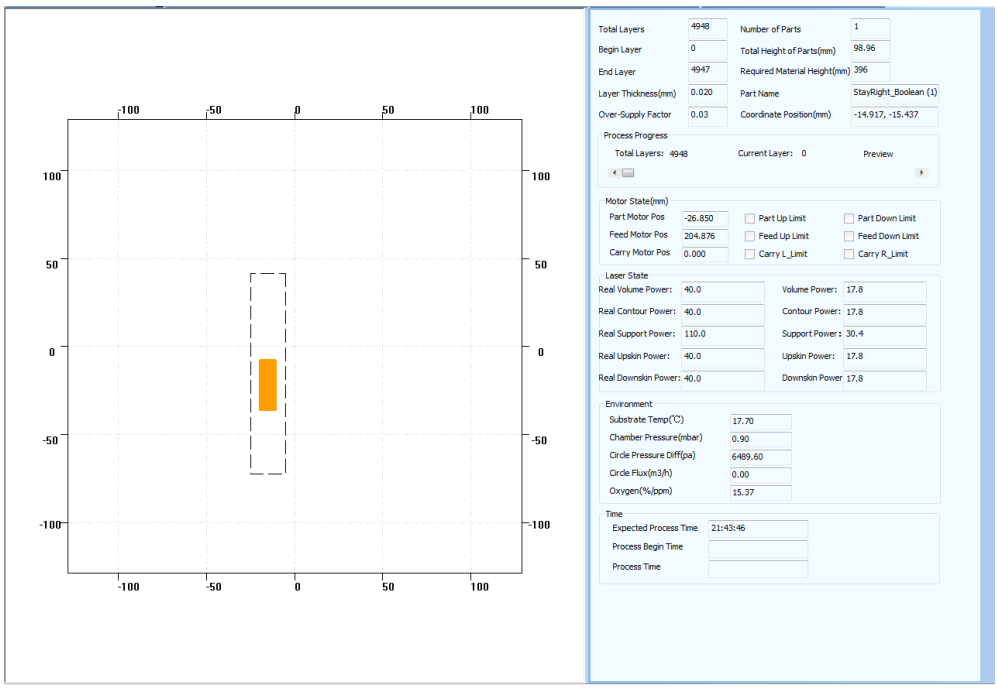

- Left dropout

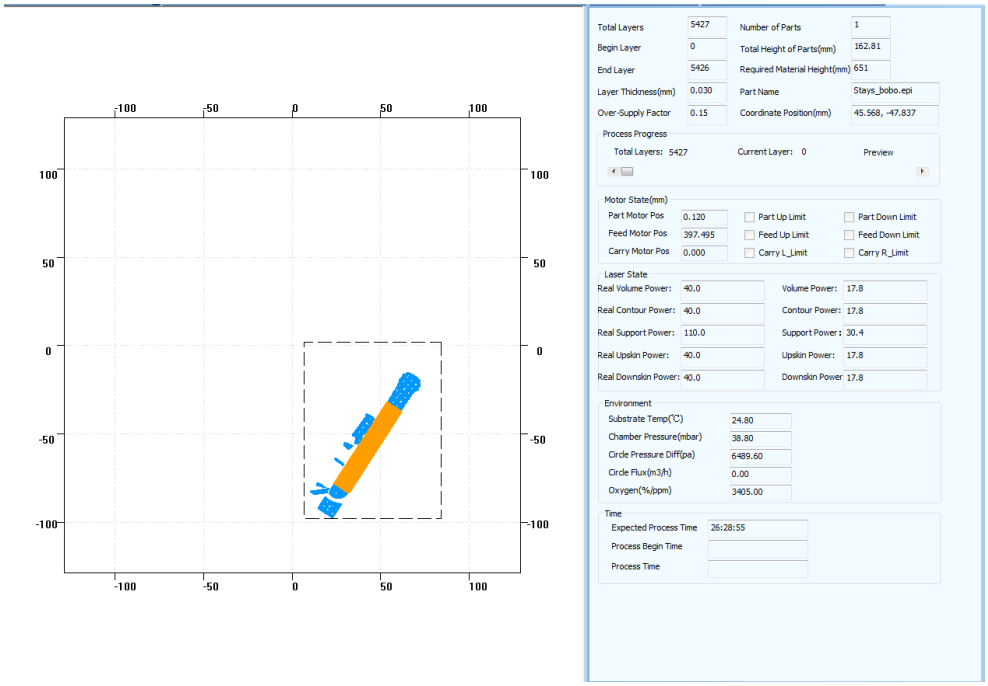

Appendix 4. Estimated cost of the parts

In this appendix are shown the screenshots of the price of the components. These prices are for guidance only; they are not the exact cost of the components. As already said in the text, they have been extracted from the Select AM website.

- Head tube

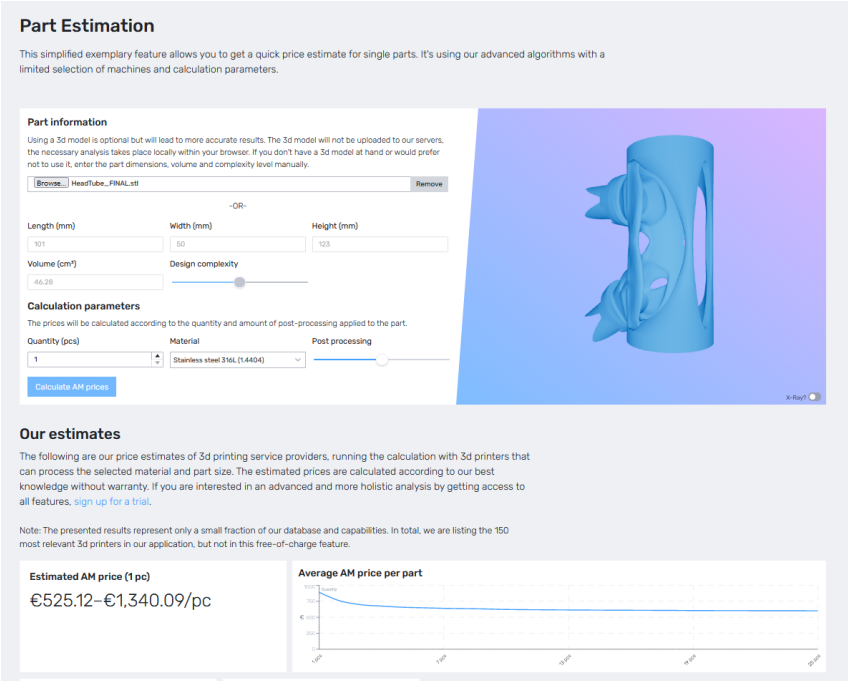

- Bottom bracket

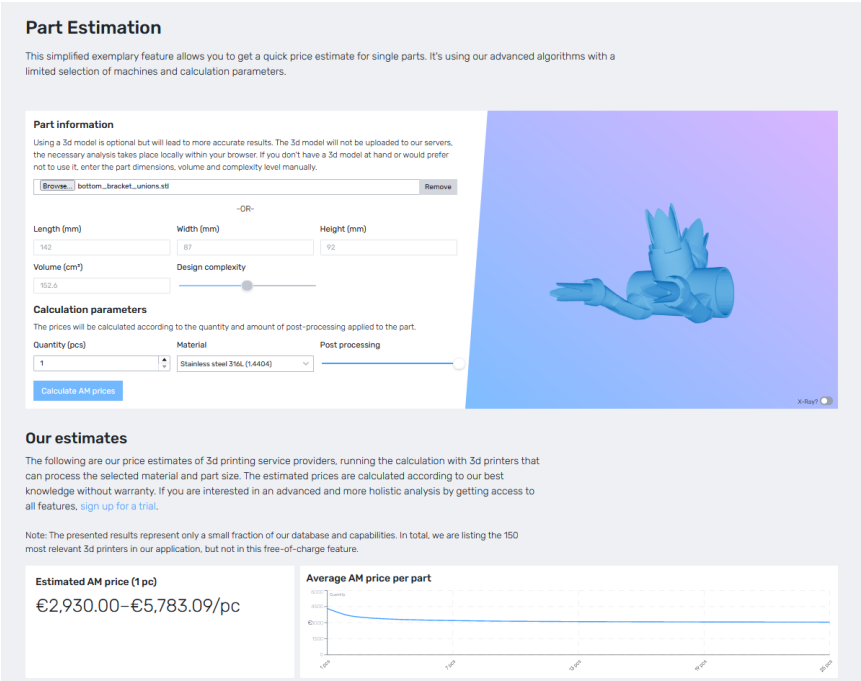

- Seat tube

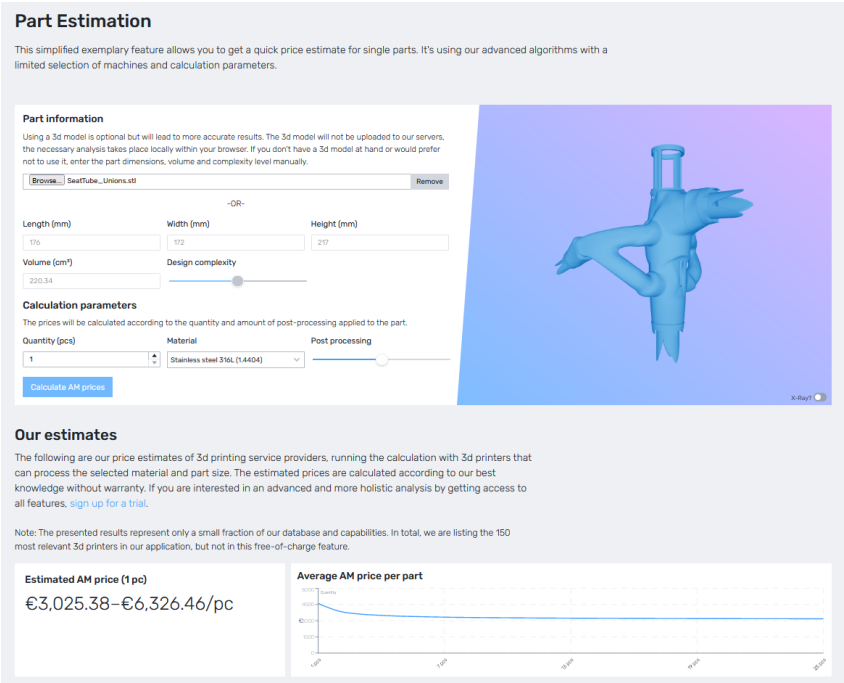

- Right dropout

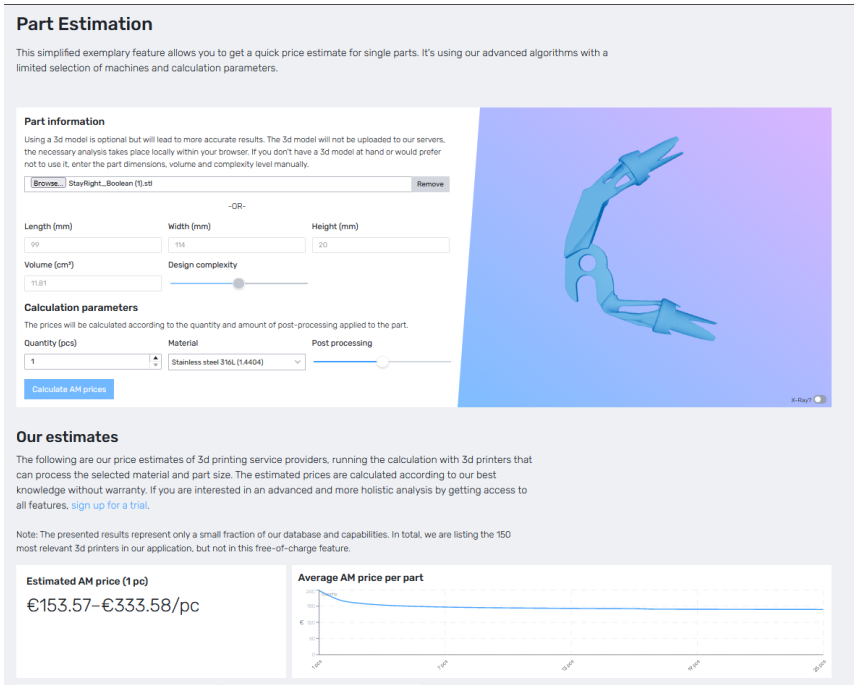

- Left dropout

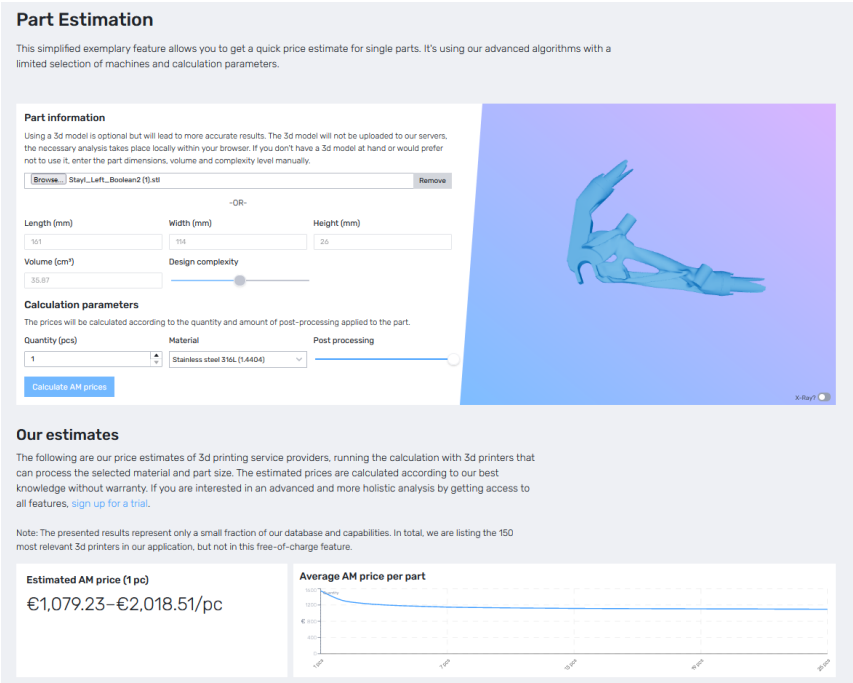

Appendix 5. Project scheduler

PROJECT: Additive Manufacturing Bike

Raúl Zurita Sánchez and Roc Font i Codinachs

On track | Low risk | Med risk | High risk | Unassigned

Project start date: 16/1/2023
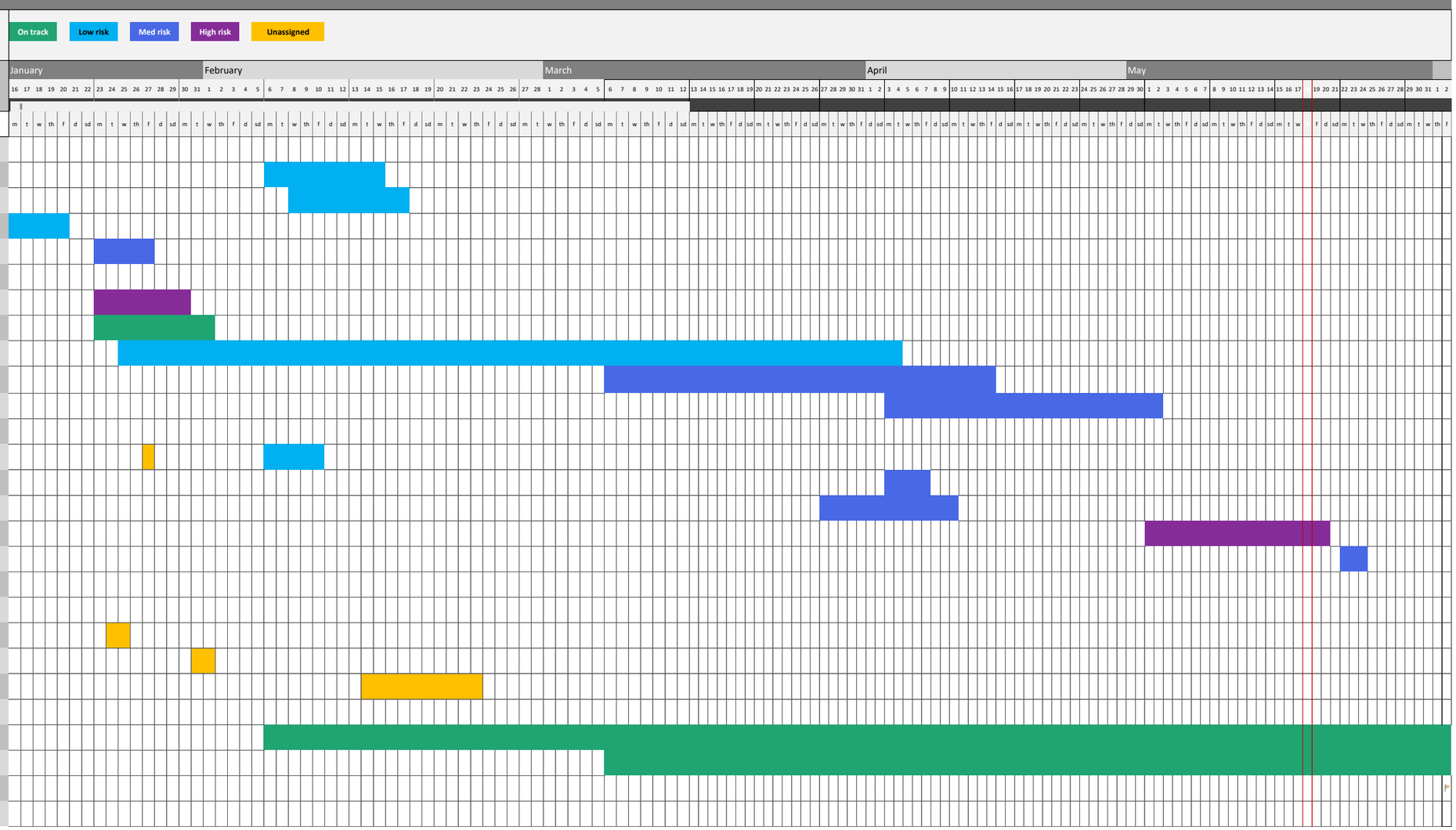
Milestone description	Category	Assigned to	Progress	Start	Days
D1 Research					
T1.1 Additive manufacturing	Low Risk	Raúl and Roc	100%	6/2/2023	10
T1.2 Topology optimisation	Low Risk	Raúl and Roc	100%	8/2/2023	10
T1.3 3D printed bikes	Low Risk	Raúl and Roc	100%	16/1/2023	5
T1.4 Forces analysis	Med Risk	Raúl and Roc	100%	23/1/2023	5
D2 Design					
T2.1 Dimensions of the frame	High Risk	Raúl and Roc	100%	23/1/2023	8
T2.2 Joints design	On Track	Raúl and Roc	100%	23/1/2023	10
T2.3 3D design with CREO	Low Risk	Raúl and Roc	100%	25/1/2023	70
T2.4 3D topology optimization with Altair and Lattice creation with nTopology	Med Risk	Raúl and Roc	100%	6/3/2023	40
T2.5 Printing preparation with materialise magics	Med Risk	Raúl and Roc	100%	3/4/2023	30
D3 Implementation					
T3.1 3D printing test of the joints in plastic	Low Risk	Raúl, Roc and Miguel	100%	6/2/2023	5
T3.2 3D printing test of the joints in metal	Med Risk	Raúl, Roc and Miguel	100%	3/4/2023	5
T3.3 3D printing of the pieces in plastics	Med Risk	Raúl, Roc and Miguel	100%	27/3/2023	15
T3.4 3D printing of the pieces in metal	High Risk	Raúl, Roc and Miguel	20%	1/5/2023	20
T3.5 Machining of the parts	Med Risk	Raúl, Roc and Miguel	0%	22/5/2023	3
T3.6 Assembly of the bike	Milestone	Raúl and Roc	0%	25/5/2023	2
D4 Documentation					
T4.1 Hi-level Planner		Raúl and Roc	100%	24/1/2023	2
T4.2 Belbin and Leadership tests		Raúl and Roc	100%	31/1/2023	2
T4.3 WBS and Scheduling		Raúl and Roc	100%	14/2/2023	10
D5 Closure					
T5.1 Writing and thesis format	On Track	Raúl, Roc and Philip	100%	6/2/2023	117
T5.2 Thesis revision	On Track	Raúl, Roc, Miguel and Philip	100%	6/3/2023	89
T5.3 Presentation	Milestone	Raúl and Roc	0%	2/6/2023	1